Protostellar Feedback Processes and the Mass of the First Stars

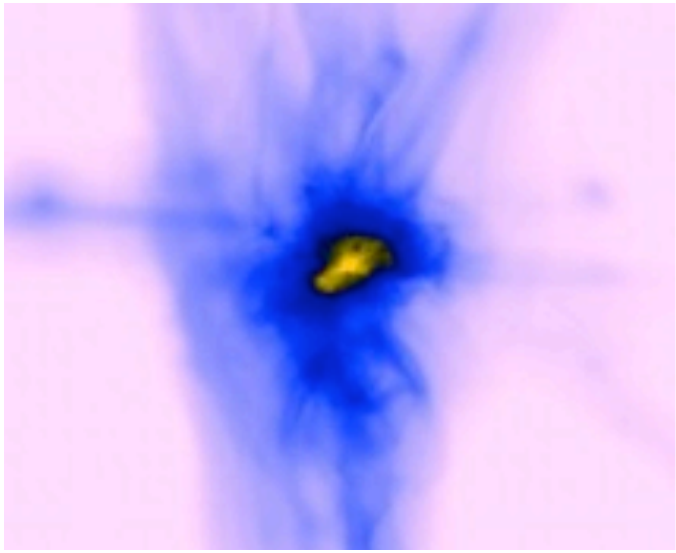

Primordial Mini-Halo (Abel, Bryan, Norman)

Jonathan Tan

(University of Florida)

In collaboration with:

Christopher McKee (Berkeley)

Eric Blackman (Rochester)

Aravind Natarajan (CMU)

Brian O'Shea (MSU)

Britton Smith (Colorado)

Dan Whalen (CMU)

Aaron Boley (Florida)

Sylvia Eksröm (Geneva)

Cyril Georgy (Geneva)

UF | Astronomy

Lessons from local star formation

A complicated, nonlinear process

Physics:

Gravity vs pressure (thermal, magnetic, turbulence, radiation, cosmic rays) and shear.

Heating and cooling, generation and decay of turbulence, generation (dynamo) and diffusion of B-fields, etc.

Chemical evolution of dust and gas.

Lessons from local star formation

A complicated, nonlinear process

Physics:

Gravity vs pressure (thermal, magnetic, turbulence, radiation, cosmic rays) and shear.

Heating and cooling, generation and decay of turbulence, generation (dynamo) and diffusion of B-fields, etc.

Chemical evolution of dust and gas.

Wide range of scales (~12 dex in space, time) and multidimensional.

Uncertain/unconstrained initial conditions/boundary conditions.

Lessons from local star formation

A complicated, nonlinear process

Physics:

Gravity vs pressure (thermal, magnetic, turbulence, radiation, cosmic rays) and shear.

Heating and cooling, generation and decay of turbulence, generation (dynamo) and diffusion of B-fields, etc.

Chemical evolution of dust and gas.

Wide range of scales (~12 dex in space, time) and multidimensional.

Uncertain/unconstrained initial conditions/boundary conditions.

Lessons from local star formation

A complicated, nonlinear process

Physics:

Gravity vs pressure (thermal, magnetic, turbulence, radiation, cosmic rays) and shear.

Heating and cooling, generation and decay of turbulence, generation (dynamo) and diffusion of B-fields, etc.

Chemical evolution of dust and gas.

Wide range of scales (~12 dex in space, time) and multidimensional.

Uncertain/unconstrained initial conditions/boundary conditions.

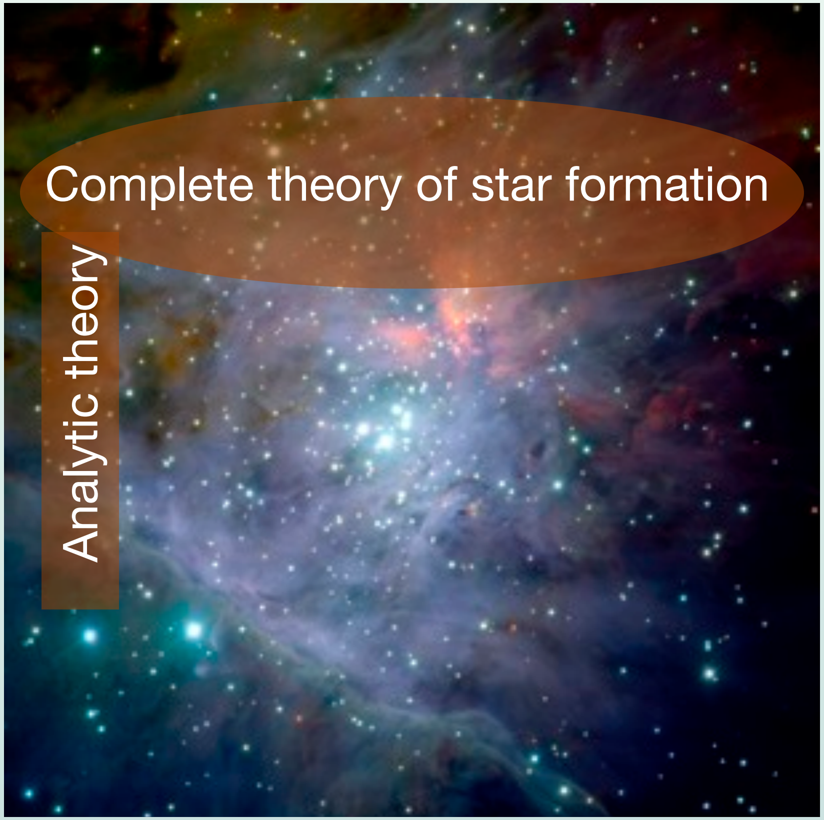

Lessons from local star formation

A complicated, nonlinear process

Physics:

Gravity vs pressure (thermal, magnetic, turbulence, radiation, cosmic rays) and shear.

Heating and cooling, generation and decay of turbulence, generation (dynamo) and diffusion of B-fields, etc.

Chemical evolution of dust and gas.

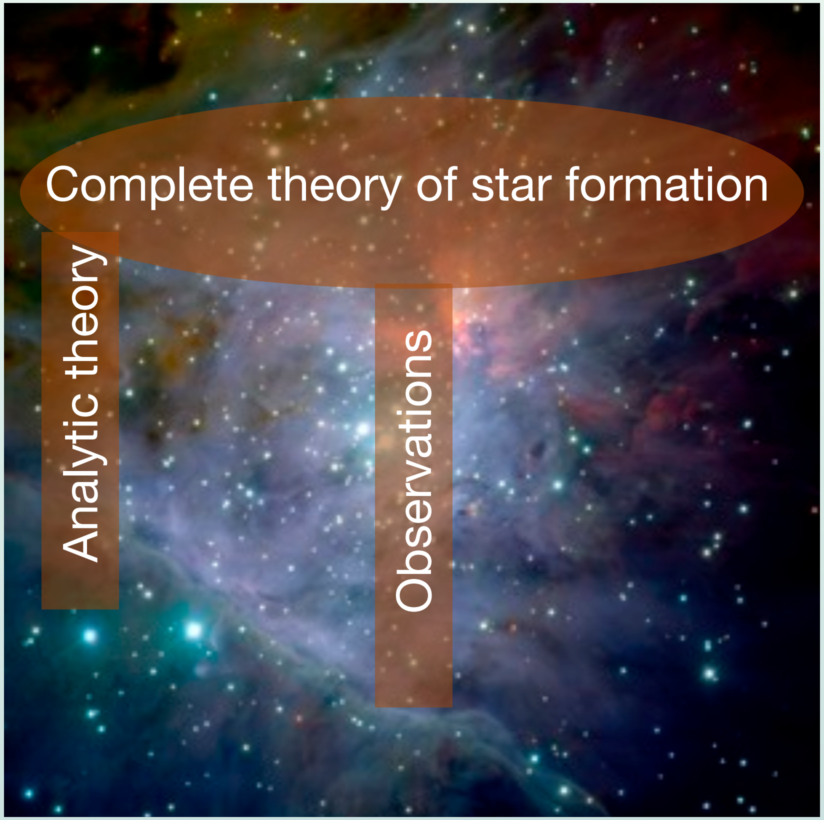

Wide range of scales (~12 dex in space, time) and multidimensional.

Uncertain/unconstrained initial conditions/boundary conditions.

Lessons from local star formation

A complicated, nonlinear process

Physics:

Gravity vs pressure (thermal, magnetic, turbulence, radiation, cosmic rays) and shear.

Heating and cooling, generation and decay of turbulence, generation (dynamo) and diffusion of B-fields, etc.

Chemical evolution of dust and gas.

Wide range of scales (~12 dex in space, time) and multidimensional.

Uncertain/unconstrained initial conditions/boundary conditions.

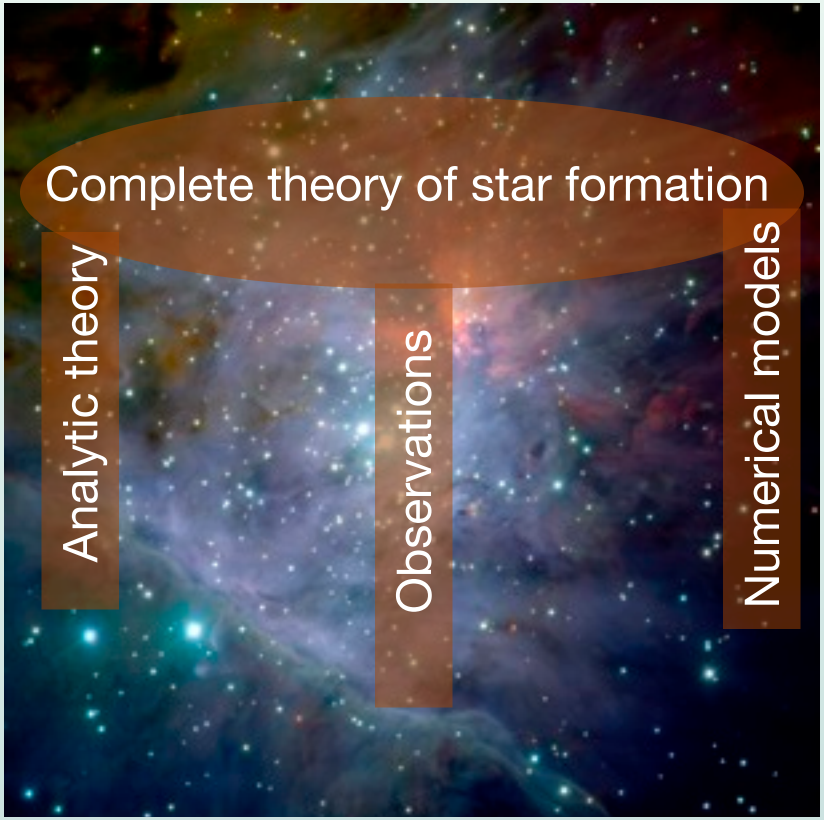

The First Stars

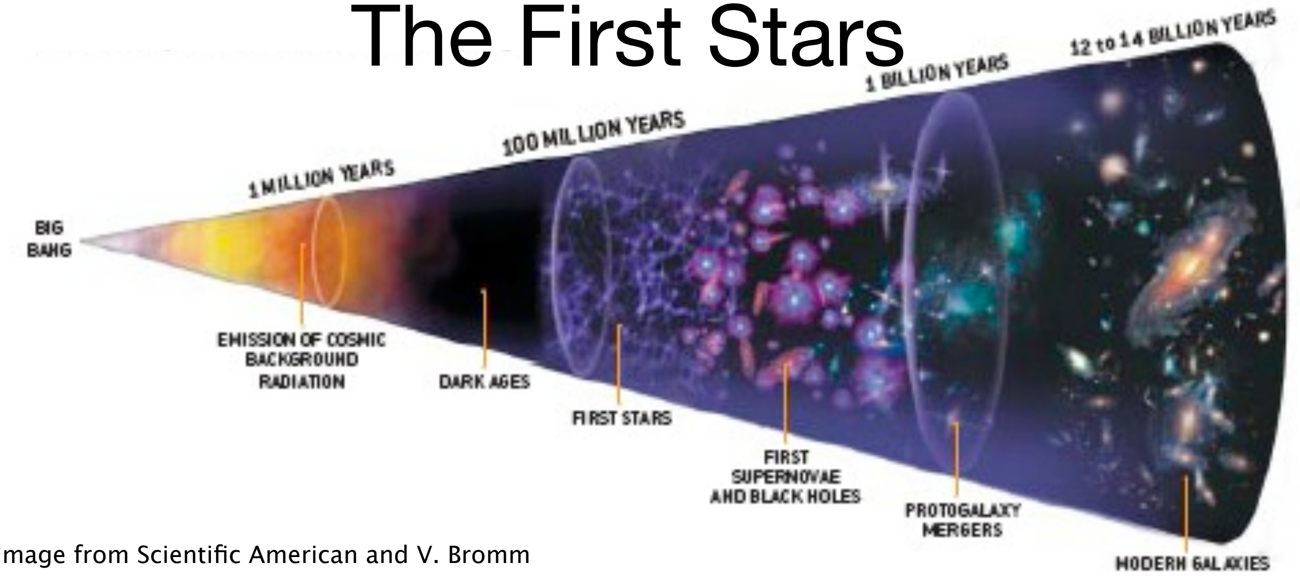

Image from Scientific American and V. Bromm

The First Stars

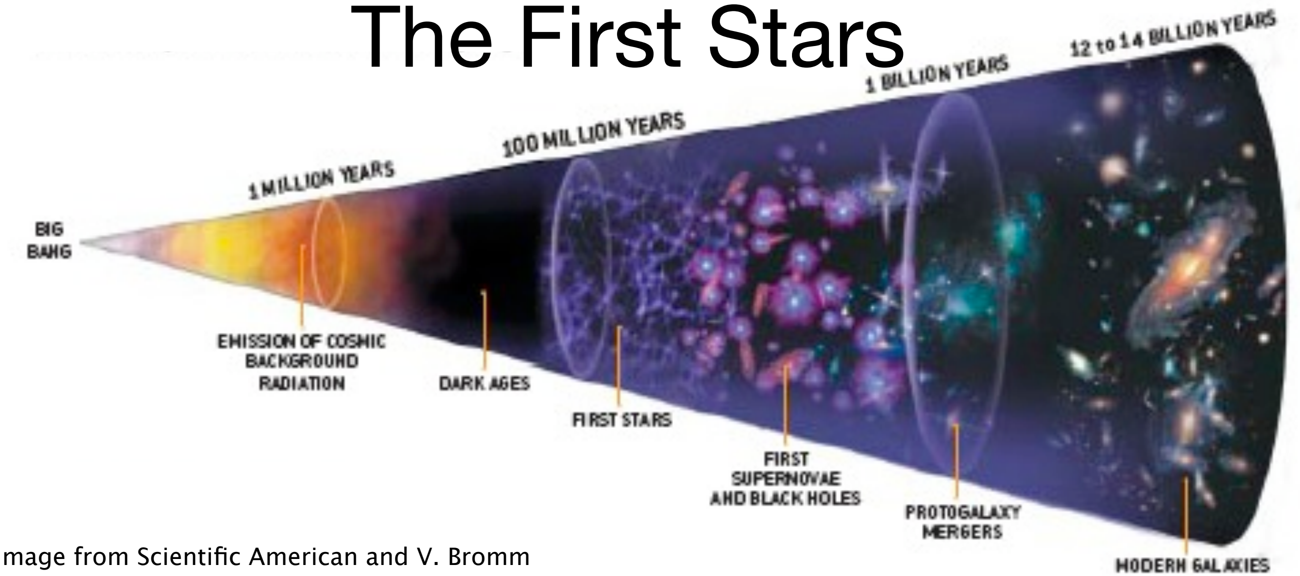

Image from Scientific American and V. Bromm

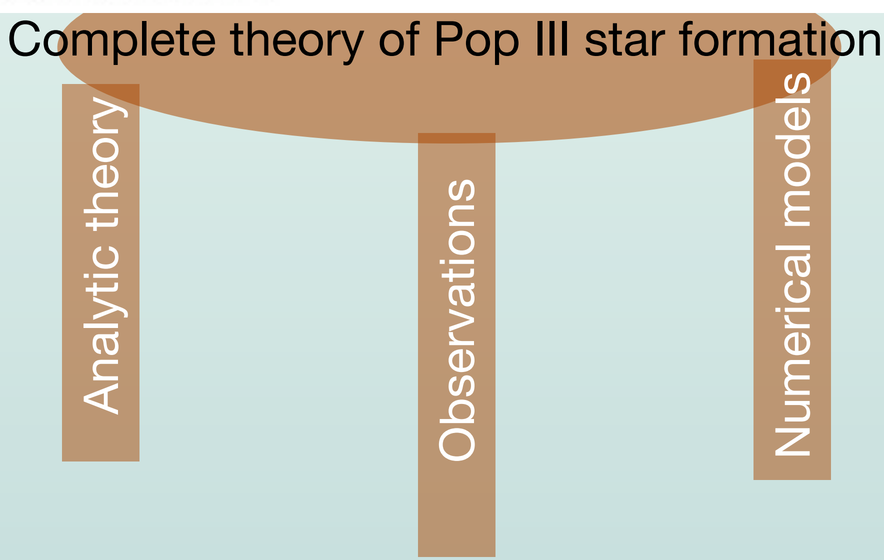

The First Stars

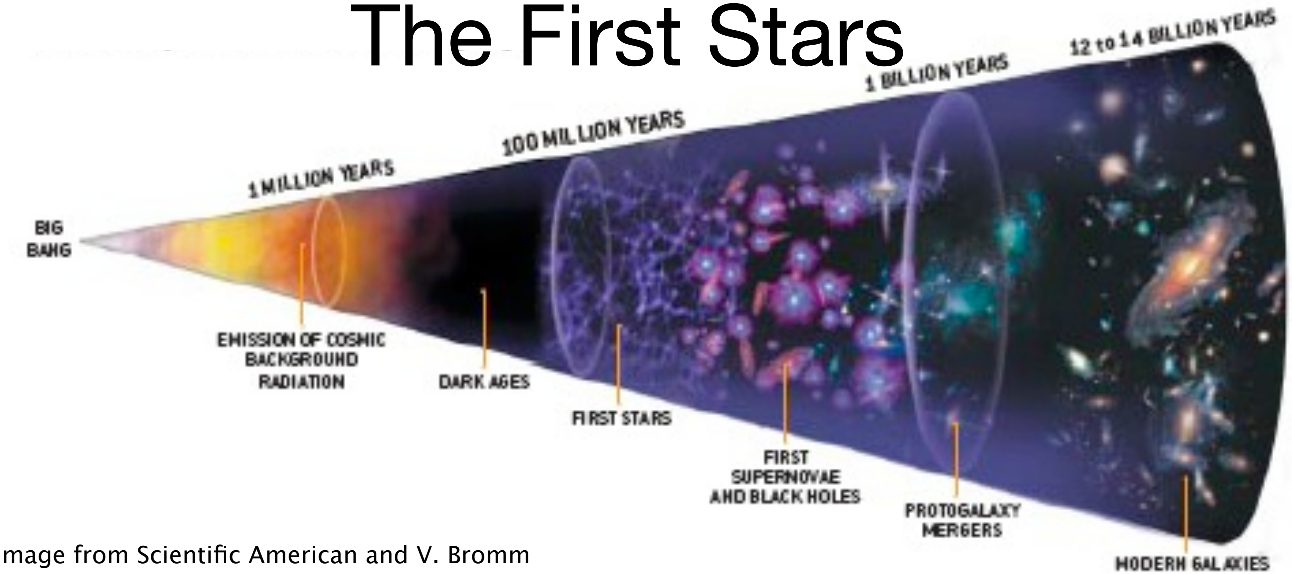

Image from Scientific American and V. Bromm

Complete theory of Pop III star formation

Analytic theory

Numerical models

The First Stars

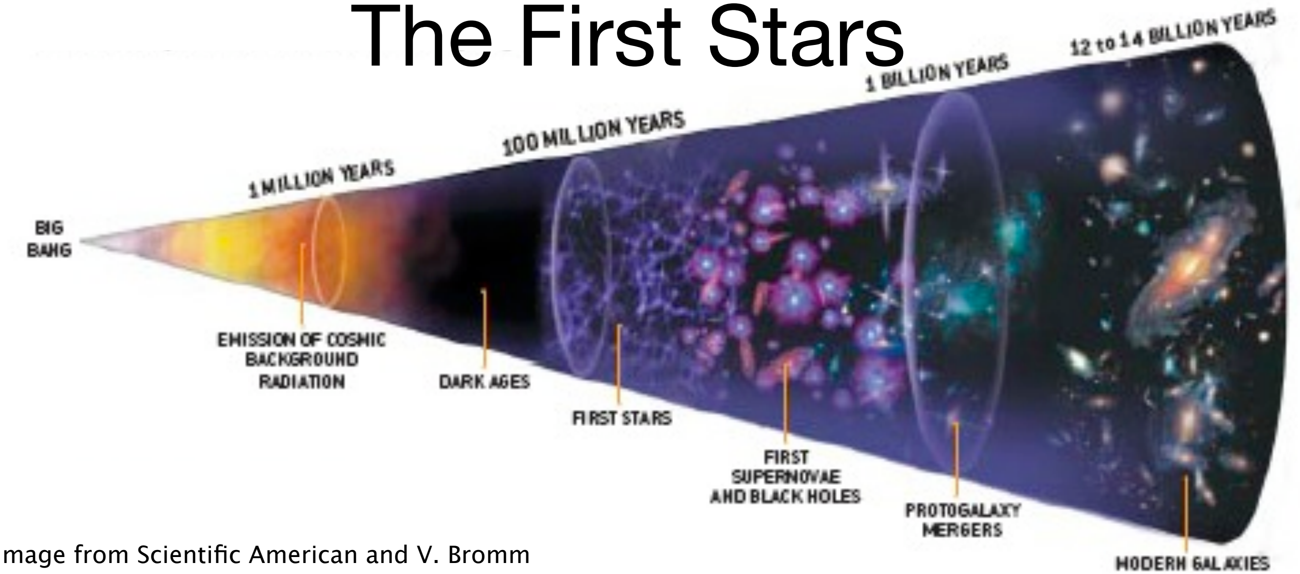

Image from Scientific American and V. Bromm

Complete theory of Pop III star formation

Analytic theory

PopIII Initial Conditions

Numerical models

The First Stars

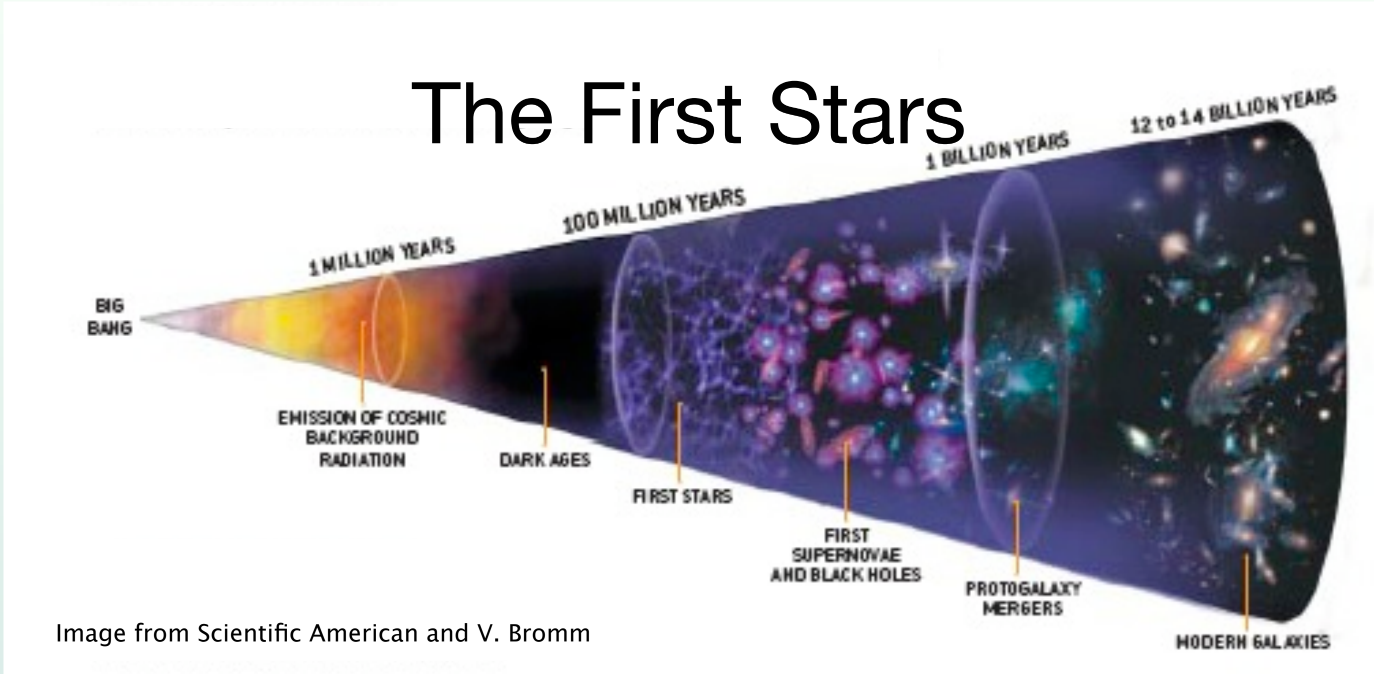

Image from Scientific American and V. Bromm

Complete theory of Pop III star formation

Analytic theory

PopIII Initial Conditions

Numerical models

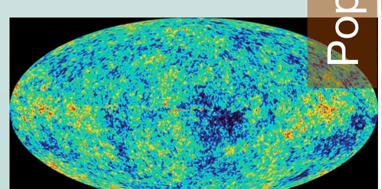

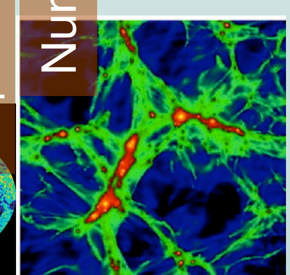

Importance of First Stars and their Mass

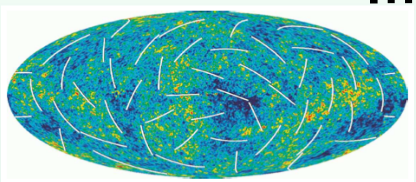

Observations

Reionization (H, He)

CMB polarization (WMAP Page et al. 07)
H 21cm (LOFAR Morales & Hewitt 04)

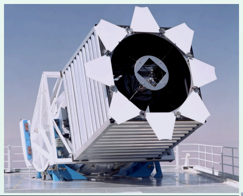

Metal Enrichment

proto-galaxies and IGM

Z of low Z halo stars (Beers & Christlieb 05, Scannapieco et al. 2006)
Z of Lya forest?(Schaye et al. 03 Norman et al. 04)

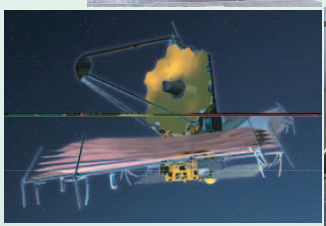

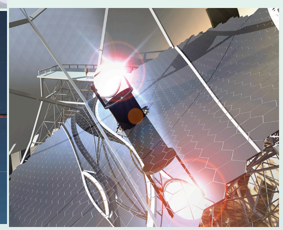

Illumination

NIR bkg. intensity (Santos et al. 02; Fernandez & Komatsu 06)
NIR bkg. fluctuations (Kashlinsky et al. 04)

SN & GRBs?

JWST (Weinmann & Lilly 2005)
SWIFT (Bromm & Loeb 2002)

Progenitors of IMBHs/SMBHs?

Early Galaxies?

ULXs (Mii & Totani 2005)
Quasars (Fan et al. 03; Willott et al. 03)
NIR cts (Stark et al. 07)

Importance of First Stars and their Mass

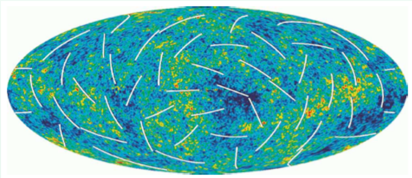

Observations

Reionization (H, He)

CMB polarization (WMAP Page et al. 07)
H 21cm (LOFAR Morales & Hewitt 04)

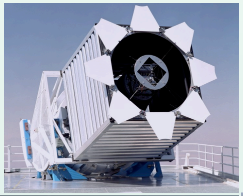

Metal Enrichment
proto-galaxies and IGM

Z of low Z halo stars (Beers & Christlieb 05, Scannapieco et al. 2006)
Z of Lya forest?(Schaye et al. 03 Norman et al. 04)

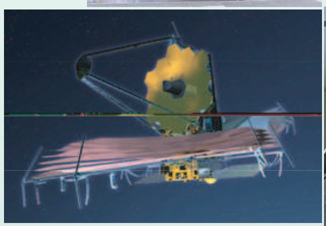

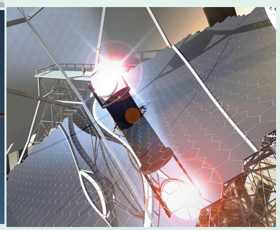

Illumination

NIR bkg. intensity (Santos et al. 02; Fernandez & Komatsu 06)

SN & GRBs?

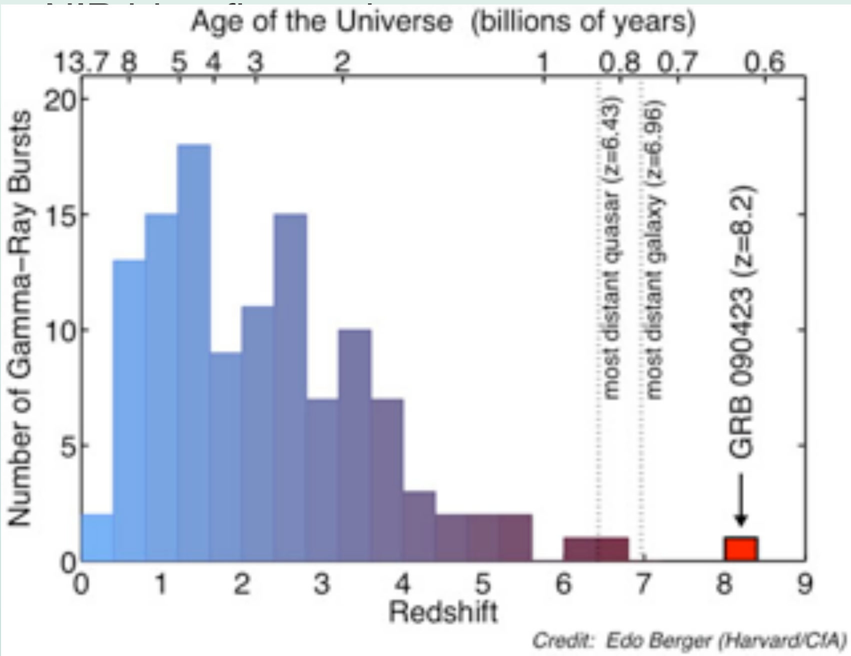

Tanvir, Berger et al. 2009

Progenitors of IMBHs/SMBHs?
Early Galaxies?

Importance of First Stars and their Mass

Observations

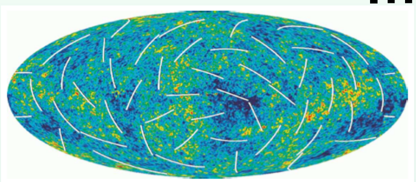

Reionization (H, He)

CMB polarization (WMAP Page et al. 07)
H 21cm (LOFAR Morales & Hewitt 04)

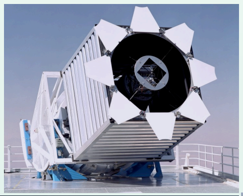

Metal Enrichment

proto-galaxies and IGM

Z of low Z halo stars (Beers & Christlieb 05, Scannapieco et al. 2006)
Z of Lya forest?(Schaye et al. 03 Norman et al. 04)

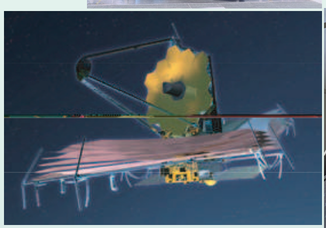

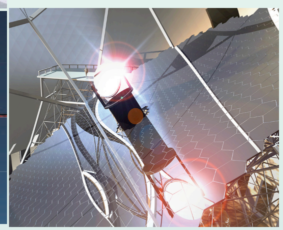

Illumination

NIR bkg. intensity (Santos et al. 02; Fernandez & Komatsu 06)
NIR bkg. fluctuations (Kashlinsky et al. 04)

SN & GRBs?

JWST (Weinmann & Lilly 2005)
SWIFT (Bromm & Loeb 2002)

Progenitors of IMBHs/SMBHs?

Early Galaxies?

ULXs (Mii & Totani 2005)
Quasars (Fan et al. 03; Willott et al. 03)
NIR cts (Stark et al. 07)

Numerical Simulations: Results Abel, Bryan, Norman (2002)

1. Form pre-galactic minihalo $\sim 10^6 M_\odot$

2. Form quasi-hydrostatic gas core inside halo:
$M \approx 4000 M_\odot$, $r \approx 10$ pc,
$n_H \approx 10$ cm^{-3}, $f_{H2} \approx 10^{-3}$,
T~>200K

3. Rapid 3-body H_2 formation at $n_H >\sim 10^{10}$cm^{-3}.
Strong cooling -> supersonic inflow.

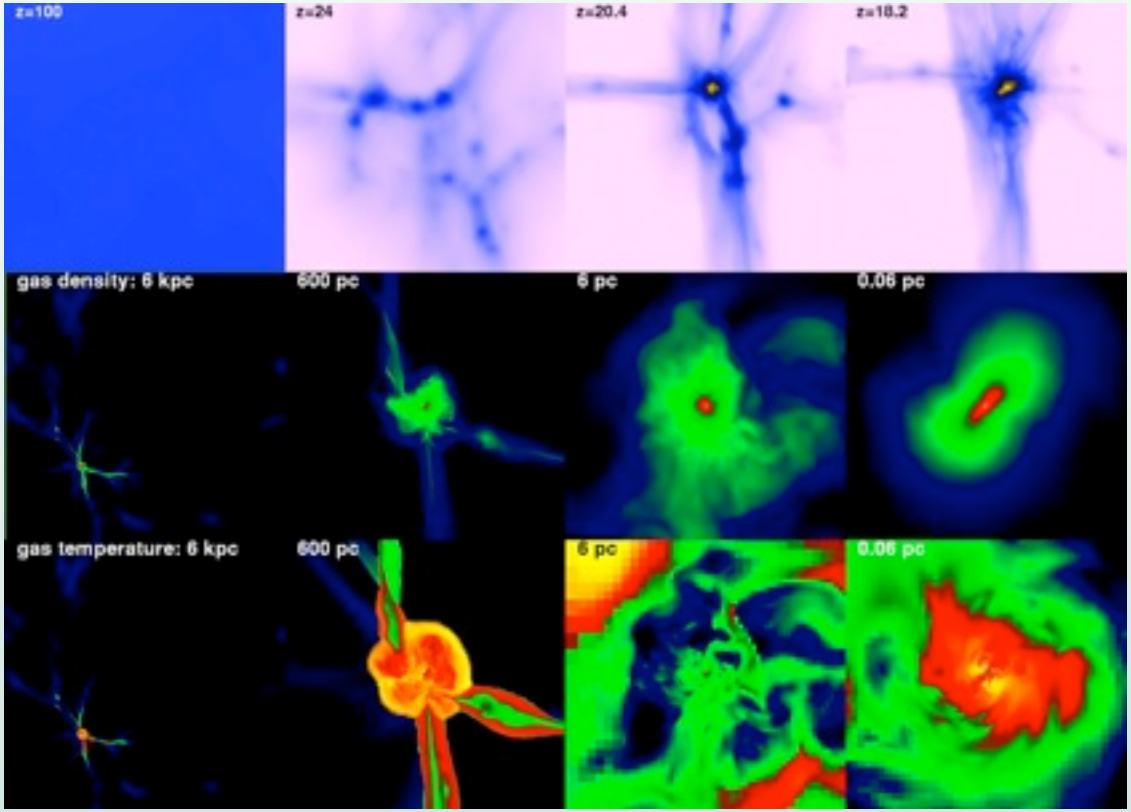

Numerical Simulations: Results Abel, Bryan, Norman (2002)

1. Form pre-galactic minihalo $\sim 10^6 M_\odot$

2. Form quasi-hydrostatic gas core inside halo:
$M \approx 4000 M_\odot$, $r \approx 10$ pc,
$n_H \approx 10$ cm^{-3}, $f_{H2} \approx 10^{-3}$,
$T \sim> 200$K

3. Rapid 3-body H_2 formation at $n_H > \sim 10^{10}$cm^{-3}.
Strong cooling -> supersonic inflow.

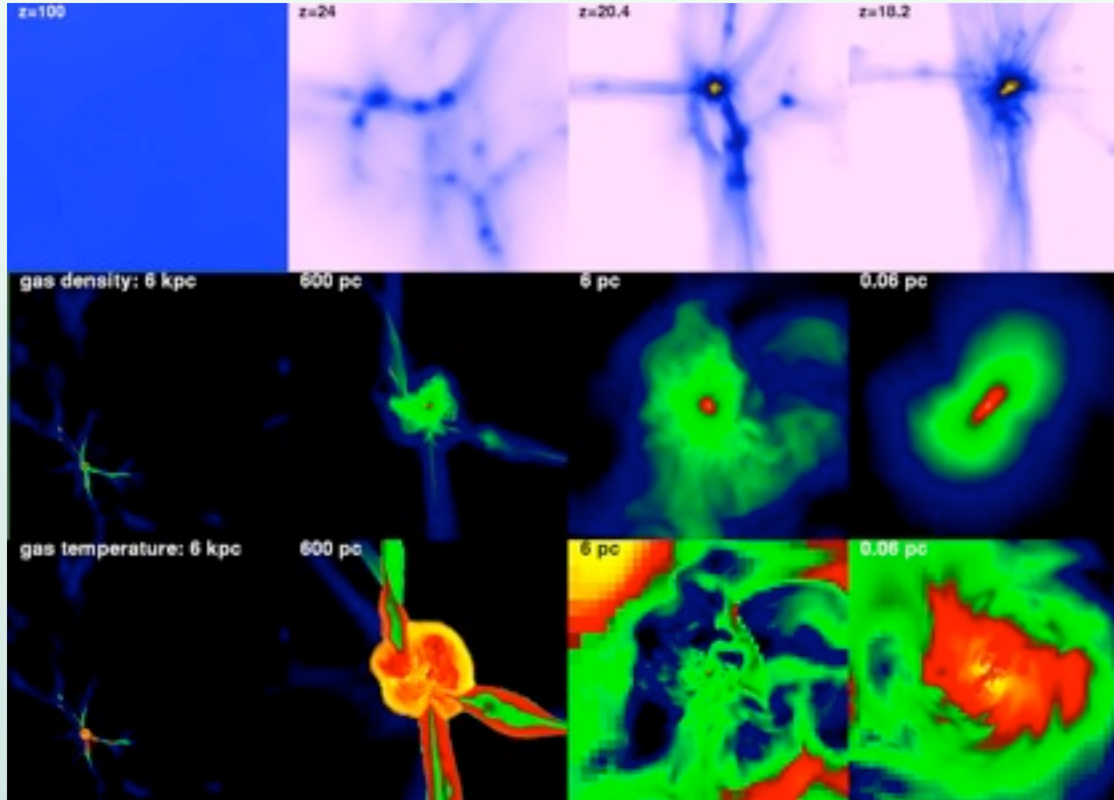

4. 1D simulations (Omukai & Nishi 1998): Form quasi-hydrostatic protostar $n_H \approx 10^{16\text{-}17}$cm^{-3}, $T \approx 2000$ K: optically thick, adiabatic contraction -> hydrostatic core with $m_* \approx 0.005 M_\odot$, $r_* \approx 14 R_\odot$

Numerical Simulations: Results Abel, Bryan, Norman (2002)

1. Form pre-galactic minihalo $\sim 10^6 M_\odot$

2. Form quasi-hydrostatic gas core inside halo:
$M \approx 4000 M_\odot$, $r \approx 10$ pc,
$n_H \approx 10$ cm^{-3}, $f_{H2} \approx 10^{-3}$,
T~>200K

3. Rapid 3-body H_2 formation at $n_H > \sim 10^{10}$cm^{-3}.
Strong cooling -> supersonic inflow.

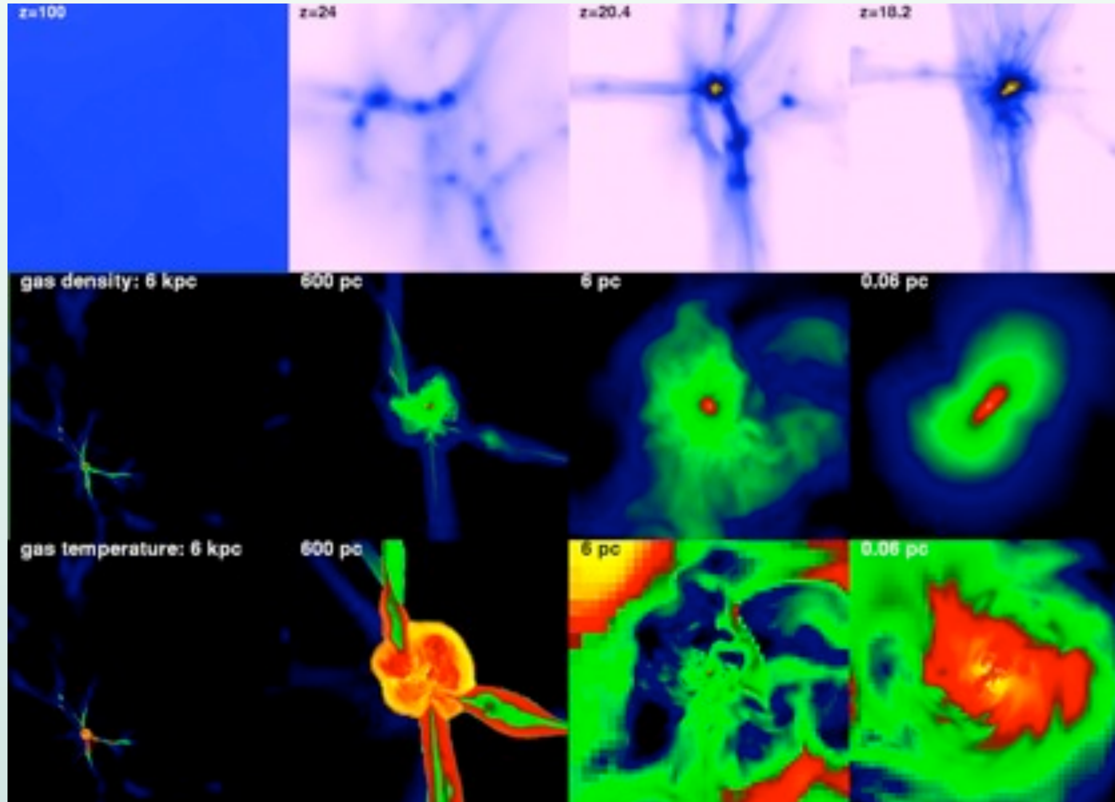

4. 1D simulations (Omukai & Nishi 1998): Form quasi-hydrostatic protostar $n_H \approx 10^{16-17}$cm^{-3}, T $\approx$2000 K: optically thick, adiabatic contraction -> hydrostatic core with $m_* \approx 0.005 M_\odot$, $r_* \approx 14 R_\odot$

More recent 3D sims. of Turk, Yoshida, Abel, Bromm, Norman etc. reach ~stellar densities, but then grind to a halt (small dynamical timescales), still at small (<<sub-solar) protostellar masses. We turn to analytic models... when does accretion stop? $100 M_\odot$??

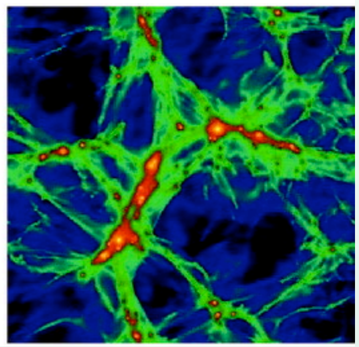

Definitions

McKee & Tan (2008); O'Shea et al. (2008; First Stars III Conference Summary)

Population III
Stars having a metallicity so low ($Z<Z_{crit}$) it has no effect on their formation (i.e. negligible cooling) or their evolution.

Population III.1
The initial conditions for the formation of Population III.1 stars (halos) are determined solely by cosmological fluctuations.

Population III.2
The initial conditions for the formation of Population III.2 stars (halos) are significantly affected by other astrophysical sources (external to their halo).

Physical Processes in Pop III.1 star formation

Accretion Rate $\dot{m}_* = 0.026 K'^{15/7} (m_*/M_\odot)^{-3/7} M_\odot yr^{-1}$ (Tan & McKee 2004)

Initial Conditions

polytropic structure: $P = K\rho^\gamma$

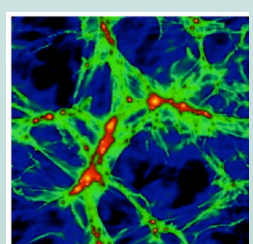

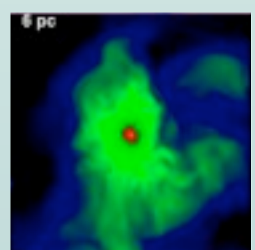

(Abel ea, Bromm ea, Yoshida ea, Omukai ea.)

Initial conditions: Entropy and Rotation

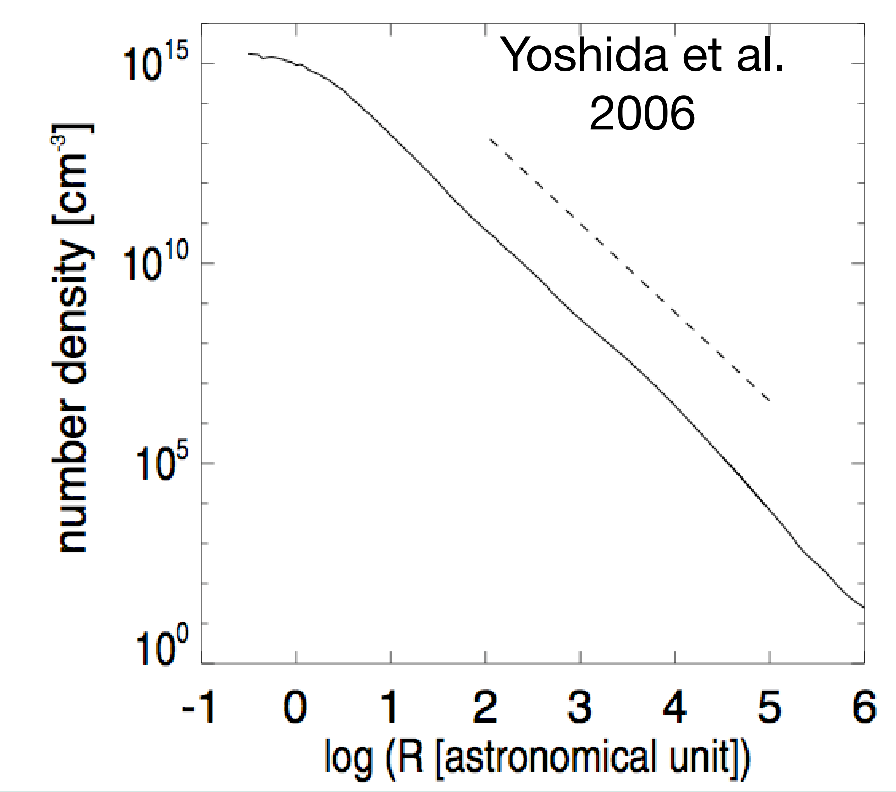

Density structure: self-similar,

$\rho \propto r^{-k}$ k≈2.2

~singular polytropic sphere in virial and hydrostatic equilibrium

Model with $P = K\rho^{\gamma}$ γ=1.1

Initial conditions: Entropy and Rotation

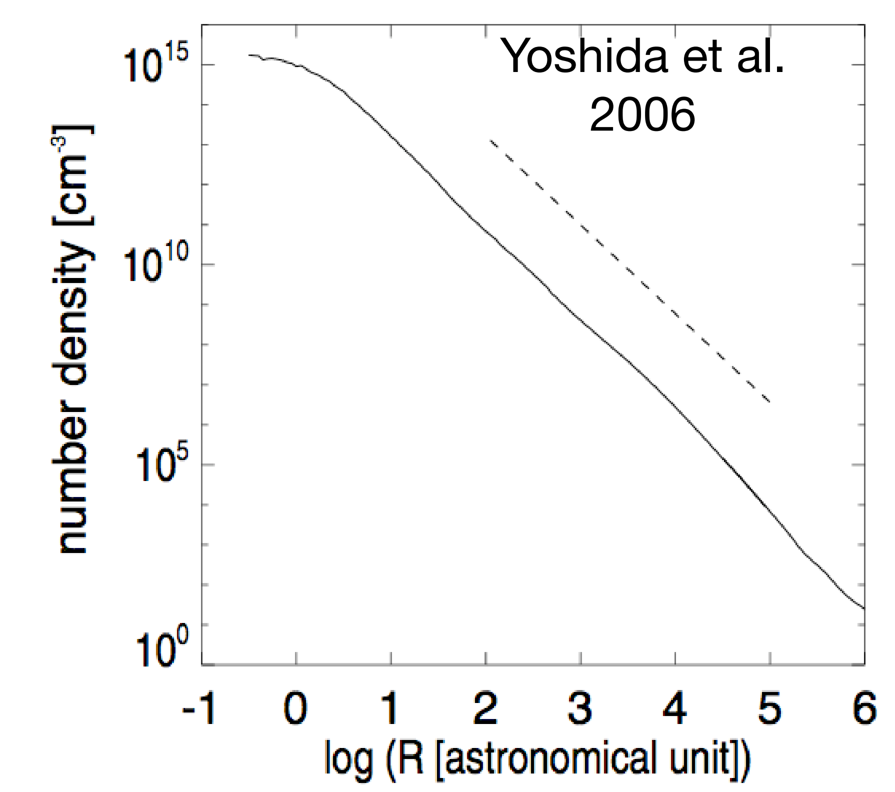

Density structure: self-similar,

$\rho \propto r^{-k}$ k≈2.2

~singular polytropic sphere in virial and hydrostatic equilibrium

Model with $P = K\rho^{\gamma}$ γ=1.1

H_2 cooling ->

T_{min} ~ 200 K, n_{crit} ~ 10^4 cm^{-3}

$$K = 1.9 \times 10^{12}(T/300K)(n_H/10^4 cm^{-3})^{-0.1} cgs$$

$$K' \equiv K/1.9 \times 10^{12} cgs$$

Initial conditions: Entropy and Rotation

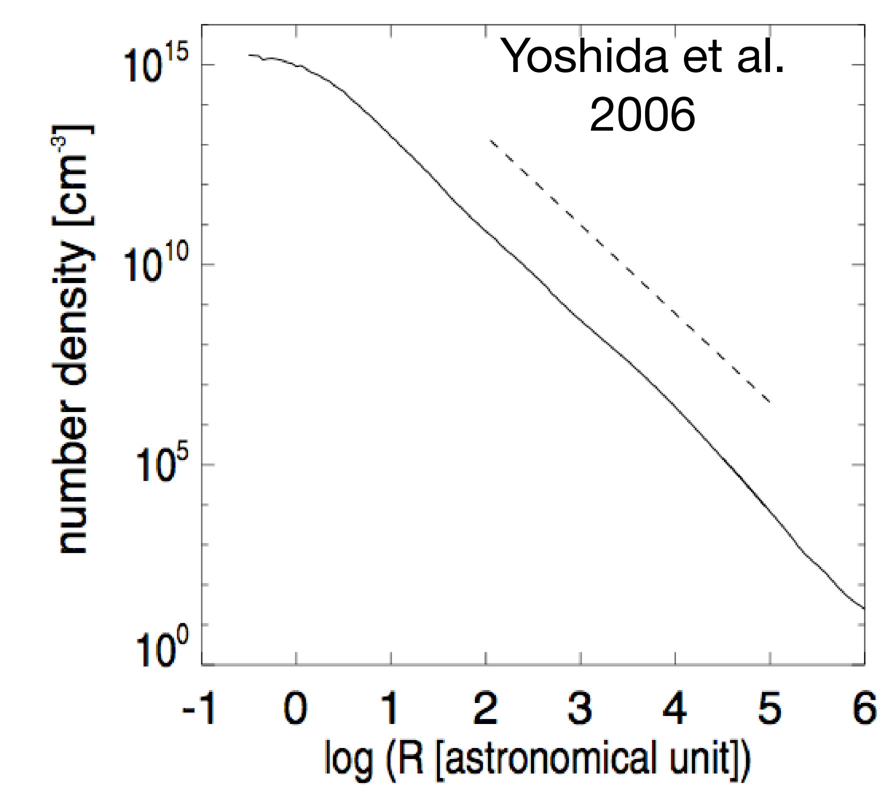

Density structure: self-similar,

$\rho \propto r^{-k}$ k≈2.2

~singular polytropic sphere in virial and hydrostatic equilibrium

Model with $P = K\rho^{\gamma}$ γ=1.1

H_2 cooling ->

T_{min} ~ 200 K, n_{crit} ~ 10^4 cm^{-3}

$$K = 1.9 \times 10^{12} (T/300K)(n_H/10^4 cm^{-3})^{-0.1} cgs$$

$$K' \equiv K/1.9 \times 10^{12} cgs$$

Resulting accretion rate

$$\dot{m}_* = 0.026 K'^{15/7} (m_*/M_\odot)^{-3/7} M_\odot yr^{-1}$$

Physical Processes in Pop III.1 star formation

Accretion Rate $\dot{m}_* = 0.026K'^{15/7}(m_*/M_\odot)^{-3/7}M_\odot yr^{-1}$ (Tan & McKee 2004)

Initial Conditions

polytropic structure: $P = K\rho^\gamma$

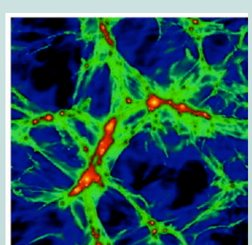

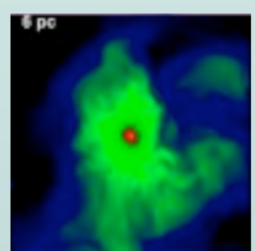

(Abel ea, Bromm ea, Yoshida ea, Omukai ea.)

Physical Processes in Pop III.1 star formation

Dark Matter Annihilation Heating? (Spolyar et al. 2008; Natarajan, Tan, O'Shea 2009)

Accretion Rate $\dot{m}_* = 0.026 K'^{15/7} (m_*/M_\odot)^{-3/7} M_\odot yr^{-1}$ (Tan & McKee 2004)

Initial Conditions

polytropic structure: $P = K\rho^\gamma$

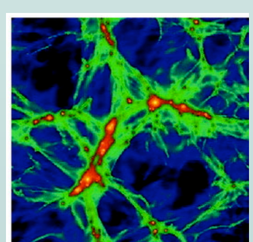

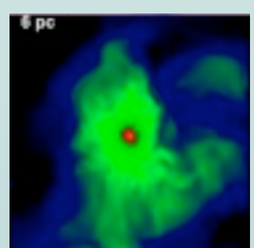

(Abel ea, Bromm ea, Yoshida ea, Omukai ea.)

Physical Processes in Pop III.1 star formation

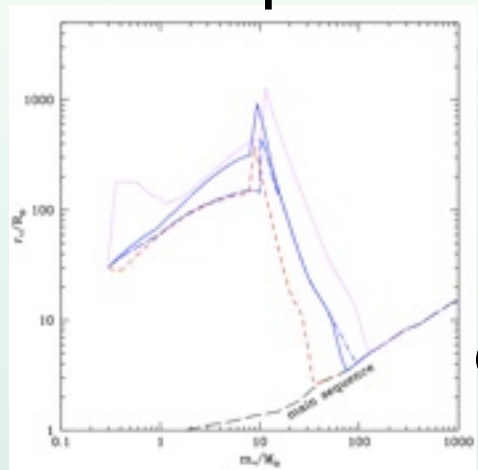

Radiative Feedback (McKee & Tan 2008)

Protostellar Evolution (Omukai & Palla 2003; Tan & McKee 2004)

Magnetic Field Generation?

$$r_d = 3.44 \left(\frac{f_{\rm Kep}}{0.5}\right)^2 \epsilon_{*d}^{-9/7} \left(\frac{m_{*d}}{M_\odot}\right)^{9/7} K'^{-10/7}\ \mathrm{AU}.$$

Rotation & Disk Structure; Fragmentation? (Tan & Blackman 2004)

Dark Matter Annihilation Heating? (Spolyar et al. 2008; Natarajan, Tan, O'Shea 2009)

Accretion Rate $\dot{m}_* = 0.026 K'^{15/7} (m_*/M_\odot)^{-3/7} M_\odot yr^{-1}$ (Tan & McKee 2004)

Initial Conditions

polytropic structure: $P = K\rho^\gamma$

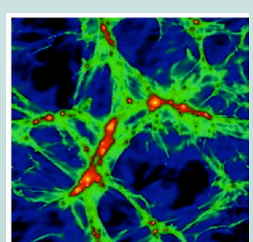

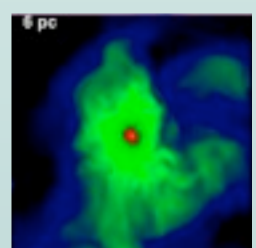

(Abel ea, Bromm ea, Yoshida ea, Omukai ea.)

Physical Processes in Pop III.1 star formation

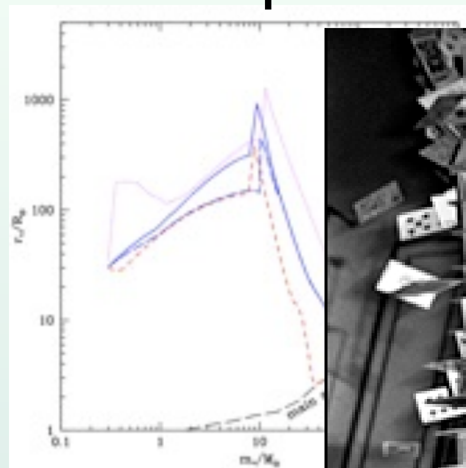

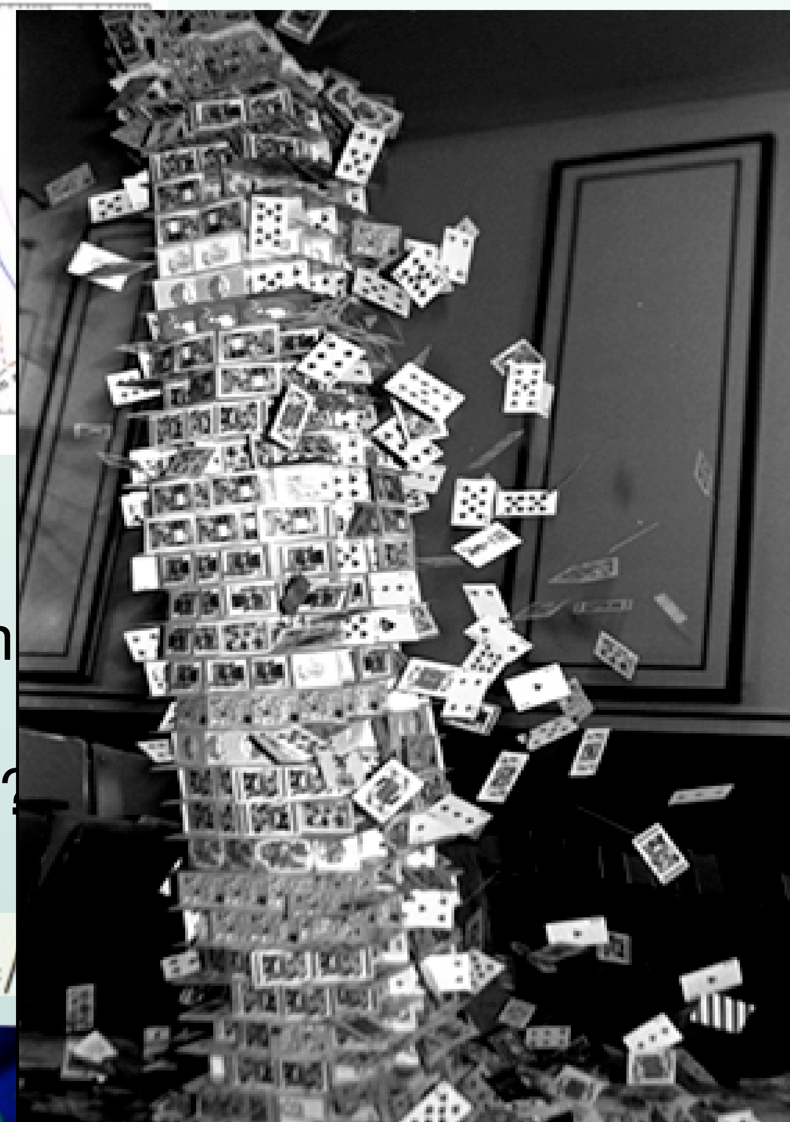

Radiative Feedback

Protostellar Evolution

Magnetic Field Generation?

$$r_d = 3.44 \left(\frac{f_{\rm Kep}}{0.5}\right)^2 \epsilon_{*d}^{-9/7} \left(\frac{m_{*d}}{M_\odot}\right)^{9/7} K'^{-10/7}\ \mathrm{AU}.$$

Rotation & Disk Structure; Fragm

Dark Matter Annihilation Heating?

Accretion Rate $\dot{m}_* = 0.026 K'^{15/7} (m_*/$

Initial Conditions

polytropic structure: $P = K\rho^\gamma$

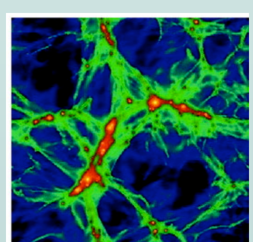

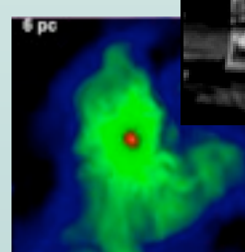

Physical Processes in Pop III.1 star formation

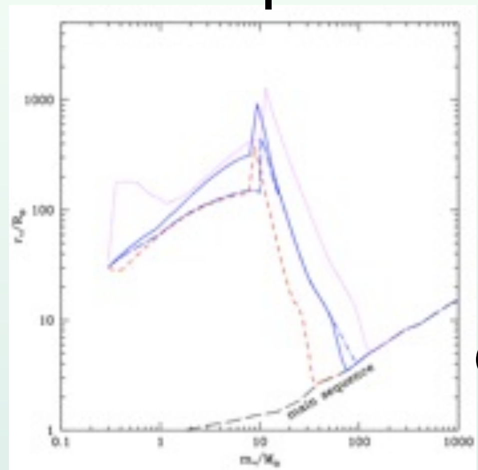

Radiative Feedback (McKee & Tan 2008)

Protostellar Evolution (Omukai & Palla 2003; Tan & McKee 2004)

Magnetic Field Generation?

$$r_d = 3.44 \left(\frac{f_{\rm Kep}}{0.5}\right)^2 \epsilon_{*d}^{-9/7} \left(\frac{m_{*d}}{M_\odot}\right)^{9/7} K'^{-10/7}\ {\rm AU}.$$

Rotation & Disk Structure; Fragmentation? (Tan & Blackman 2004)

Dark Matter Annihilation Heating? (Spolyar et al. 2008; Natarajan, Tan, O'Shea 2009)

Accretion Rate $\dot{m}_* = 0.026 K'^{15/7} (m_*/M_\odot)^{-3/7} M_\odot yr^{-1}$ (Tan & McKee 2004)

Initial Conditions

polytropic structure: $P = K\rho^\gamma$

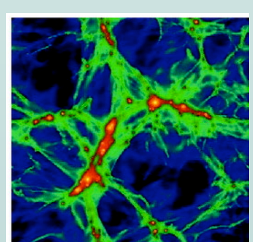

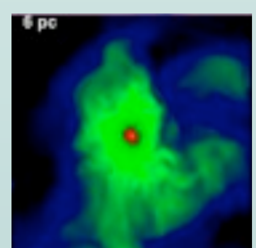

(Abel ea, Bromm ea, Yoshida ea, Omukai ea.)

Physical Processes in Pop III.1 star formation

Stellar Evolution $t_{ms} \simeq 2.7 m_{*,2}^{-0.24}\, Myr \rightarrow m_{*,max} \simeq 1900 K'^{1.28} M_{\odot}$

Schaerer 2002

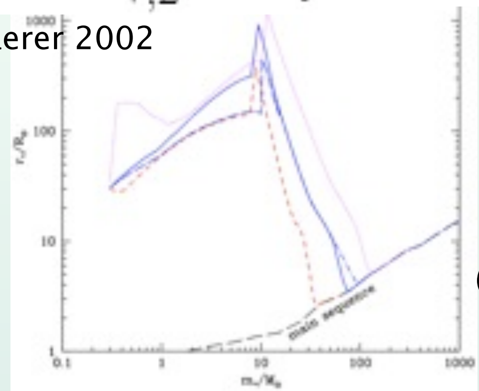

Radiative Feedback (McKee & Tan 2008)

Protostellar Evolution (Omukai & Palla 2003; Tan & McKee 2004)

Magnetic Field Generation?

$$r_d = 3.44 \left(\frac{f_{\rm Kep}}{0.5}\right)^2 \epsilon_{*d}^{-9/7} \left(\frac{m_{*d}}{M_{\odot}}\right)^{9/7} K'^{-10/7}\ {\rm AU.}$$

Rotation & Disk Structure; Fragmentation? (Tan & Blackman 2004)

~~Dark Matter Annihilation Heating?~~ (Spolyar et al. 2008; Natarajan, Tan, O'Shea 2009)

Accretion Rate $\dot{m}_* = 0.026 K'^{15/7} (m_*/M_{\odot})^{-3/7} M_{\odot} yr^{-1}$ (Tan & McKee 2004)

Initial Conditions

polytropic structure: $P = K\rho^{\gamma}$

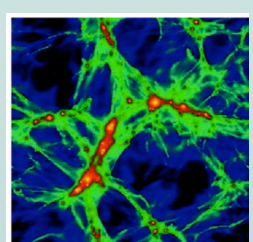

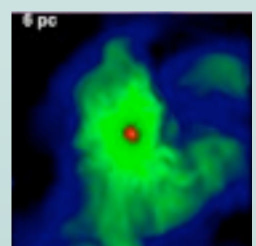

(Abel ea, Bromm ea, Yoshida ea, Omukai ea.)

Collapse to a disk around a central protostar

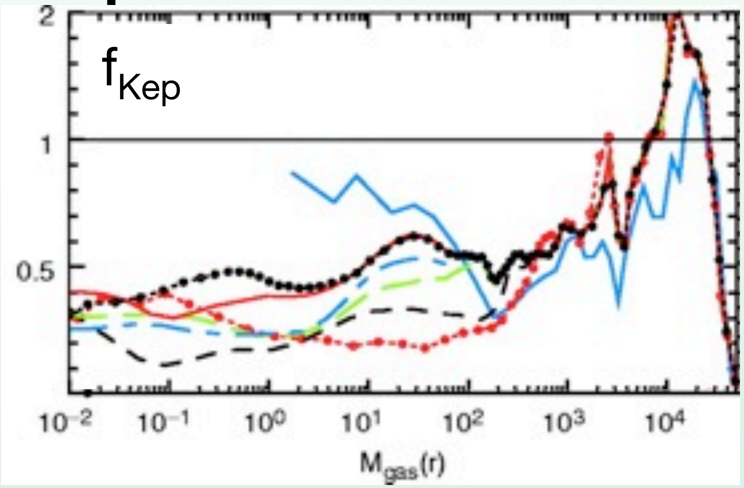

Rotation: core forms from mergers and collapse along filaments: expect J>0

$f_{Kep} \equiv v_{circ} / v_{Kep} \sim 0.5$

$$r_d = f_{Kep}^2 r_0 \rightarrow 3.4(M/M_\odot)^{9/7} AU$$

Collapse to a disk around a central protostar

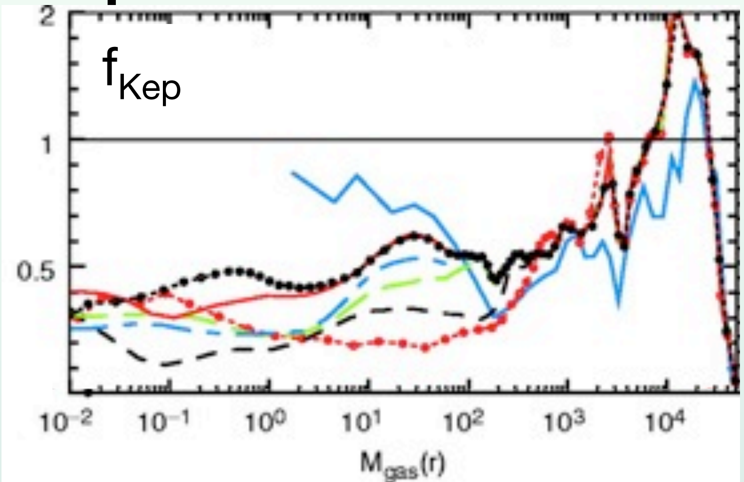

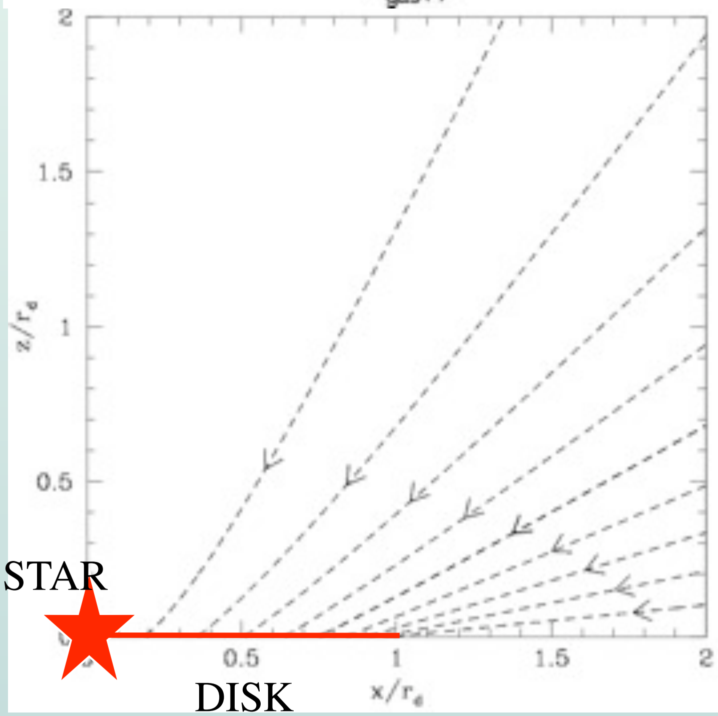

Rotation: core forms from mergers and collapse along filaments: expect J>0

$f_{Kep} \equiv v_{circ} / v_{Kep} \sim 0.5$

$$r_d = f_{Kep}^2 r_0 \rightarrow 3.4(M/M_\odot)^{9/7} AU$$

Collapse to a disk around a central protostar

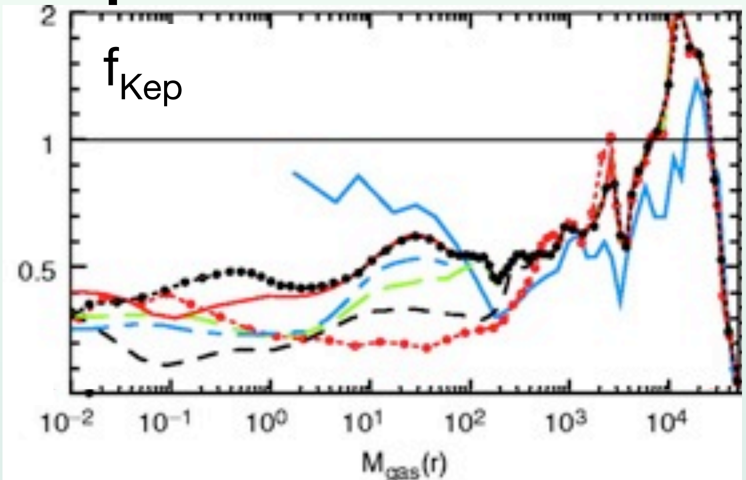

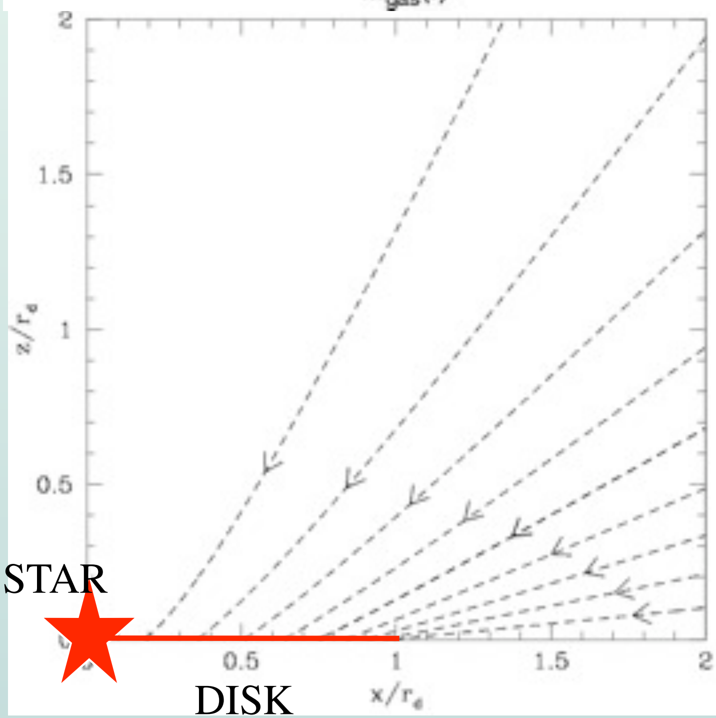

Rotation: core forms from mergers and collapse along filaments: expect J>0

$f_{Kep} \equiv v_{circ} / v_{Kep} \sim 0.5$

$$r_d = f_{Kep}^2 r_0 \rightarrow 3.4(M/M_\odot)^{9/7} AU$$

Expect accretion within the disk is driven by large scale gravitational instabilities and local gravitational viscosity (Gammie 2001).

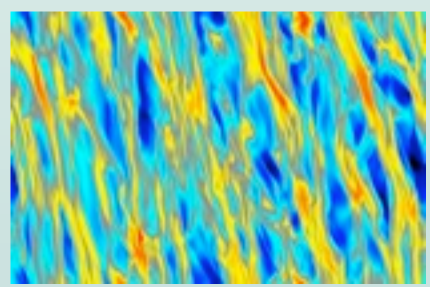

viscosity

$\nu = \alpha\, c_s\, h$,

$\alpha < 0.3$

Collapse to a disk around a central protostar

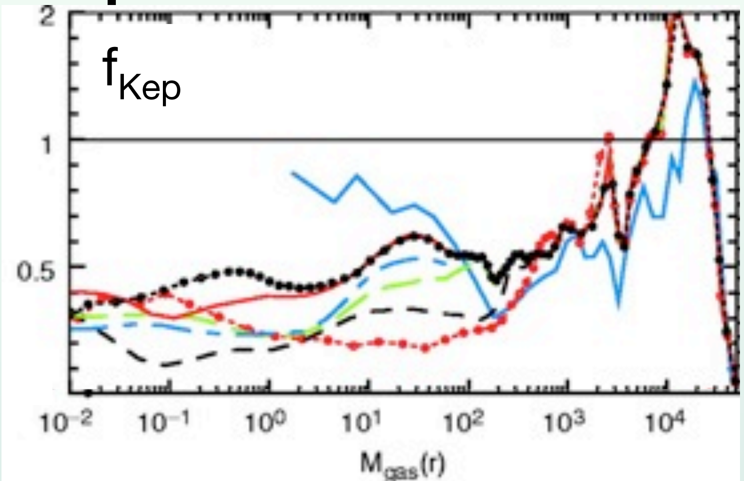

Rotation: core forms from mergers and collapse along filaments: expect J>0

$f_{Kep} \equiv v_{circ} / v_{Kep} \sim 0.5$

$$r_d = f_{Kep}^2 r_0 \rightarrow 3.4(M/M_\odot)^{9/7} AU$$

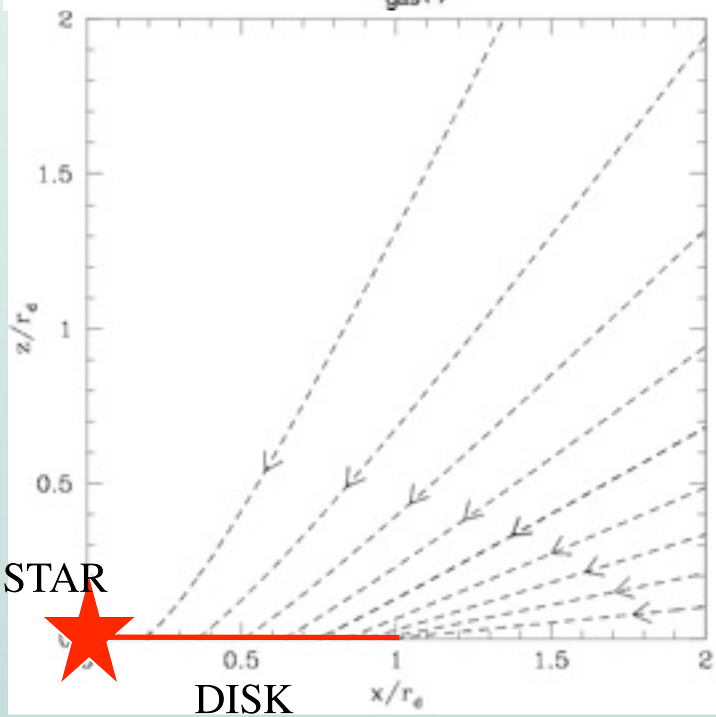

Expect accretion within the disk is driven by large scale gravitational instabilities and local gravitational viscosity (Gammie 2001).

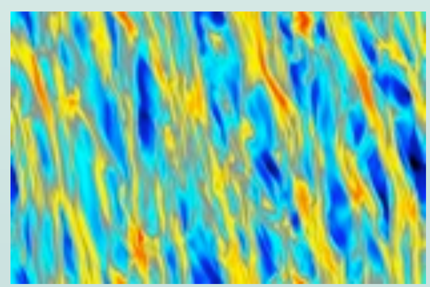

viscosity

$\nu = \alpha\, c_s\, h$,

$\alpha < 0.3$

We now construct simple models for the protostar and disk

Collapse to a disk around a central protostar

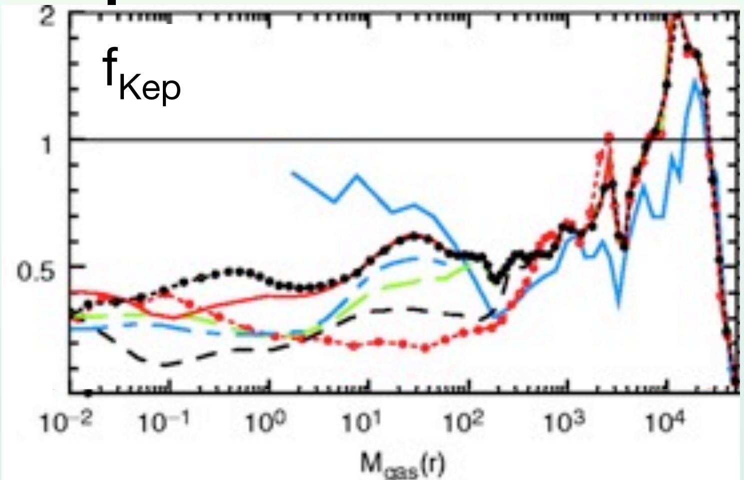

Rotation: core forms from mergers and collapse along filaments: expect J>0

$f_{Kep} \equiv v_{circ} / v_{Kep} \sim 0.5$

$$r_d = f_{Kep}^2 r_0 \rightarrow 3.4(M/M_\odot)^{9/7} AU$$

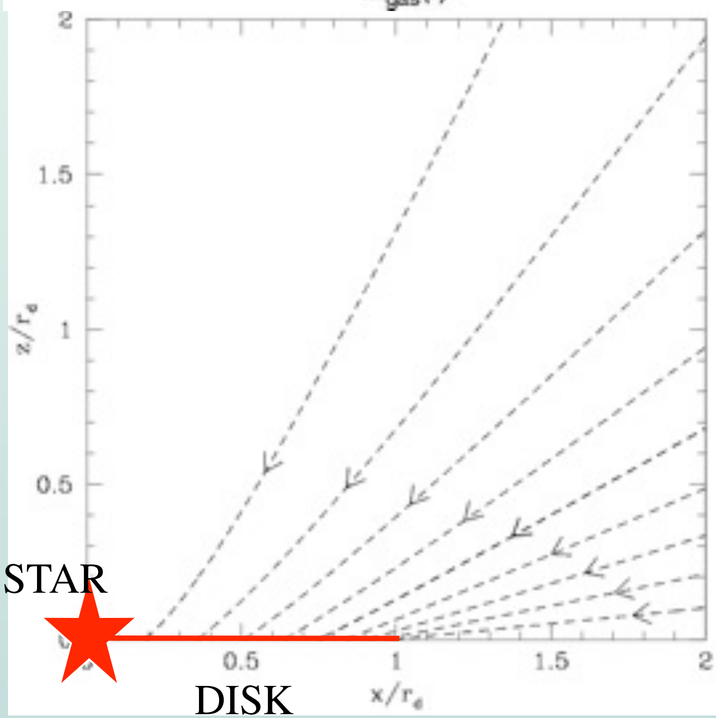

Expect accretion within the disk is driven by large scale gravitational instabilities and local gravitational viscosity (Gammie 2001).

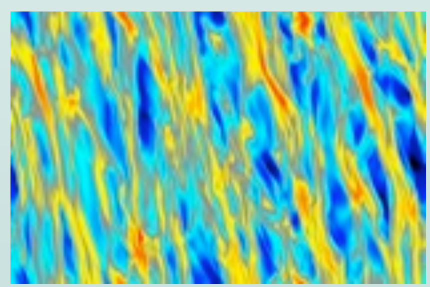

viscosity

$\nu = \alpha\, c_s\, h,$

$\alpha < 0.3$

We now construct simple models for the protostar and disk [Toomre stable]

Evolution of the Protostar depends on Accretion Rate

(Stahler et al. 1980; Palla & Stahler 1991; Nakano 1995; Omukai & Palla 2003; Tan & McKee 2004; Hosokawa & Omukai 2009; Ohkubo et al. 2009)

Assume polytropic stellar structure and continuous sequence of equilibria

One zone model: follow energy of protostar as it accretes

$$E = -\frac{a_g \beta}{2}\frac{G m_*^2}{r_*} + m_* \bar{\varepsilon}_I$$

$$\frac{dE}{dt} = \dot{m}_* < w > - L + \dot{E}_{nuc}$$

$$< w > \equiv \frac{5}{3}\varepsilon_{th} + \varepsilon_I - \frac{1}{2}(1 - f_k) v_{ff}^2$$

Evolution of the Protostar depends on Accretion Rate

(Stahler et al. 1980; Palla & Stahler 1991; Nakano 1995; Omukai & Palla 2003; Tan & McKee 2004; Hosokawa & Omukai 2009; Ohkubo et al. 2009)

Assume polytropic stellar structure and continuous sequence of equilibria

One zone model: follow energy of protostar as it accretes

$$E = -\frac{a_g \beta}{2}\frac{G m_*^2}{r_*} + m_* \bar{\varepsilon}_I$$

$$\frac{dE}{dt} = \dot{m}_* < w > - L + \dot{E}_{nuc}$$

$$< w > \equiv \frac{5}{3}\varepsilon_{th} + \varepsilon_I - \frac{1}{2}(1 - f_k) v_{ff}^2$$

Deuterium burning for $T_c > 10^6$ K

Structural rearrangement after t_{Kelvin}

Eddington model for β

Solve for $r_*(m_*)$, until reach main sequence

Evolution of the Protostar depends on Accretion Rate

(Stahler et al. 1980; Palla & Stahler 1991; Nakano 1995; Omukai & Palla 2003; Tan & McKee 2004; Hosokawa & Omukai 2009; Ohkubo et al. 2009)

Assume polytropic stellar structure and continuous sequence of equilibria

One zone model: follow energy of protostar as it accretes

$$E = -\frac{a_g \beta}{2} \frac{G m_*^2}{r_*} + m_* \bar{\varepsilon}_I \qquad \frac{dE}{dt} = \dot{m}_* < w > -L + \dot{E}_{nuc}$$

$$< w > \equiv \frac{5}{3}\varepsilon_{th} + \varepsilon_I - \frac{1}{2}(1 - f_k) v_{ff}^2$$

Deuterium burning for $T_c > 10^6$K

Structural rearrangement after t_{Kelvin}

Eddington model for β

Solve for $r_*(m_*)$, until reach main sequence

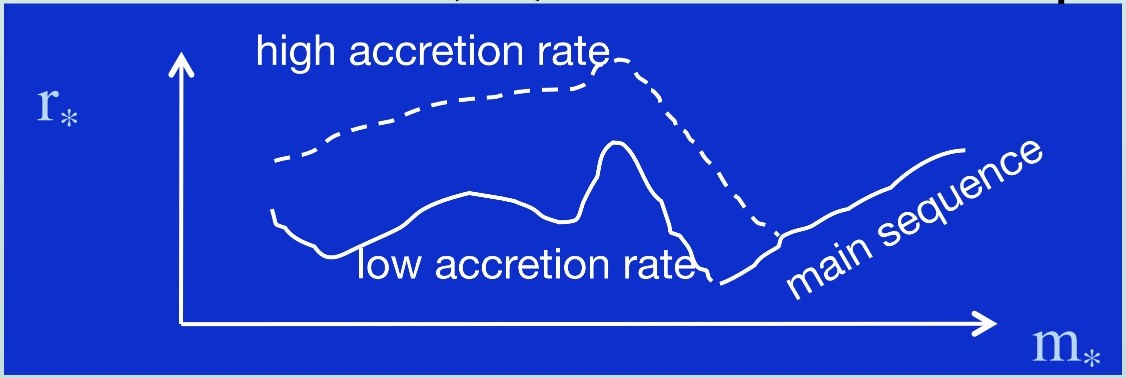

Evolution of the Protostar depends on Accretion Rate

(Stahler et al. 1980; Palla & Stahler 1991; Nakano 1995; Omukai & Palla 2003; Tan & McKee 2004; Hosokawa & Omukai 2009; Ohkubo et al. 2009)

Assume polytropic stellar structure and continuous sequence of equilibria

One zone model: follow energy of protostar as it accretes

$$E = -\frac{a_g \beta}{2}\frac{Gm_*^2}{r_*} + m_* \bar{\varepsilon}_I \qquad \frac{dE}{dt} = \dot{m}_* < w > -L + \dot{E}_{nuc}$$

$$< w > \equiv \frac{5}{3}\varepsilon_{th} + \varepsilon_I - \frac{1}{2}(1 - f_k) v_{ff}^2$$

Deuterium burning for $T_c > 10^6$K

Structural rearrangement after t_{Kelvin}

Eddington model for β

Solve for $r_*(m_*)$, until reach main sequence

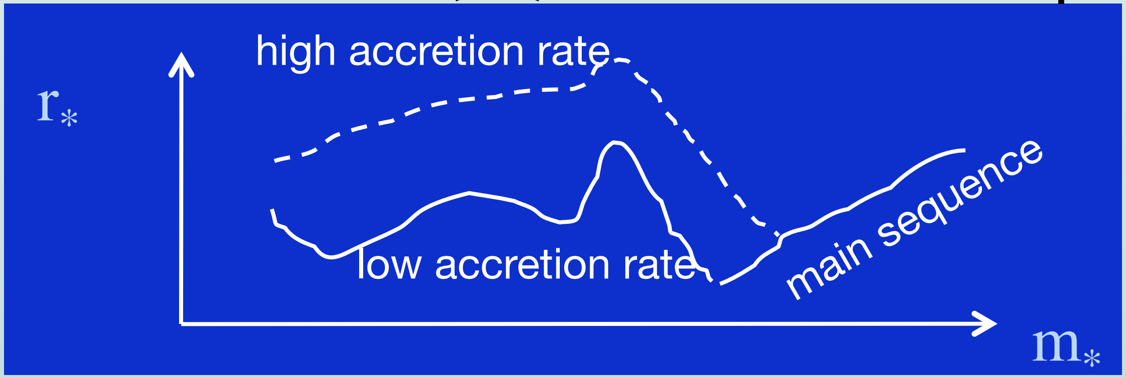

Here we assume dark matter annihilation heating is negligible

Protostar Evolution: Ionizing Luminosity

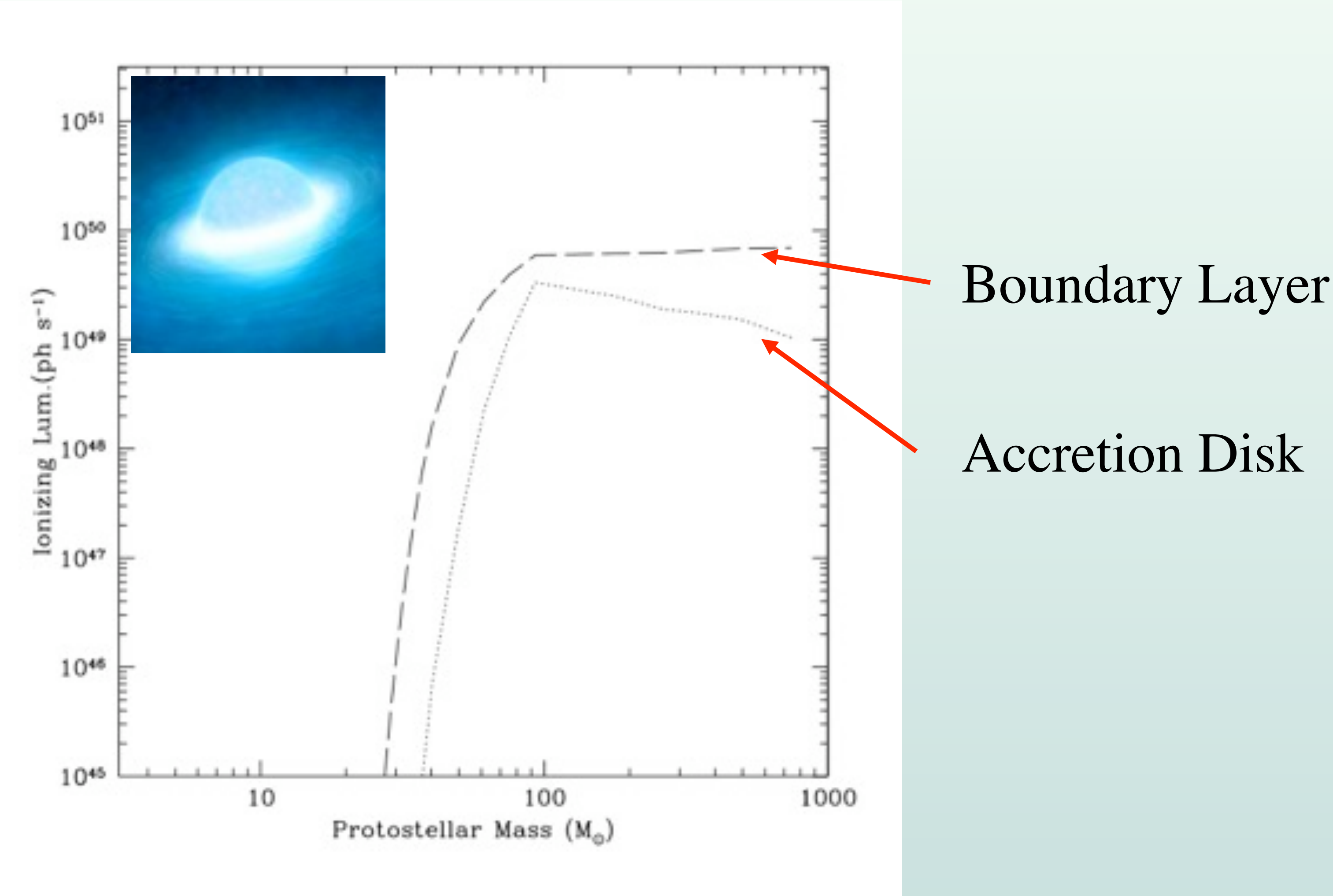

Protostar Evolution: Ionizing Luminosity

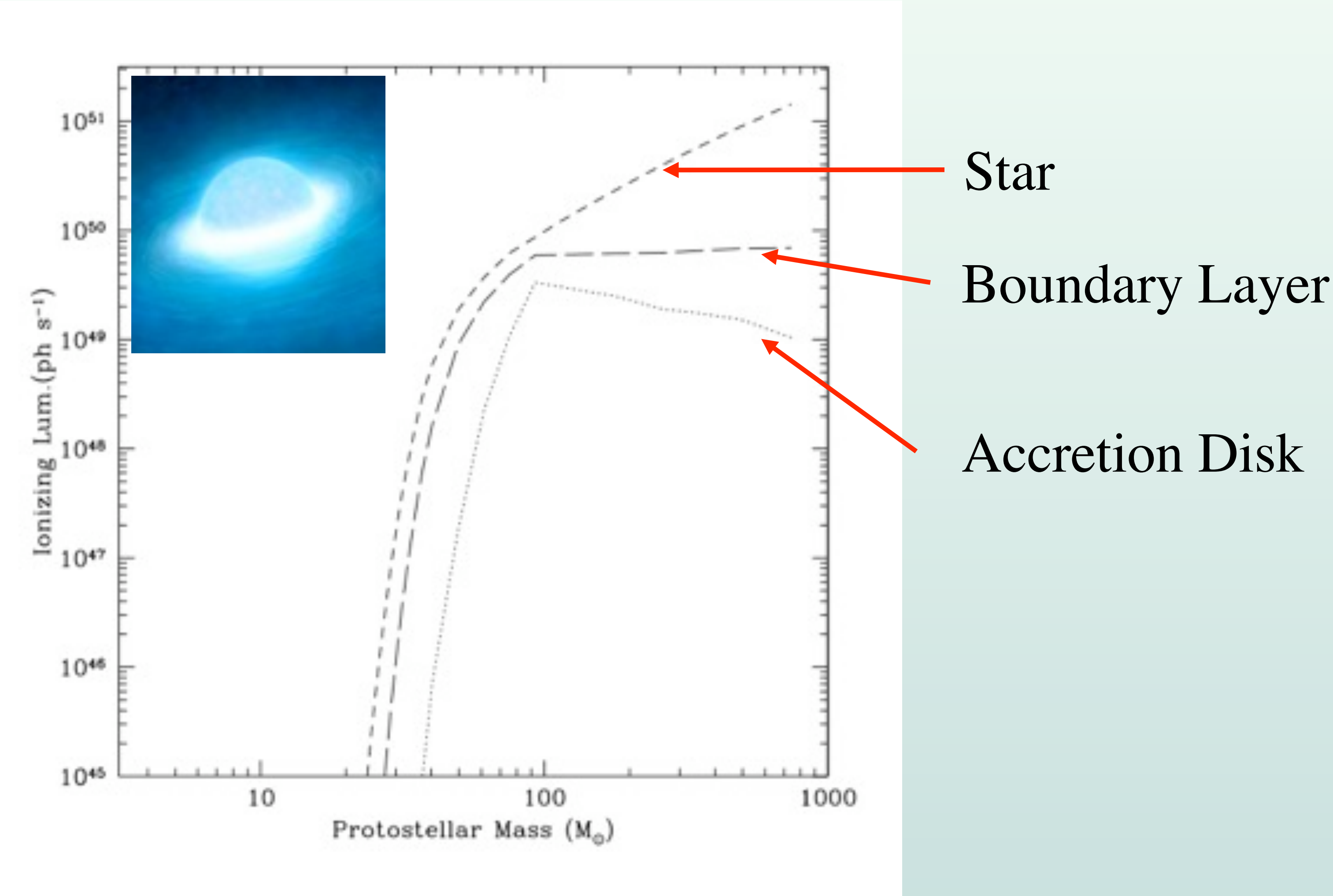

Protostar Evolution: Ionizing Luminosity

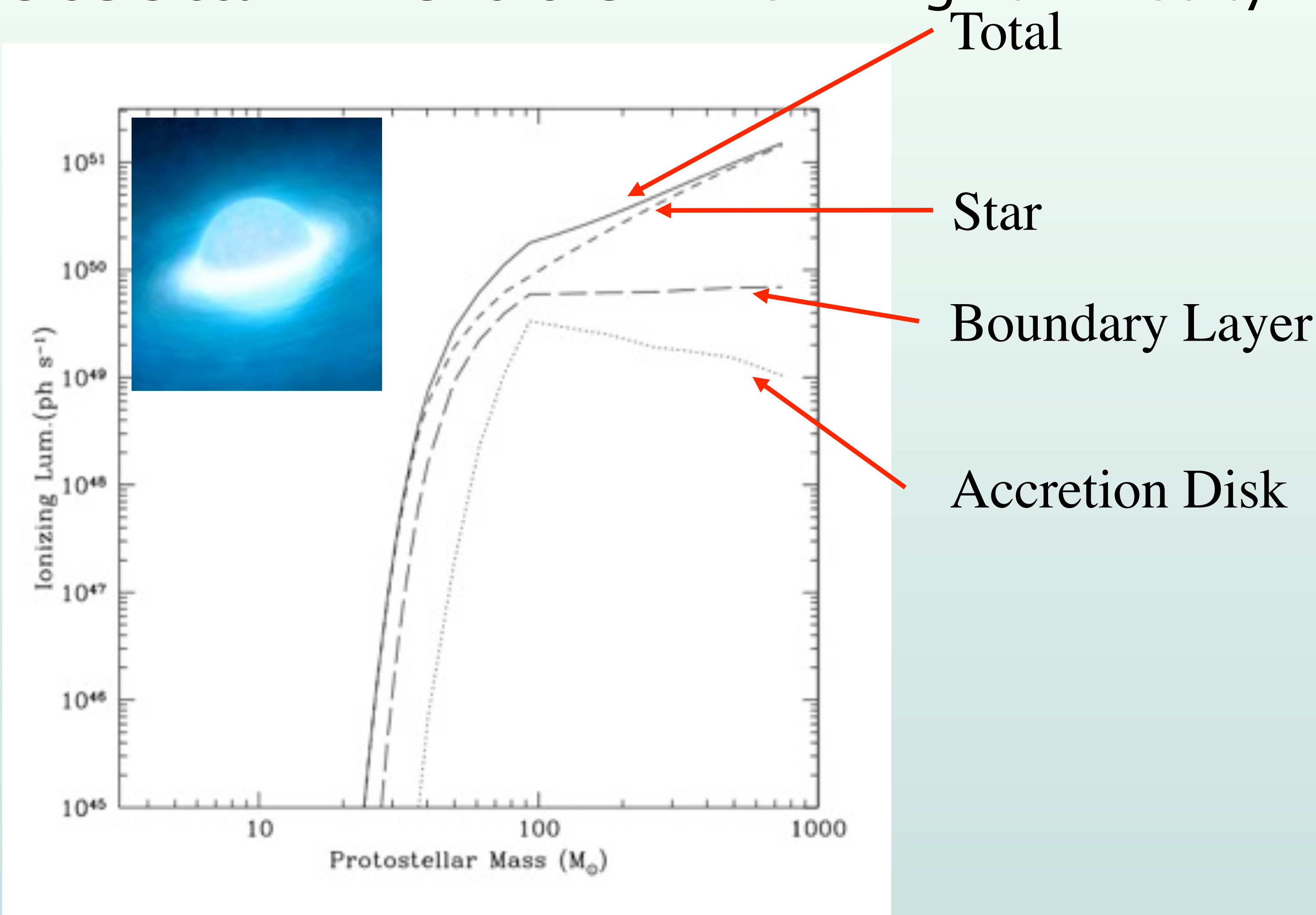

Protostar Evolution: Ionizing Luminosity

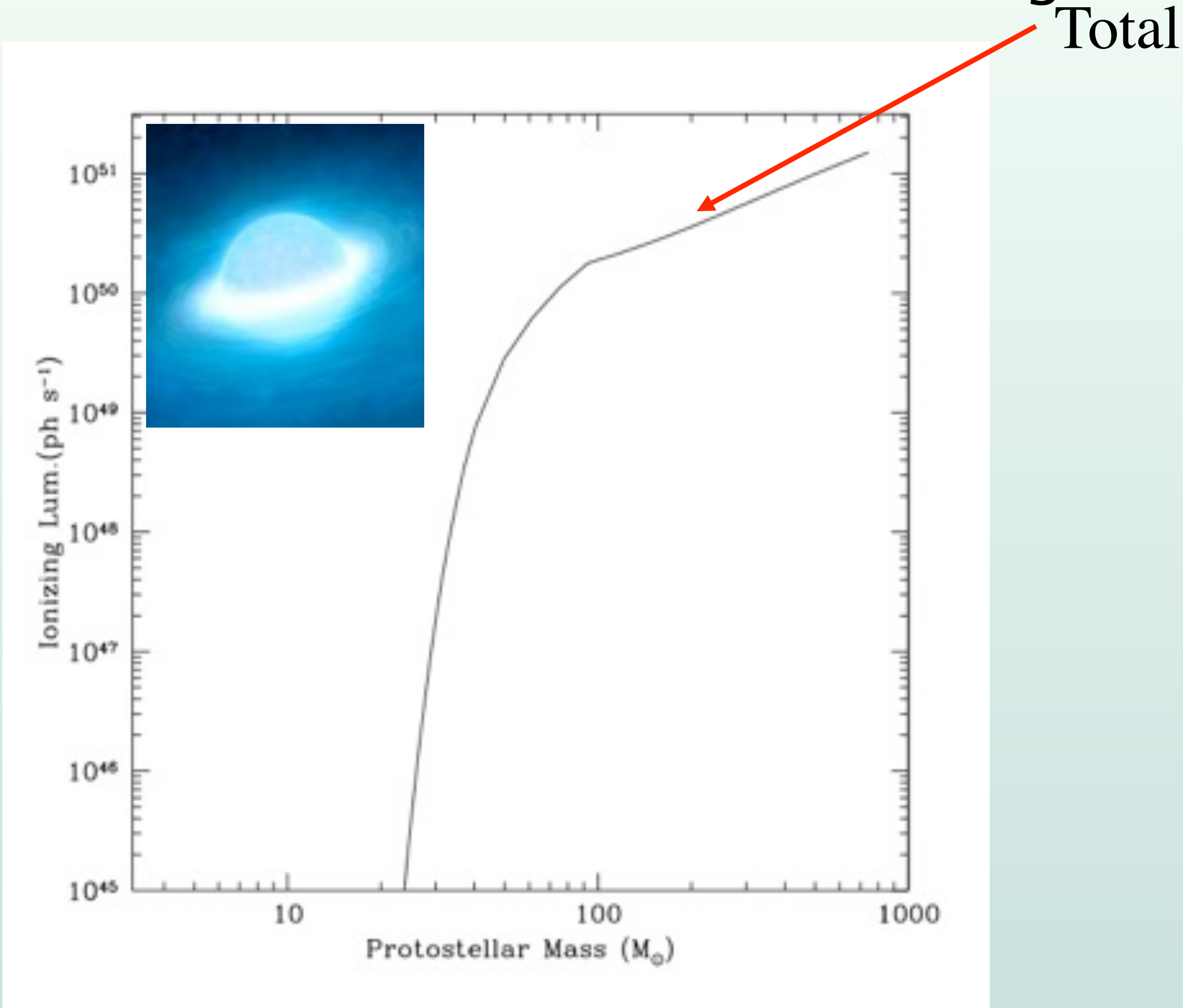

Protostar Evolution: Ionizing Luminosity

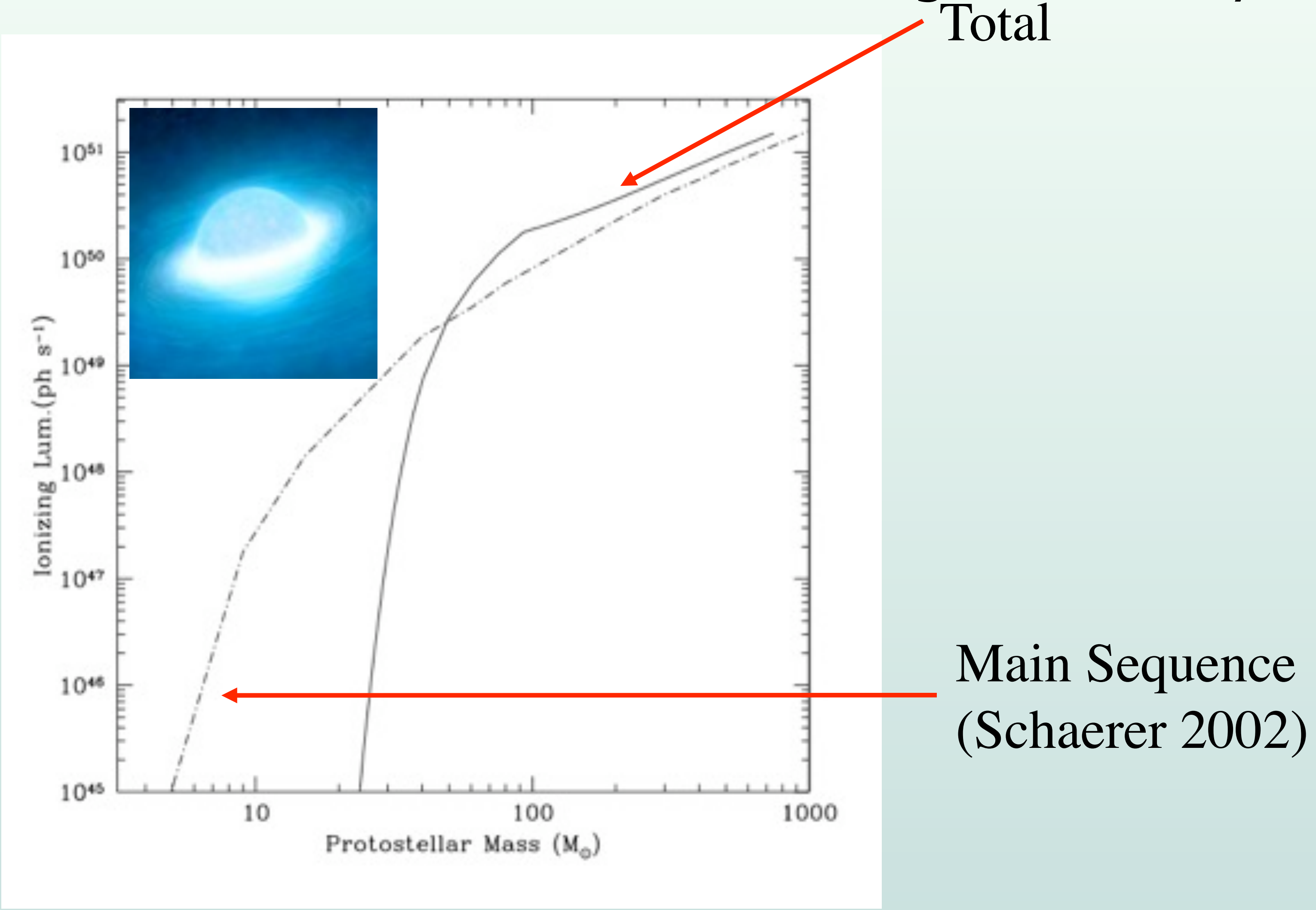

Protostar Evolution: Ionizing Luminosity

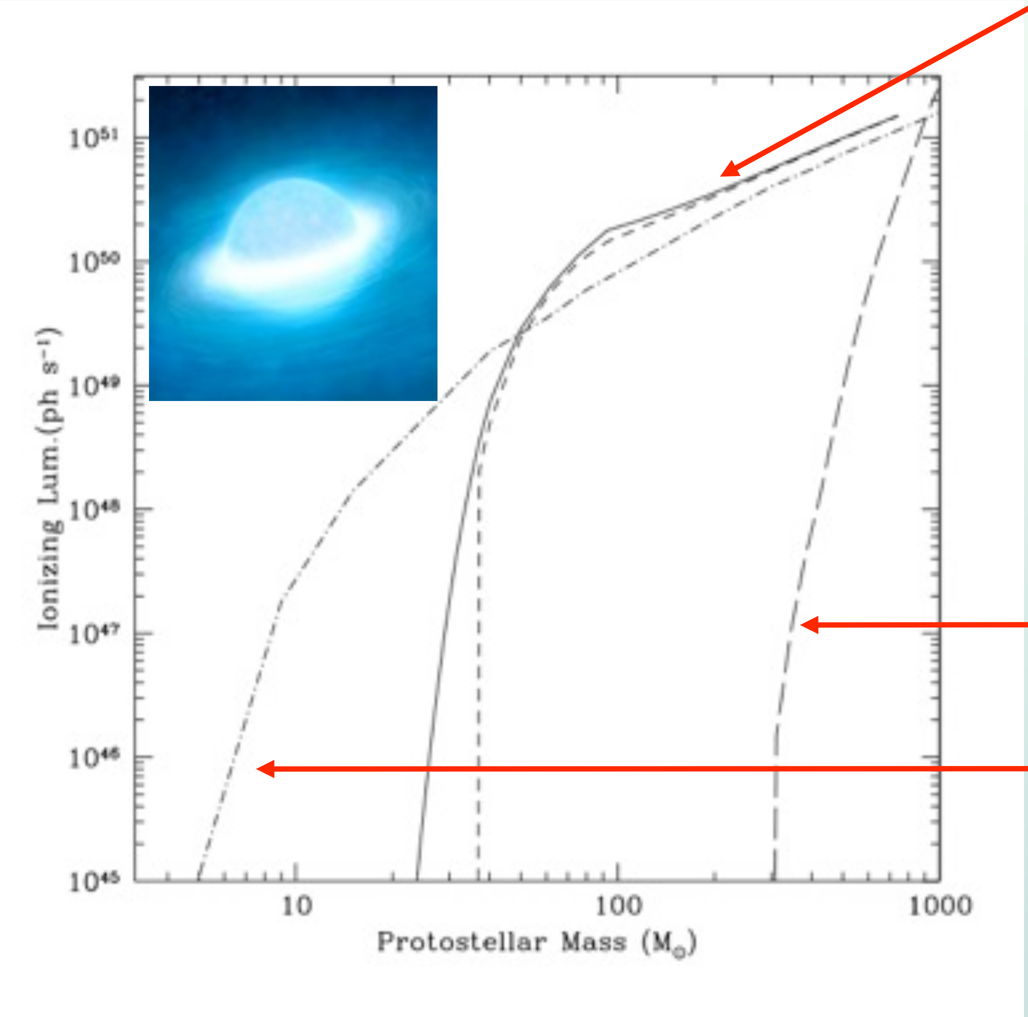

Total f_{Kep}=0.5

Spherical, f_{Kep}=0

Main Sequence (Schaerer 2002)

Spectrum depends on initial rotation

c.f. Omukai & Palla (2003)

Overview of Radiative Feedback

McKee & Tan (2008)

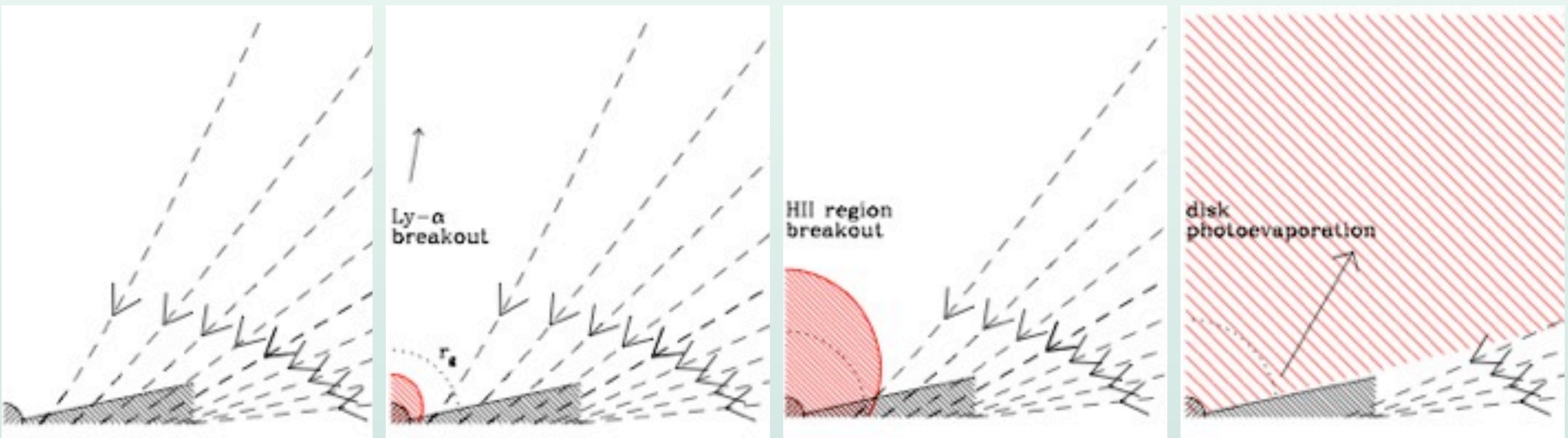

Hollenbach et al. (1994)

$m_* \longrightarrow$

See also Omukai & Inutsuka (2002); Hosokawa & Omukai (2009)

Feedback-limited accretion McKee & Tan (2008)

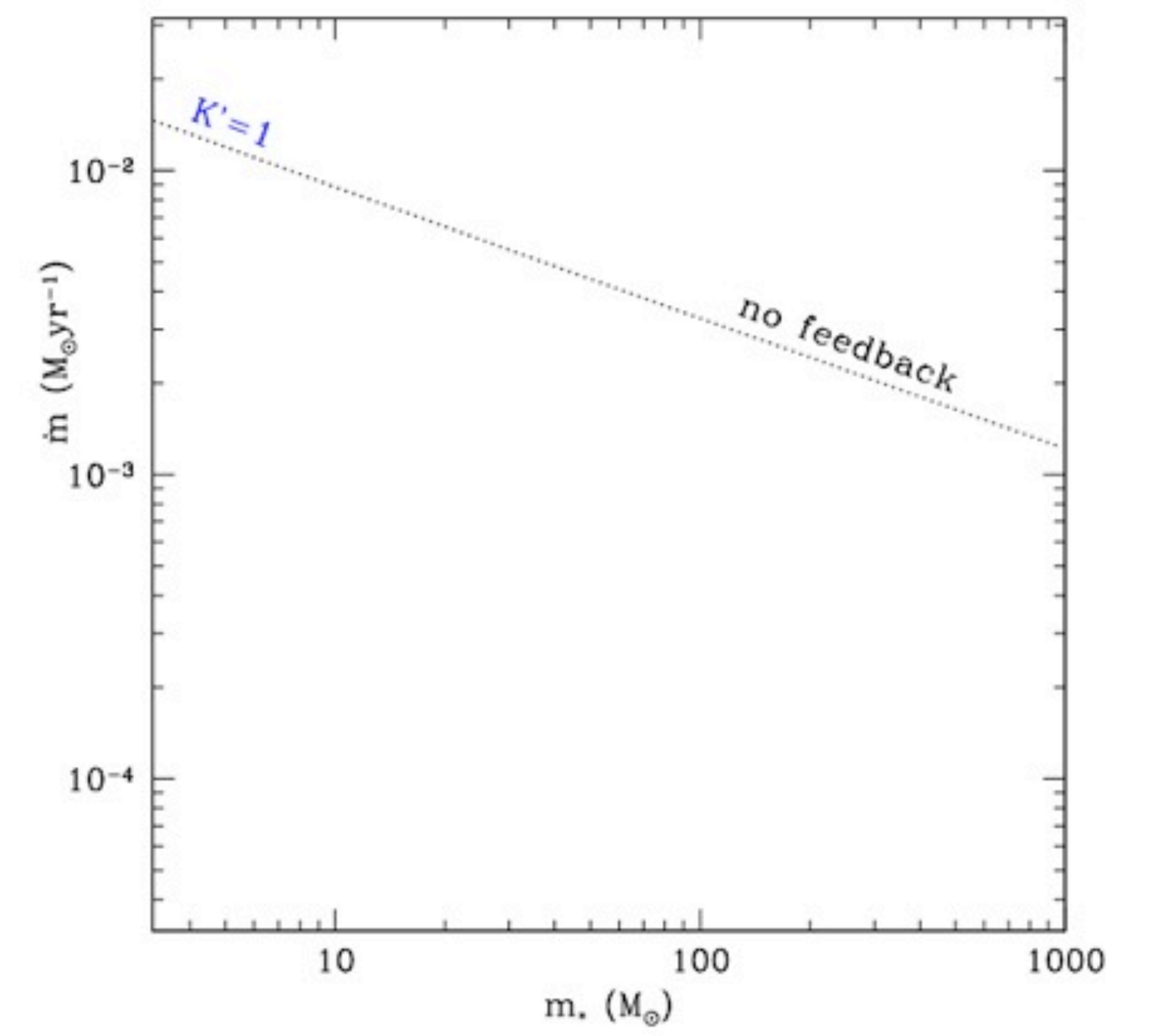

Self-consistent model for growth & evolution of protostar including:
-accretion rate(t)
-accretion disk(t,r,z)
-protostellar structure(t)
-ionizing feedback(t)

Feedback-limited accretion

McKee & Tan (2008)

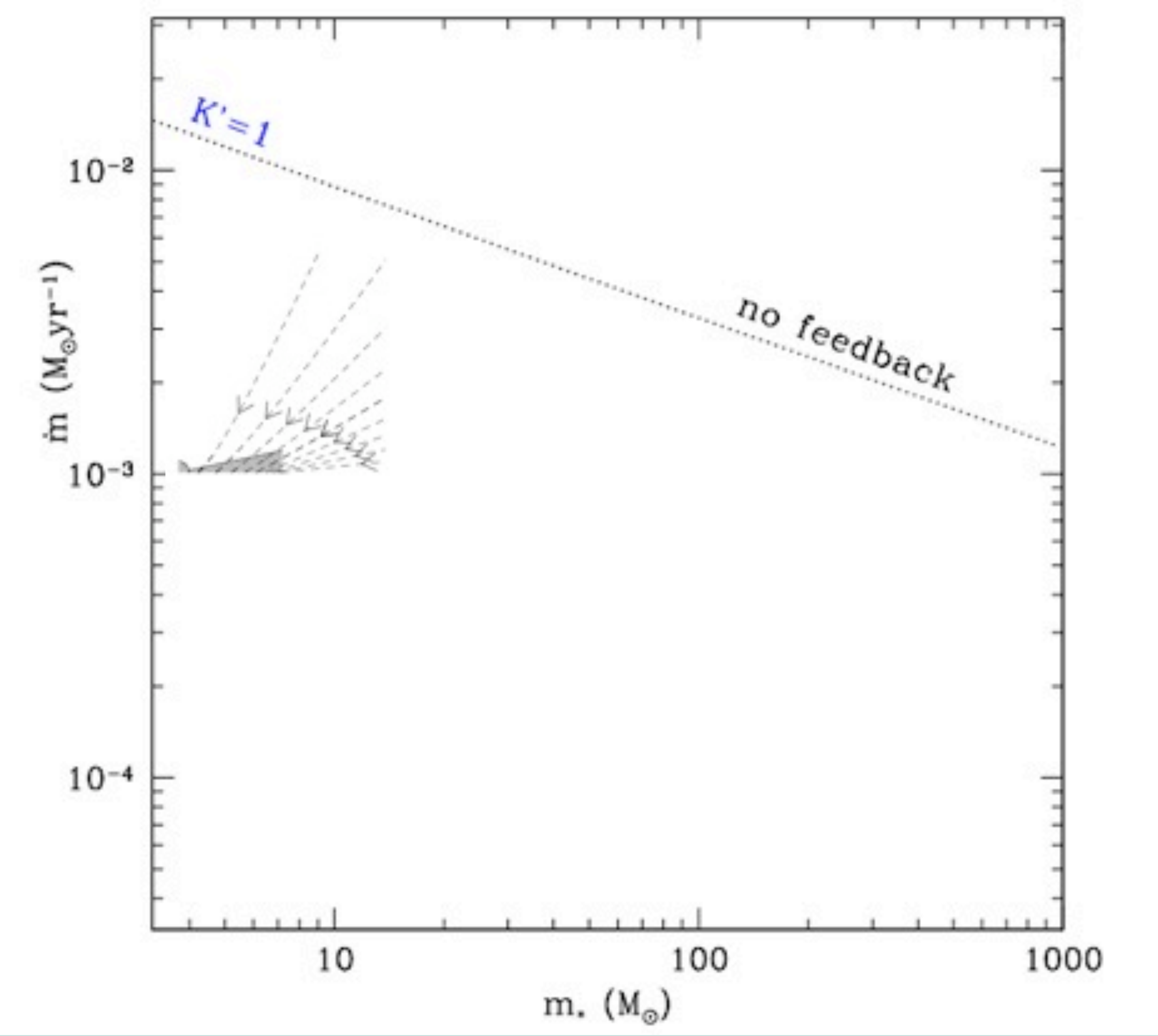

Self-consistent model for growth & evolution of protostar including:

-accretion rate(t)

-accretion disk(t,r,z)

-protostellar structure(t)

-ionizing feedback(t)

Feedback-limited accretion McKee & Tan (2008)

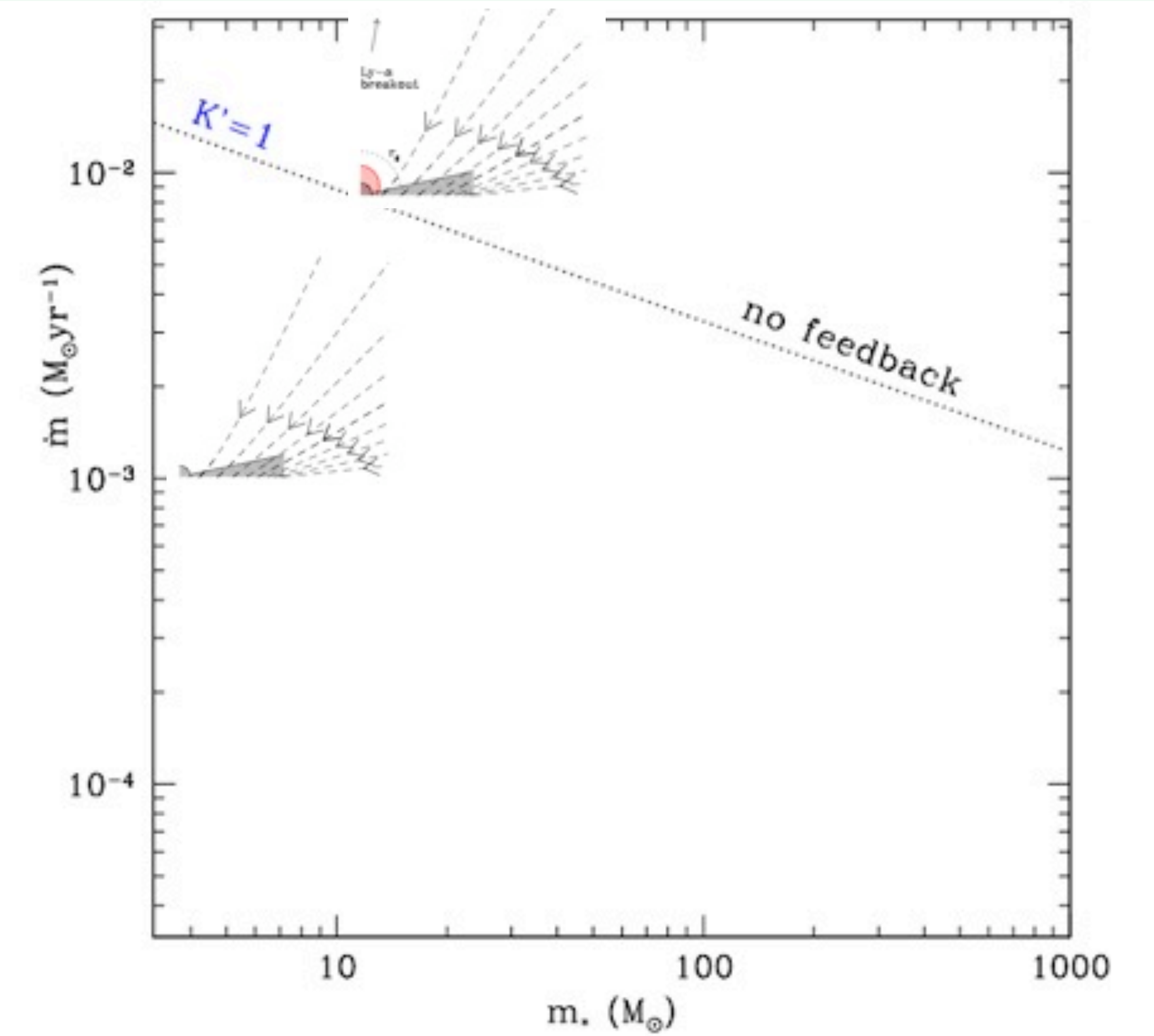

Self-consistent model for growth & evolution of protostar including:
- -accretion rate(t)
- -accretion disk(t,r,z)
- -protostellar structure(t)
- -ionizing feedback(t)

Feedback-limited accretion McKee & Tan (2008)

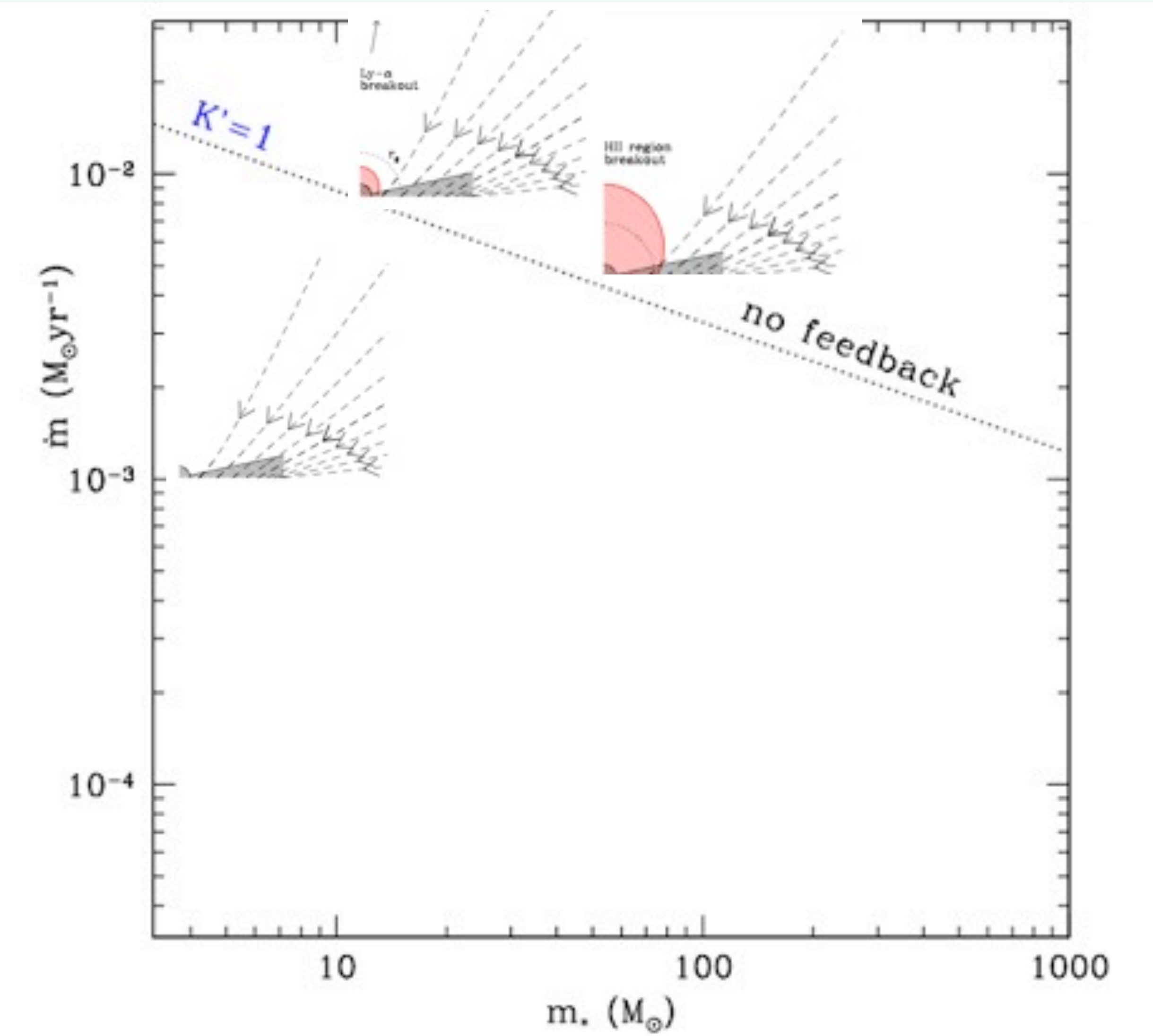

Self-consistent model for growth & evolution of protostar including:
- accretion rate(t)
- accretion disk(t,r,z)
- protostellar structure(t)
- ionizing feedback(t)

Feedback-limited accretion

McKee & Tan (2008)

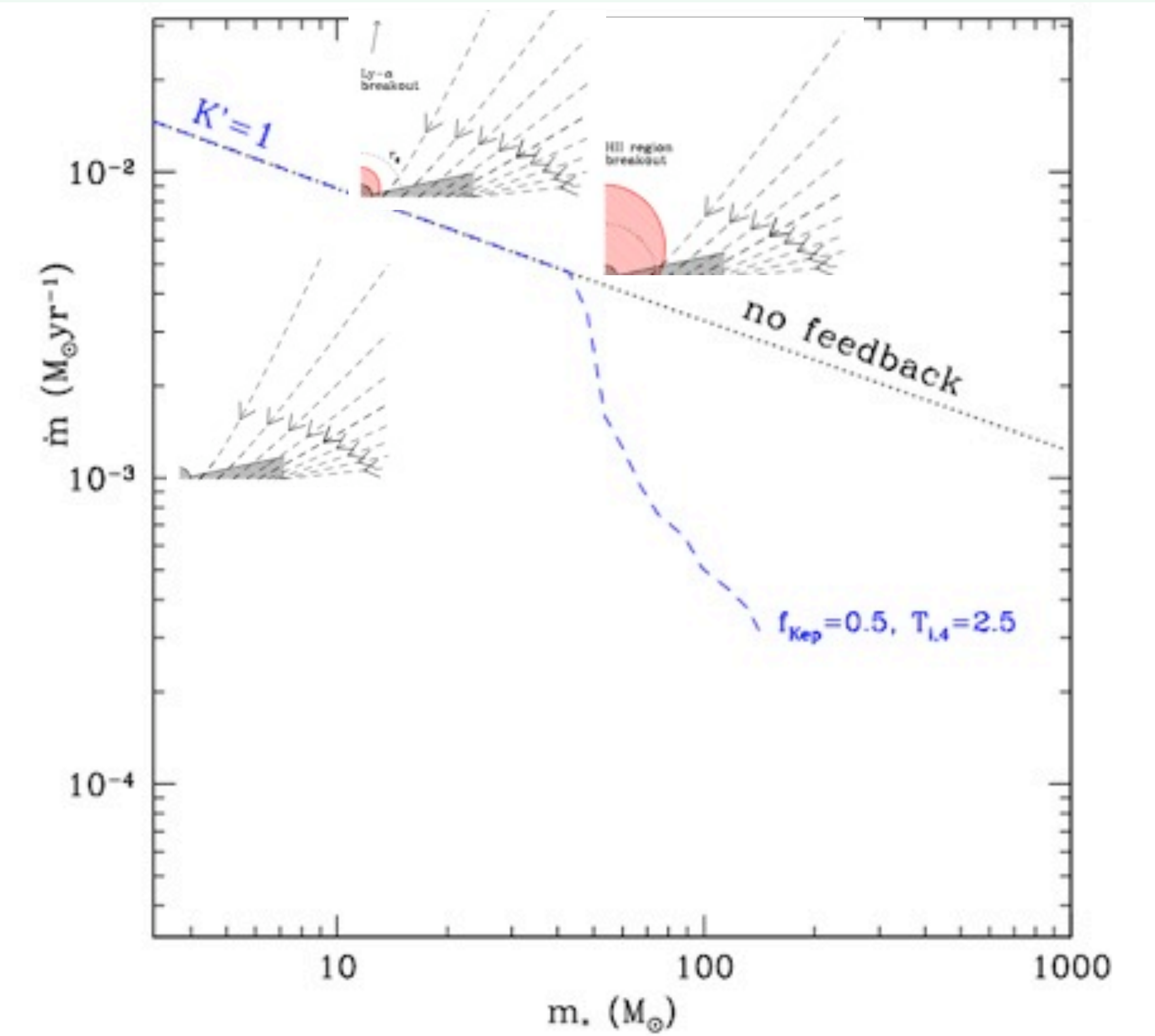

Self-consistent model for growth & evolution of protostar including:
- accretion rate(t)
- accretion disk(t,r,z)
- protostellar structure(t)
- ionizing feedback(t)

Feedback-limited accretion

McKee & Tan (2008)

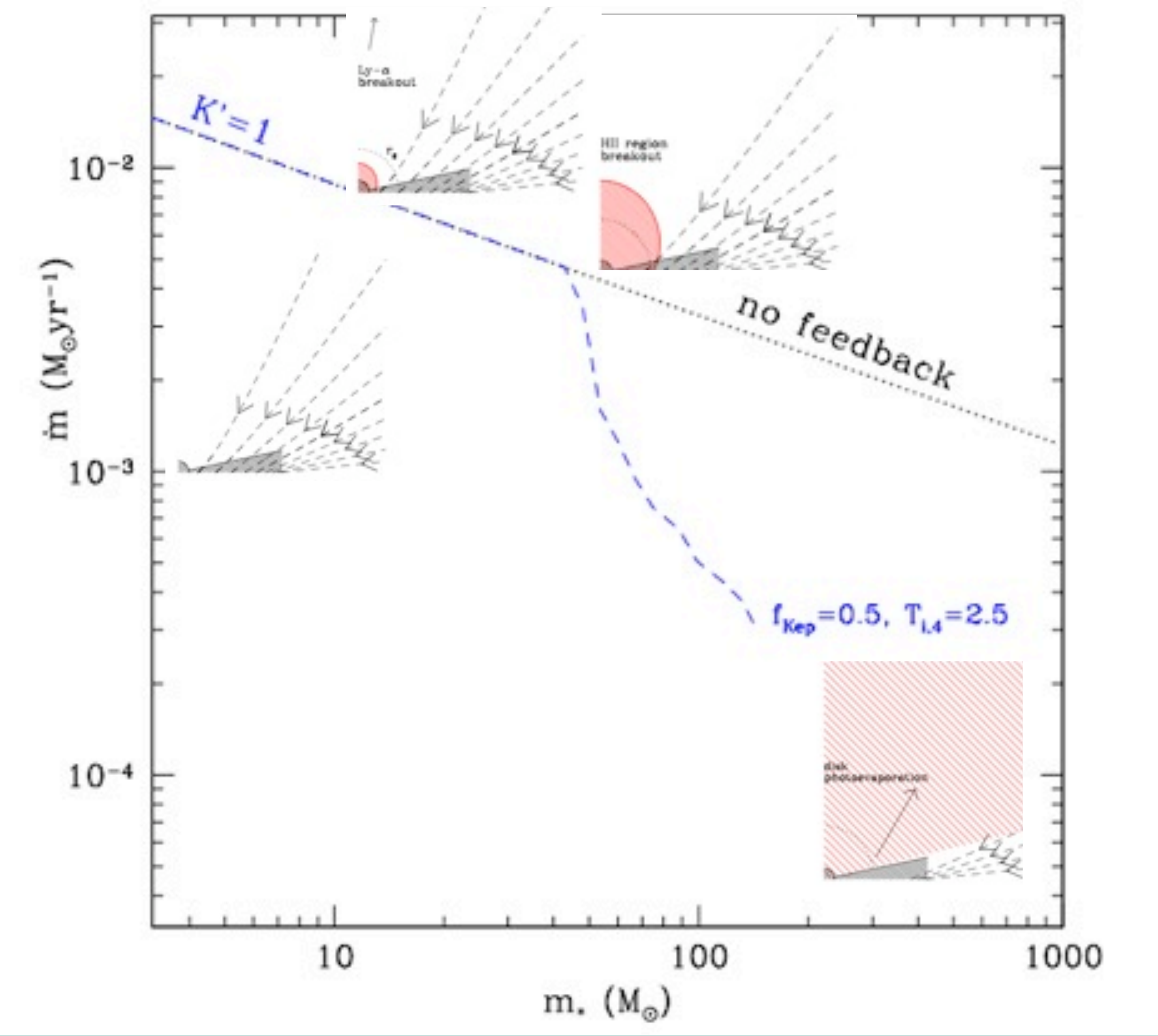

Self-consistent model for growth & evolution of protostar including:
- accretion rate(t)
- accretion disk(t,r,z)
- protostellar structure(t)
- ionizing feedback(t)

Feedback-limited accretion McKee & Tan (2008)

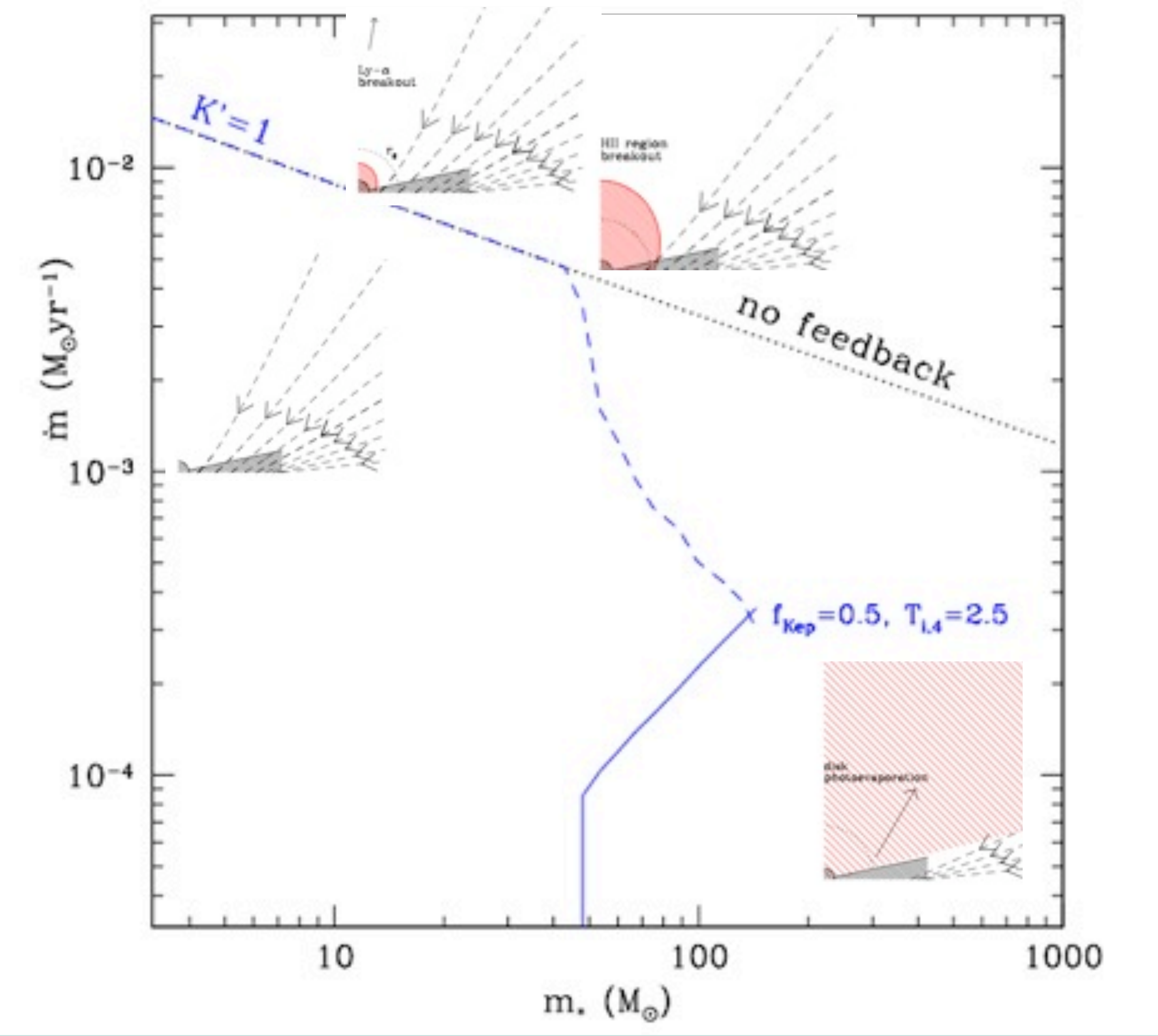

Self-consistent model for growth & evolution of protostar including:
- accretion rate(t)
- accretion disk(t,r,z)
- protostellar structure(t)
- ionizing feedback(t)

Feedback-limited accretion McKee & Tan (2008)

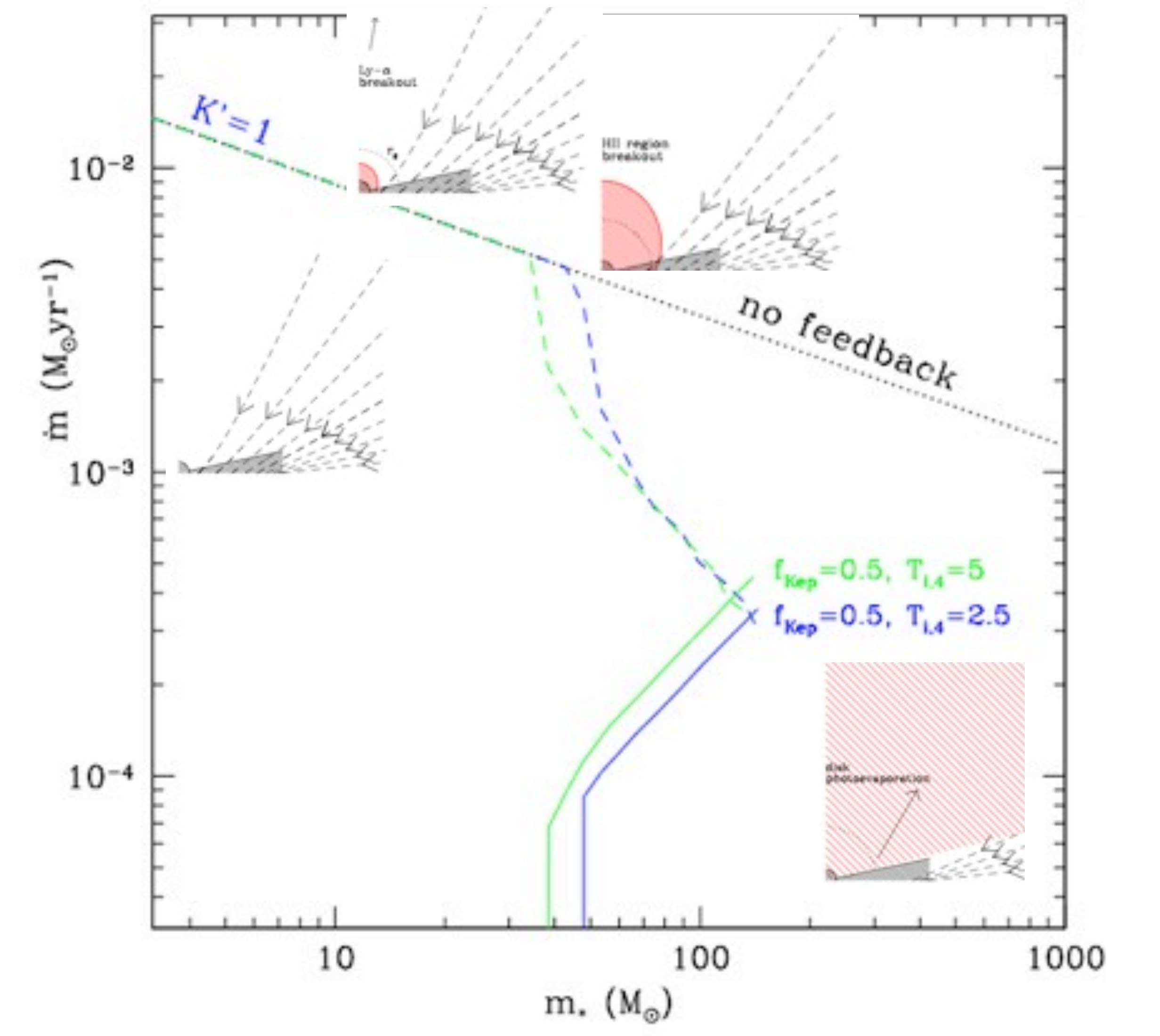

Self-consistent model for growth & evolution of protostar including:
- accretion rate(t)
- accretion disk(t,r,z)
- protostellar structure(t)
- ionizing feedback(t)

Feedback-limited accretion McKee & Tan (2008)

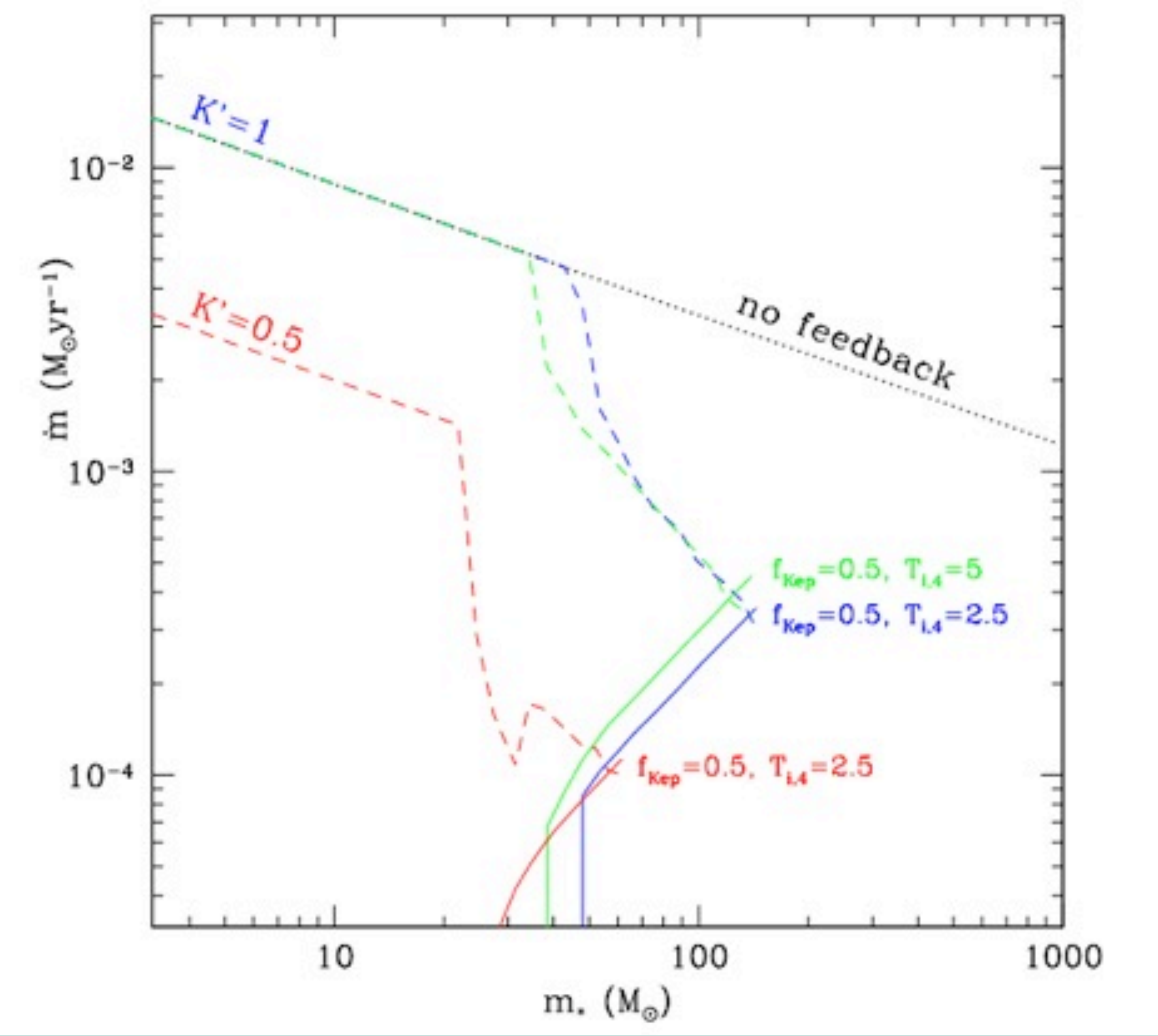

Self-consistent model for growth & evolution of protostar including:
- accretion rate(t)
- accretion disk(t,r,z)
- protostellar structure(t)
- ionizing feedback(t)

Feedback-limited accretion McKee & Tan (2008)

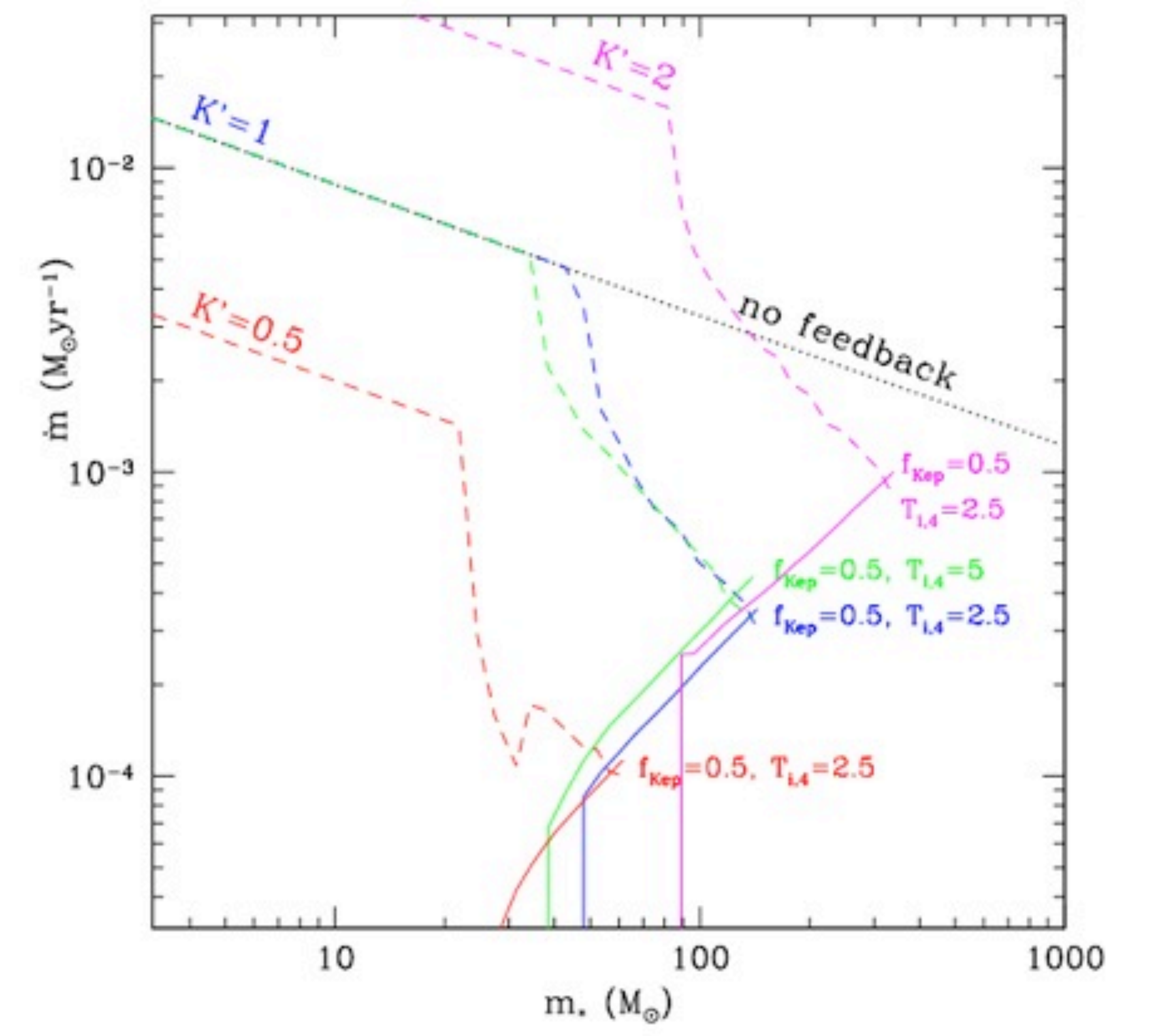

Self-consistent model for growth & evolution of protostar including:

- accretion rate(t)
- accretion disk(t,r,z)
- protostellar structure(t)
- ionizing feedback(t)

Feedback-limited accretion McKee & Tan (2008)

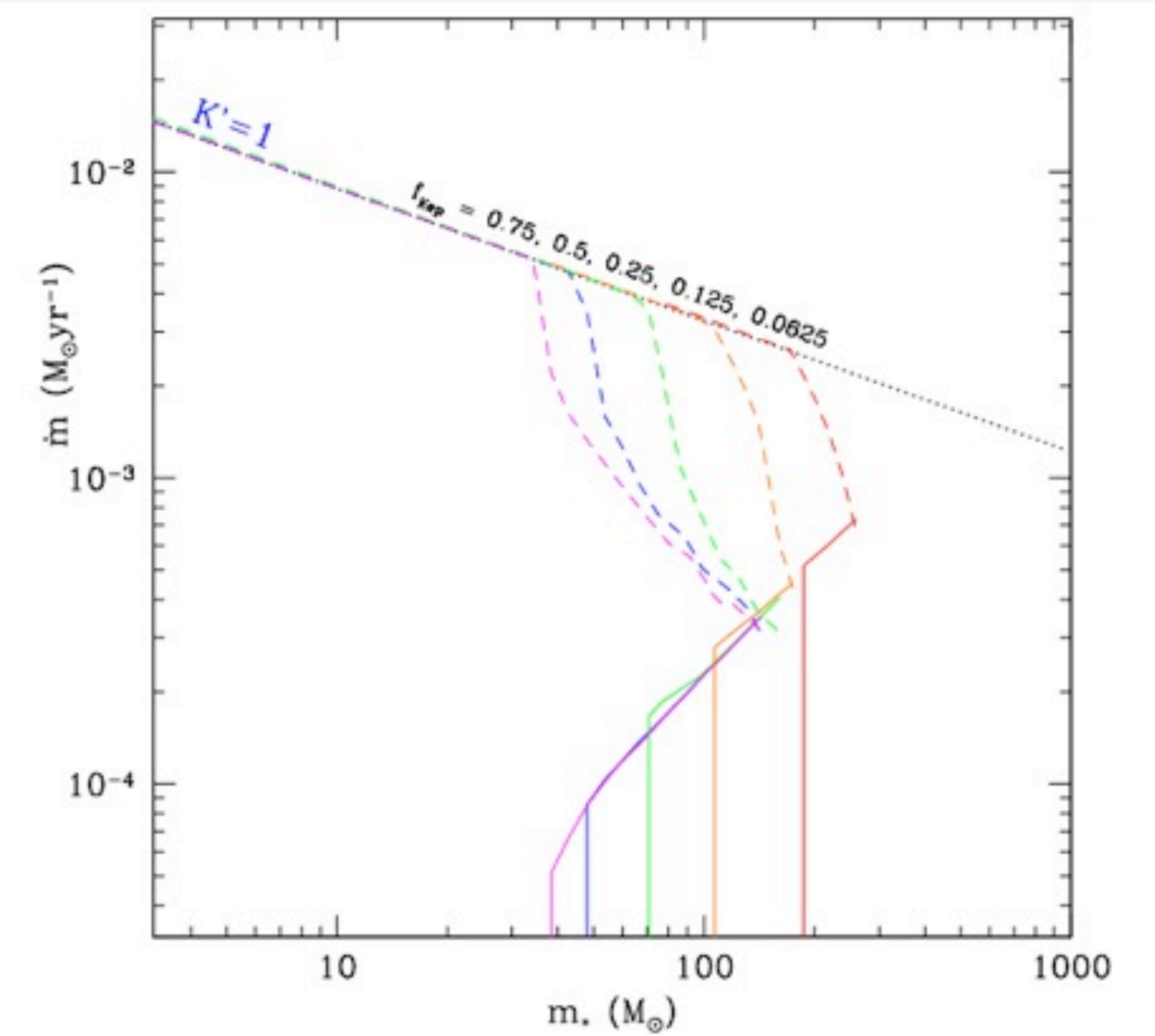

Self-consistent model
for growth & evolution of
protostar including:
-accretion rate(t)
-accretion disk(t,r,z)
-protostellar structure(t)
-ionizing feedback(t)

Feedback-limited accretion

McKee & Tan (2008)

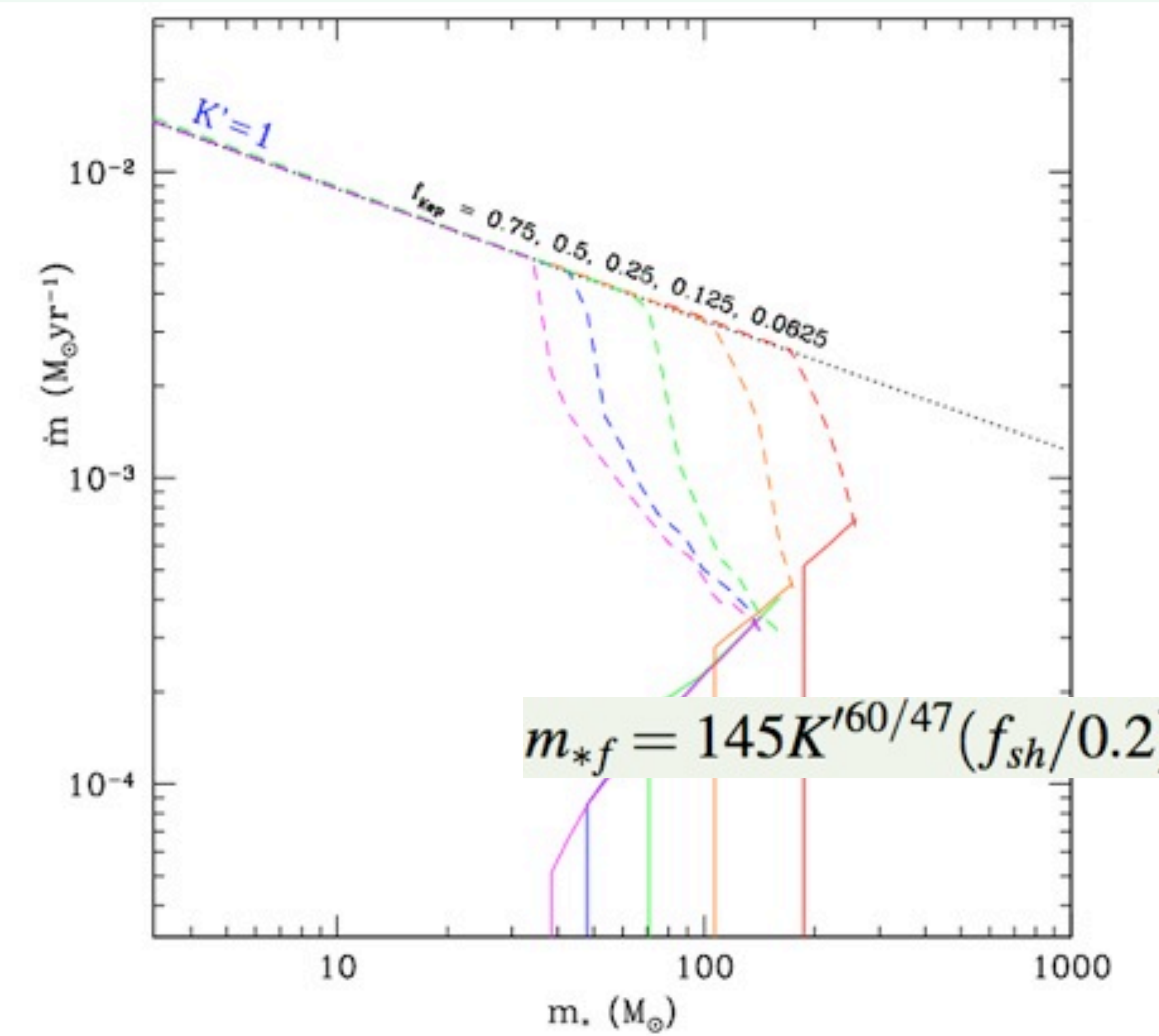

Self-consistent model for growth & evolution of protostar including:

- accretion rate(t)
- accretion disk(t,r,z)
- protostellar structure(t)
- ionizing feedback(t)

$$m_{*f} = 145K'^{60/47}(f_{sh}/0.2)^{28/47}(\bar{\varepsilon}_{*d}/0.25)^{12/47}M_\odot$$

A Population of Pop III.1 Halos

O'Shea &Norman 2007

Halo Properties

Run	z_{coll}	M_{vir}	R_{vir}	T_{vir}	M_b	f_{bar}	λ_{dm}	λ_{gas}	θ
L0_30 simulations:									
L0_30A	19.28	4.18×10^5	118.1	1120.0	4.59×10^4	0.823	0.050	0.022	55.1
L0_30B	22.19	2.92×10^5	91.7	1009.6	2.91×10^4	0.753	0.066	0.029	3.3
L0_30C	20.31	6.92×10^5	132.9	1646.8	7.56×10^4	0.819	0.053	0.034	17.3
L0_30D	24.74	1.36×10^5	64.0	671.4	1.29×10^4	0.711	0.046	0.014	12.7
L0_45 simulations:									
L0_45A	28.70	2.41×10^5	67.4	1131.7	2.03×10^4	0.631	0.108	0.056	8.4
L0_45B	26.46	2.42×10^5	72.7	1052.8	2.28×10^4	0.706	0.019	0.019	34.0
L0_45C	24.74	5.21×10^5	100.1	1645.6	5.21×10^4	0.750	0.054	0.015	97.4
L0_45D	28.67	5.89×10^5	90.5	2060.0	5.71×10^4	0.727	0.059	0.071	11.4
L0_60 simulations:									
L0_60A	24.10	3.96×10^5	93.8	1338.0	4.29×10^4	0.813	0.052	0.027	26.0
L0_60B	25.64	3.82×10^5	87.3	1385.6	3.72×10^4	0.730	0.047	0.056	11.0
L0_60C	28.13	1.68×10^5	60.7	876.9	1.29×10^4	0.575	0.027	0.016	40.0
L0_60D	32.70	2.85×10^5	62.5	1440.9	2.06×10^4	0.542	0.049	0.033	10.0

Notes.—Mean halo properties at the collapse redshift. Here z_{coll} is the collapse redshift of the halo, defined as the redshift at which the central baryon density of the halo reaches $n_H \simeq 10^{10}$ cm^{-3}; M_{vir}, R_{vir}, and T_{vir} are the halo virial mass, radius, and temperature at that epoch, respectively; M_b is the total baryon mass within the virial radius at that epoch, and f_{bar} is the baryon mass fraction (in units of Ω_b/Ω_m); λ_{dm} and λ_{gas} are the halo dark matter and gas spin parameters, respectively, and θ is the angle of separation (in degrees) between the bulk dark matter and gas angular momentum vectors. M_{vir} and M_b are in units of $M_\odot$, R_{vir} is in units of proper parsecs, and T_{vir} is in units of kelvins.

Numerical K’ Profiles and Accretion Rates

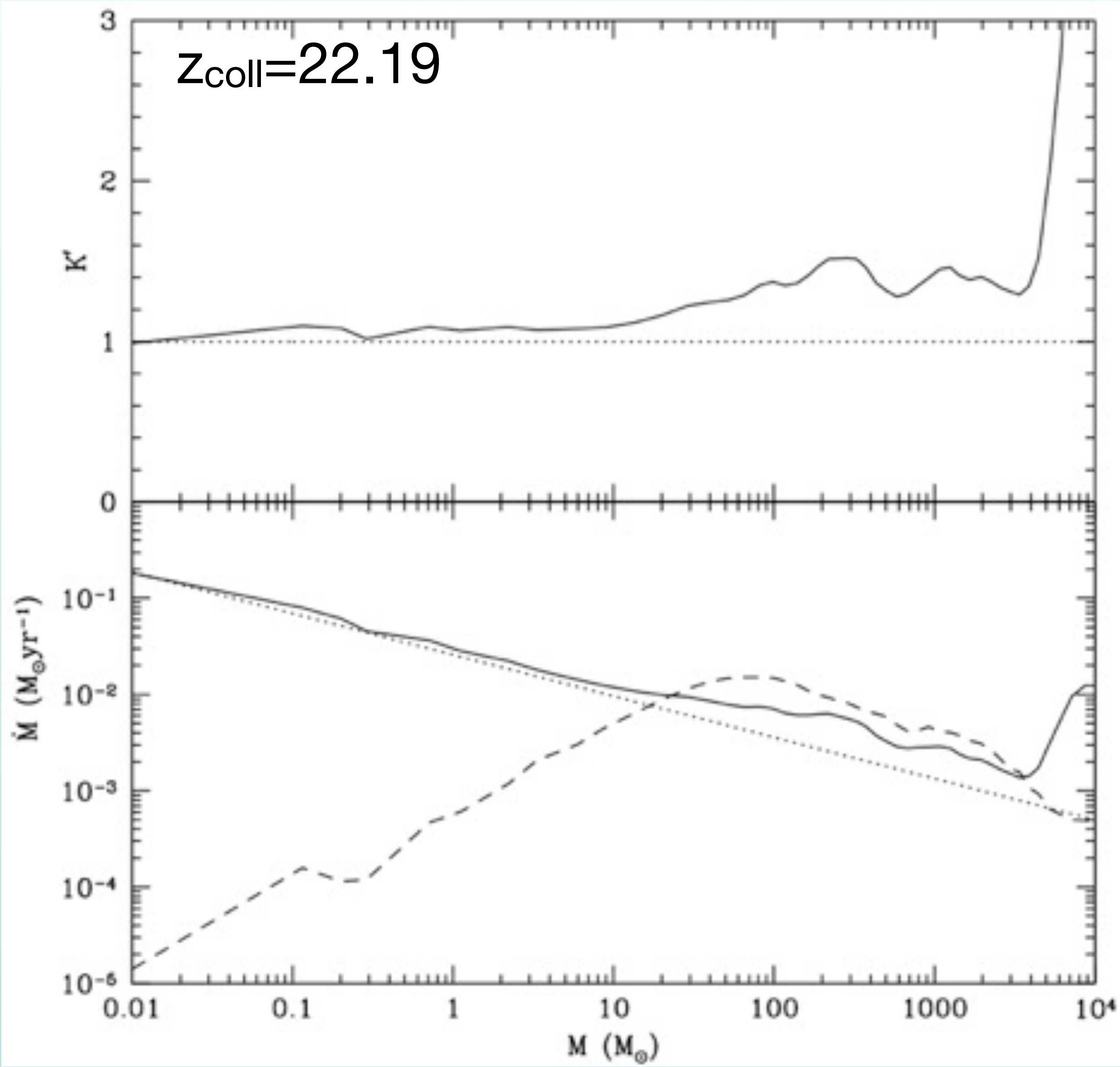

Tan, Smith et al., in prep

$\dot{m}_{*(infall,SPS)} = \dot{m}_{evap}$

$m_{*f(SPS)} = 220 M_\odot$

$m_{*f(infall)} = 310 M_\odot$

Numerical K' Profiles and Accretion Rates

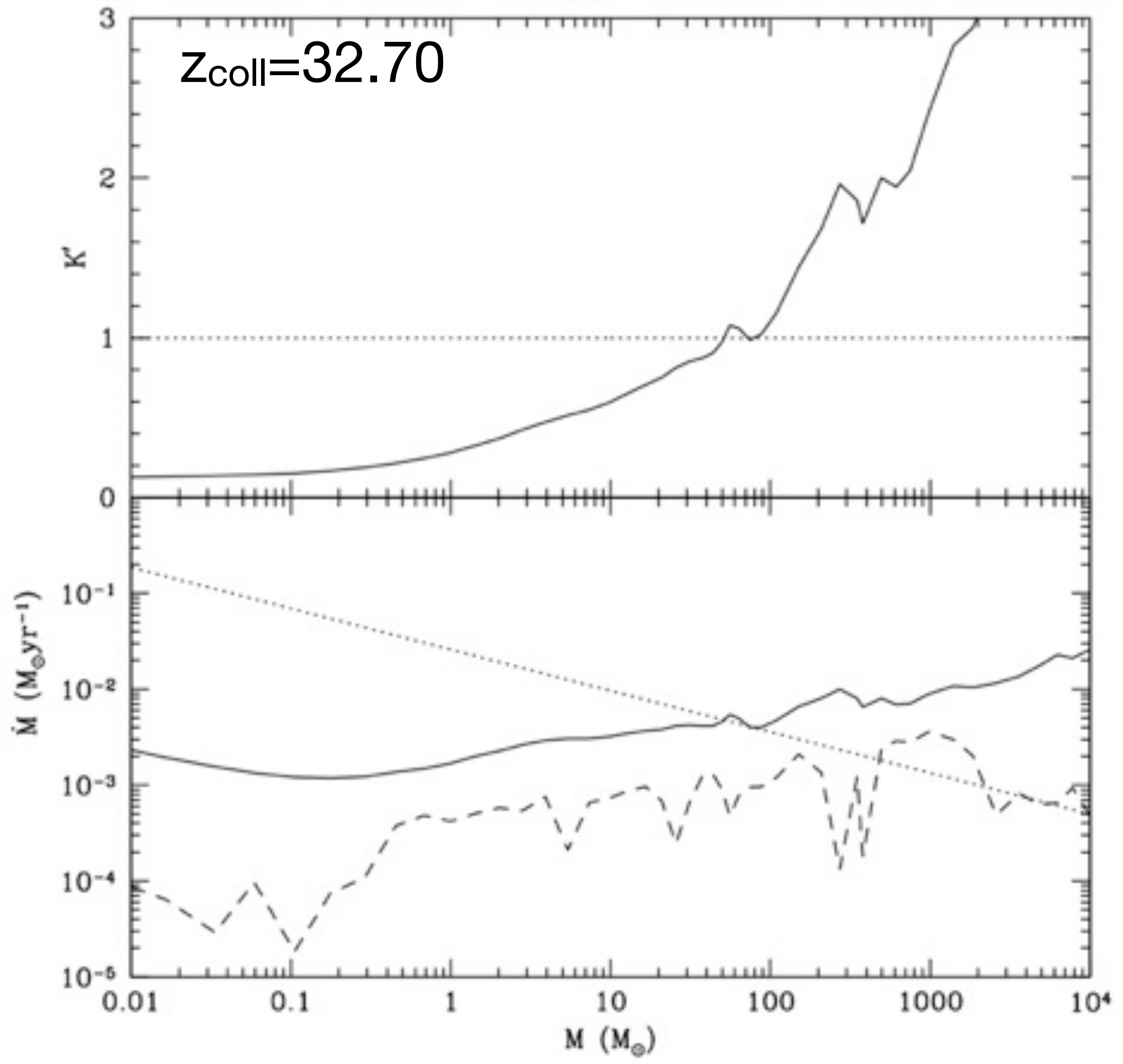

Tan, Smith et al., in prep

$\dot{m}_{*(infall,SPS)} = \dot{m}_{evap}$

$m_{*f(SPS)} = 690 M_\odot$

$m_{*f(infall)} = 59 M_\odot$

Pop III.1 IMF [$m_{*f(infall)}$]

Tan, Smith et al., in prep

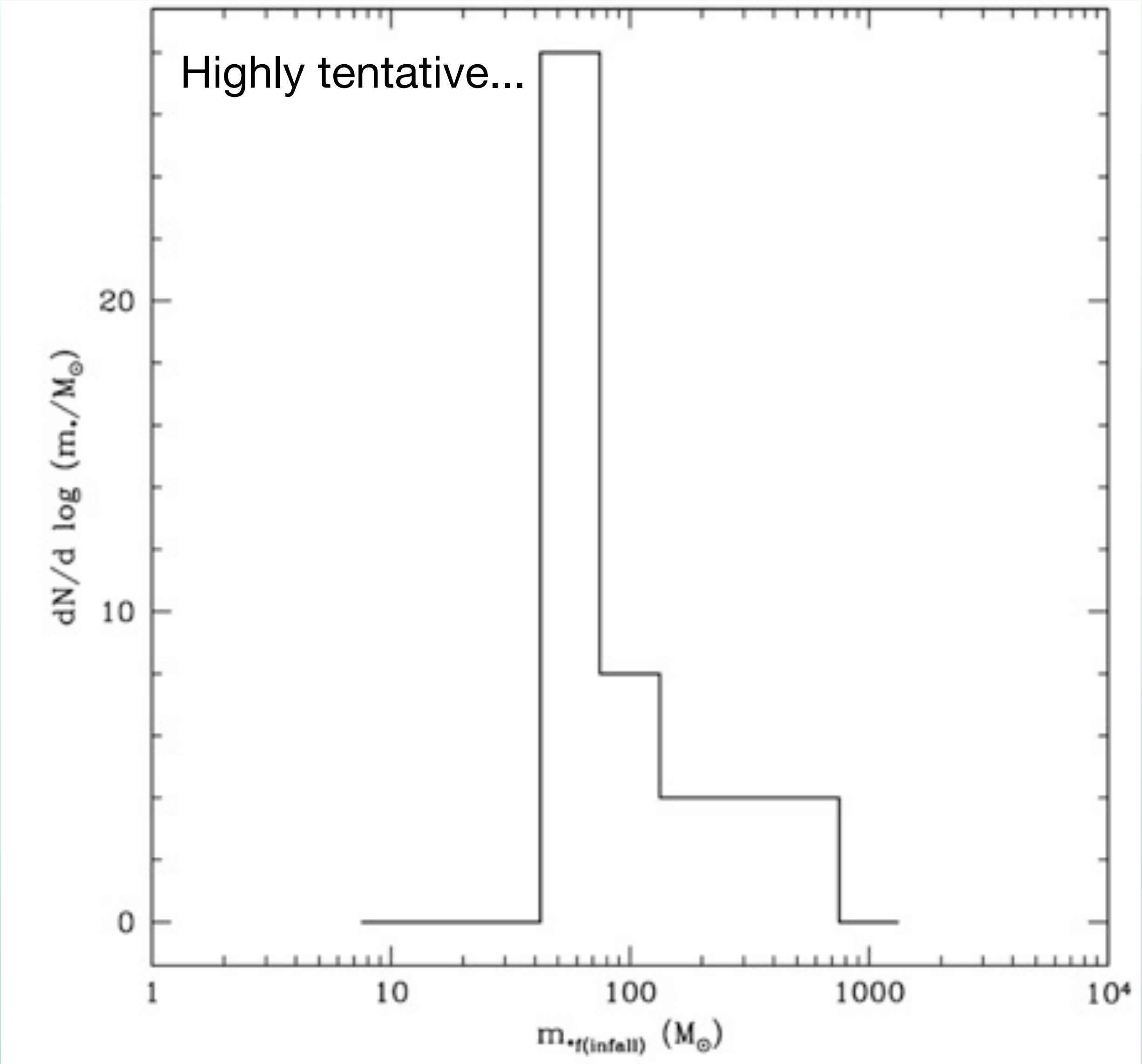

Pop III.1 m_{*f} versus z

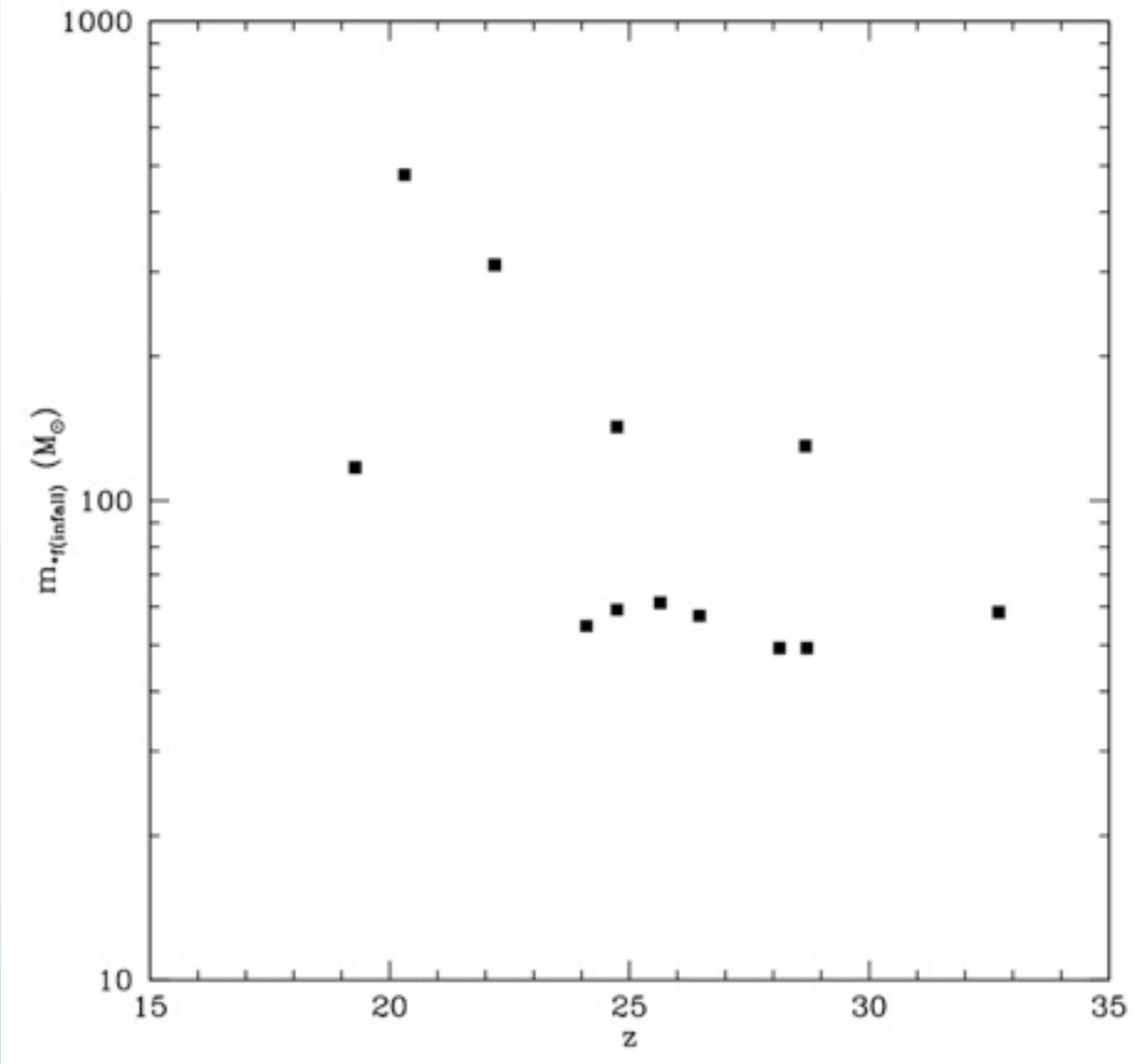

Model uncertainties

-HII region breakout

-Disk photoevaporation

-Protostellar evolution

Model uncertainties

-HII region breakout

Rayleigh-Taylor instabilities (Whalen & Norman 2008)
Diversion of accretion flow to
equatorial plane (rather than radial expulsion)

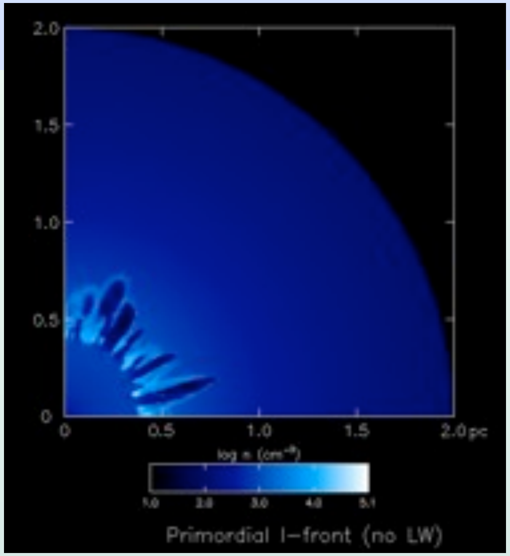

-Disk photoevaporation

-Protostellar evolution

Model uncertainties

-HII region breakout

Rayleigh-Taylor instabilities (Whalen & Norman 2008)
Diversion of accretion flow to
equatorial plane (rather than radial expulsion)

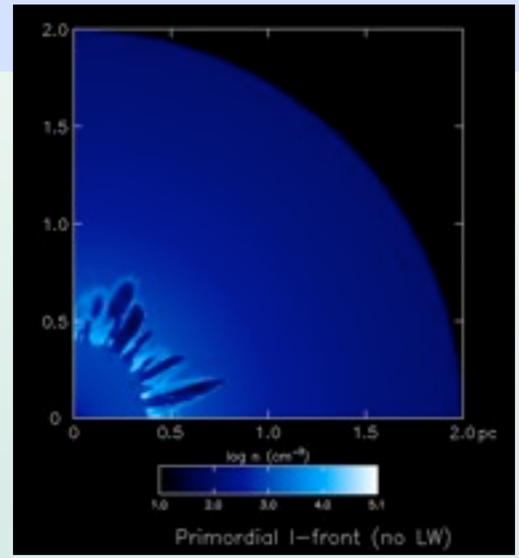

-Disk photoevaporation

Normalization of basic Hollenbach et al. model
Effect of protostellar outflow
Non-spherical large-scale accretion to core

-Protostellar evolution

Model uncertainties

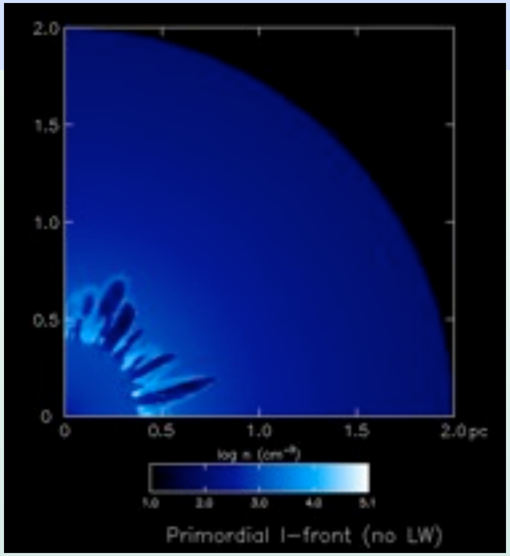

-HII region breakout

Rayleigh-Taylor instabilities (Whalen & Norman 2008)
Diversion of accretion flow to
equatorial plane (rather than radial expulsion)

-Disk photoevaporation

Normalization of basic Hollenbach et al. model
Effect of protostellar outflow
Non-spherical large-scale accretion to core

-Protostellar evolution

Rotation, especially anisotropic ionizing flux

Model uncertainties

-HII region breakout

Rayleigh-Taylor instabilities (Whalen & Norman 2008)
Diversion of accretion flow to
equatorial plane (rather than radial expulsion)

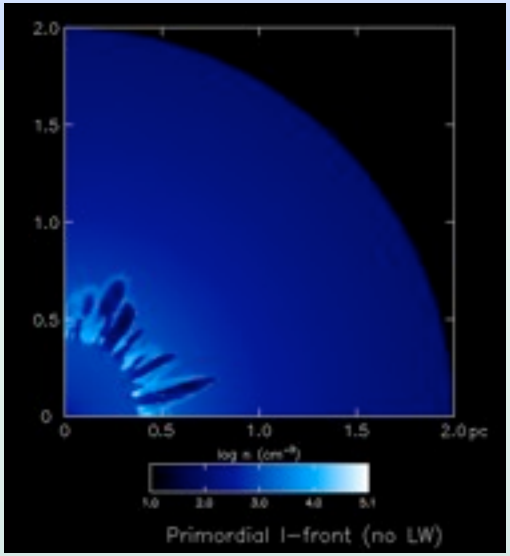

-Disk photoevaporation

Normalization of basic Hollenbach et al. model
Effect of protostellar outflow
Non-spherical large-scale accretion to core

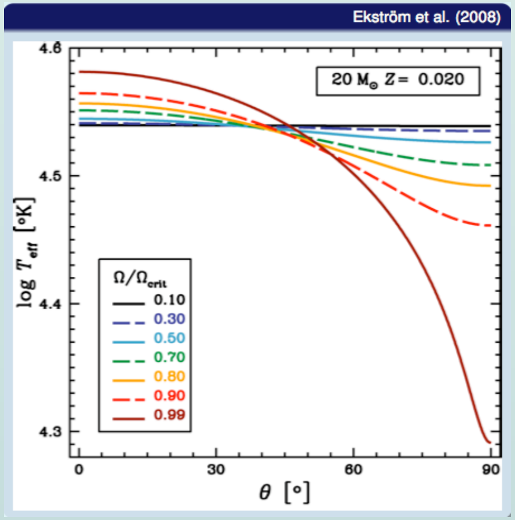

-Protostellar evolution

Rotation, especially anisotropic ionizing flux

Model uncertainties

-HII region breakout

Rayleigh-Taylor instabilities (Whalen & Norman 2008)
Diversion of accretion flow to
equatorial plane (rather than radial expulsion)

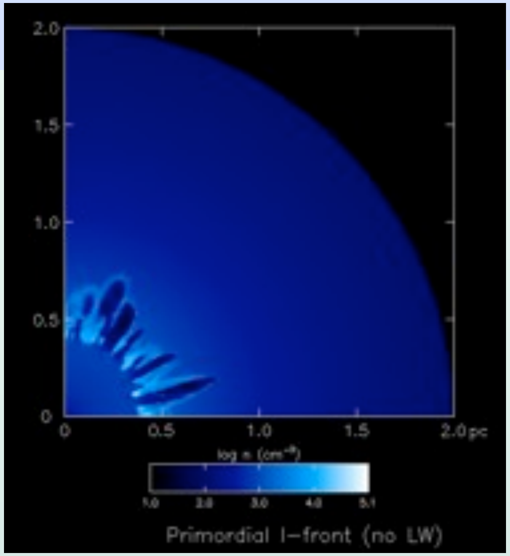

-Disk photoevaporation

Normalization of basic Hollenbach et al. model
Effect of protostellar outflow
Non-spherical large-scale accretion to core

-Protostellar evolution

Rotation, especially anisotropic ionizing flux

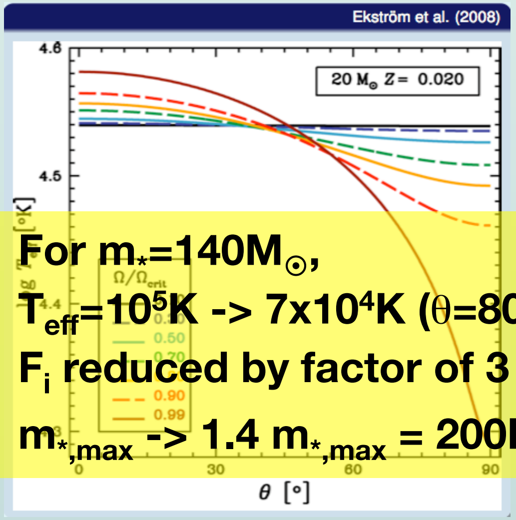

For m_*=140$M_\odot$,
T_{eff}=10^5K -> 7x10^4K (θ=80º)
F_i reduced by factor of 3
$m_{*,max}$ -> 1.4 $m_{*,max}$ = 200$M_\odot$

Model uncertainties

-Dark Matter Annihilation Heating

Delayed contraction to the main sequence

-HII region breakout

Rayleigh-Taylor instabilities (Whalen & Norman 2008)
Diversion of accretion flow to
equatorial plane (rather than radial expulsion)

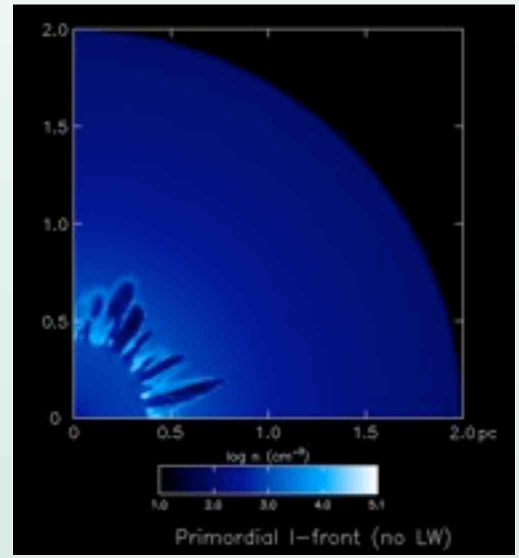

-Disk photoevaporation

Normalization of basic Hollenbach et al. model
Effect of protostellar outflow
Non-spherical large-scale accretion to core

-Protostellar evolution

Rotation, especially anisotropic ionizing flux

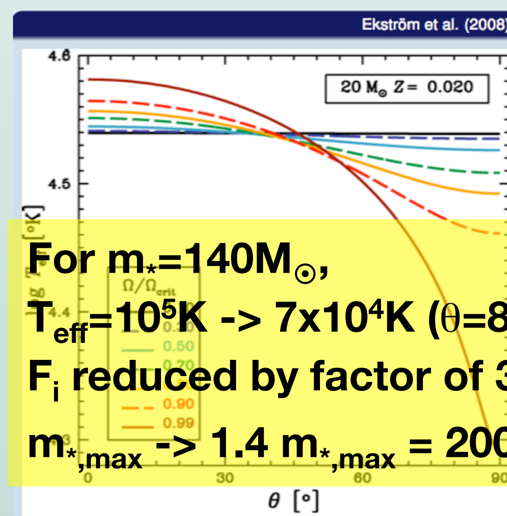

For m_*=140$M_\odot$,
T_{eff}=10^5K -> 7x10^4K (θ=80º)
F_i reduced by factor of 3
$m_{*,max}$ -> 1.4 $m_{*,max}$ = 200$M_\odot$

Heating by WIMP Dark Matter Annihilation?

Spolyar, Freese, Gondolo (2008) conclude WIMP annihilation heating is important for $n > 10^{13}\text{cm}^{-3}$ or $r < 20$ AU. Could delay or halt collapse: dark matter powered protostar. Main uncertainties: $\rho_{DM}(r<10^{-3}\text{pc})$, m_χ, $<\sigma v>$, f_{trap}

Heating by WIMP Dark Matter Annihilation?

Spolyar, Freese, Gondolo (2008) conclude WIMP annihilation heating is important for $n > 10^{13}cm^{-3}$ or $r < 20$ AU. Could delay or halt collapse: dark matter powered protostar. Main uncertainties: $\rho_{DM}(r<10^{-3}pc)$, m_χ, $<\sigma v>$, f_{trap}

Natarajan, Tan, O'Shea (2009) examined the ρ_{DM} profiles of 3 simulated minihalos, finding steepening for r<0.5pc, i.e. where baryons dominate. Here $\rho_{DM} \propto r^{-2}$.

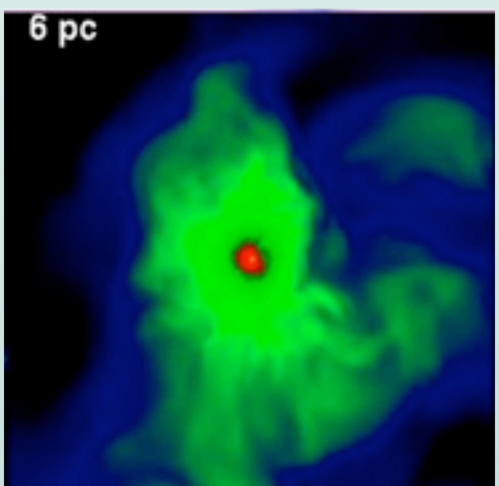

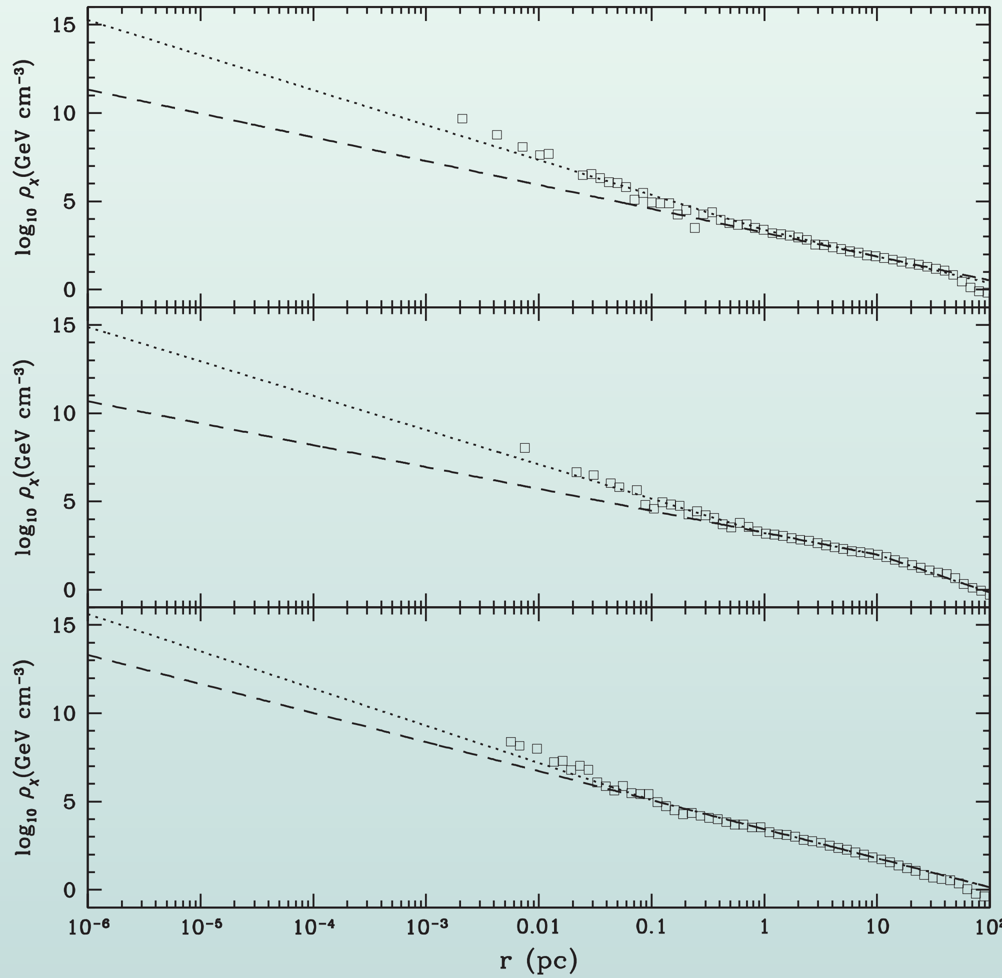

WIMP Annihilation Heating Rate / Baryonic Cooling Rate

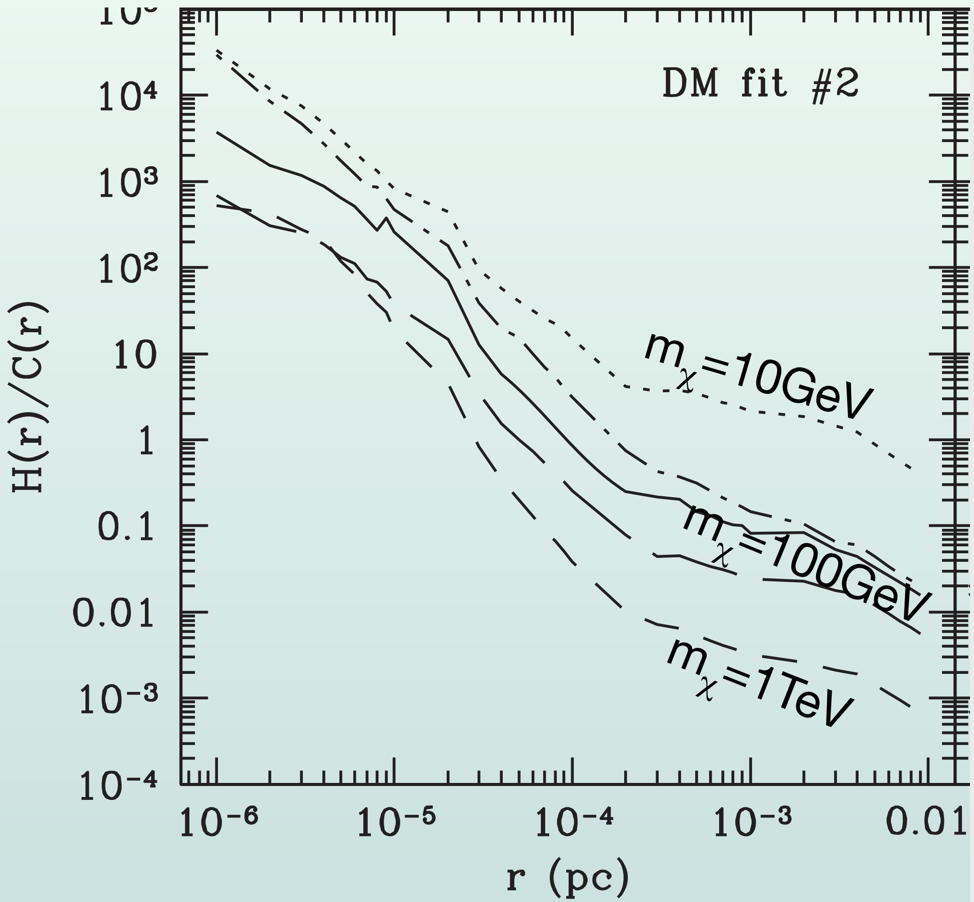

Models assume annihilation rate coefficient <σv>=3×10^{-26}cm^{3}s^{-1}

WIMP Annihilation Heating Rate / Baryonic Cooling Rate

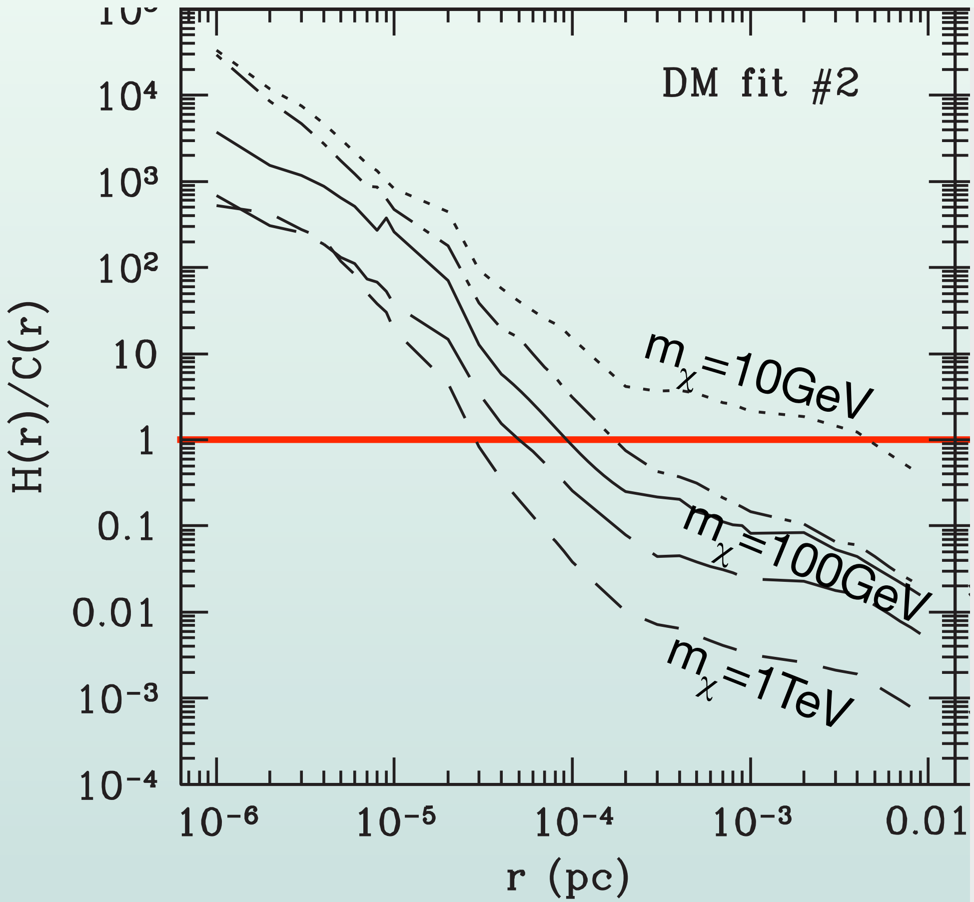

Models assume annihilation rate coefficient $\langle\sigma v\rangle = 3\text{x}10^{-26}\text{cm}^3\text{s}^{-1}$

WIMP Annihilation Heating Rate / Baryonic Cooling Rate

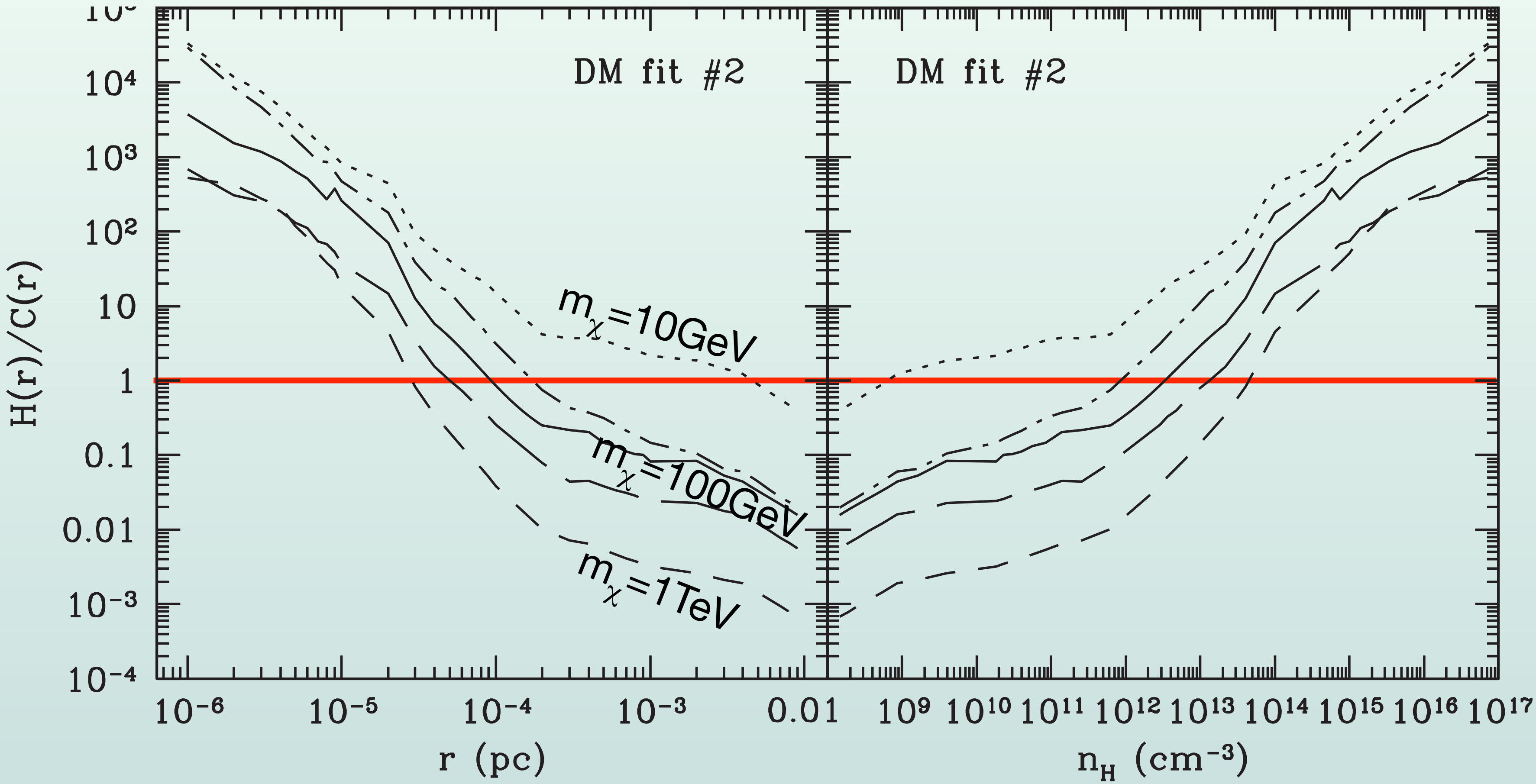

Models assume annihilation rate coefficient $\langle\sigma v\rangle = 3\times10^{-26} cm^3 s^{-1}$

Evolution of Protostellar Radius

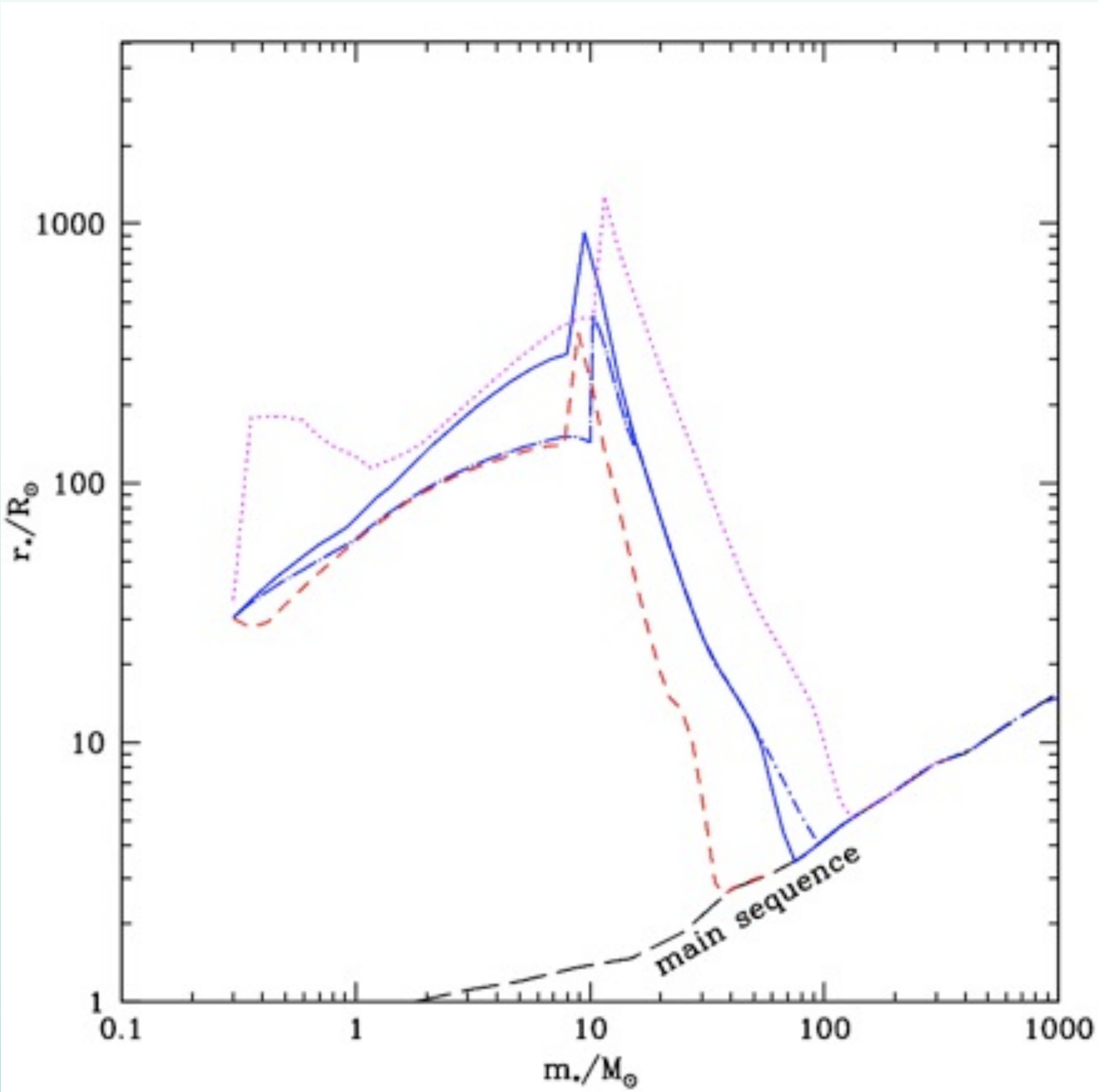

See also Spolyar et al. 2009

Talks by Freese, Iocco

Evolution of Protostellar Radius

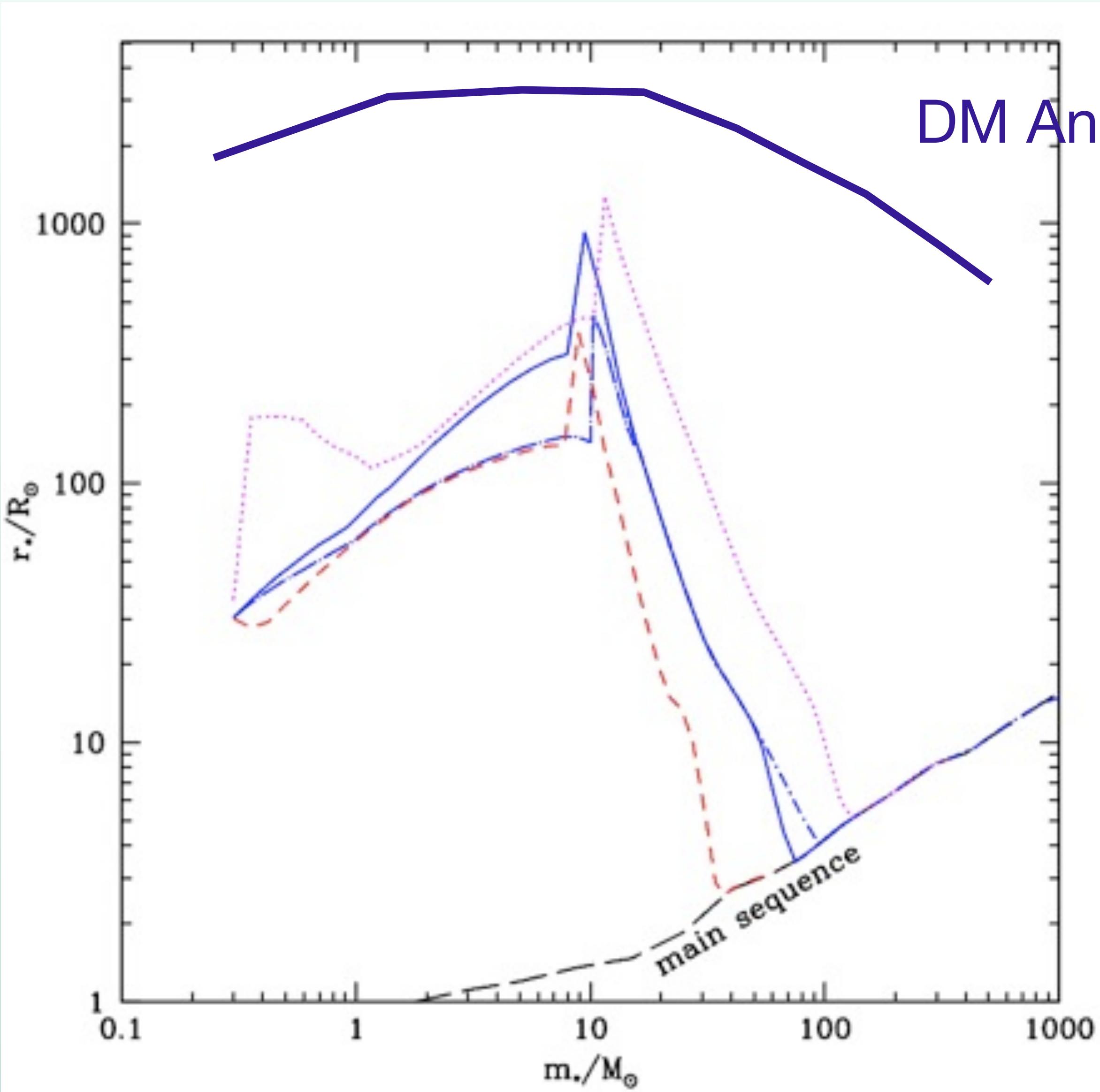

See also Spolyar et al. 2009

Talks by Freese, Iocco

Summary: Population III.1 Star Formation

- Quasi equilibrium massive cores form in dark matter mini halos (simulations of structure formation)
- Standard accretion physics suggests single (or binary) stars form in each minihalo
- Mass likely to set by radiative (ionization) feedback -> $m_* \sim 100 M_\odot$

Summary: Population III.1 Star Formation

- Quasi equilibrium massive cores form in dark matter mini halos (simulations of structure formation)
- Standard accretion physics suggests single (or binary) stars form in each minihalo
- Mass likely to set by radiative (ionization) feedback -> $m_* \sim 100 M_\odot$
- Dark Matter (WIMP) annihilation may change this story.
- Pop III.2: may be lower-mass stars due to external radiative feedback, but more complicated.

Enclosed Luminosity Profiles of "Equilibrium" Configurations

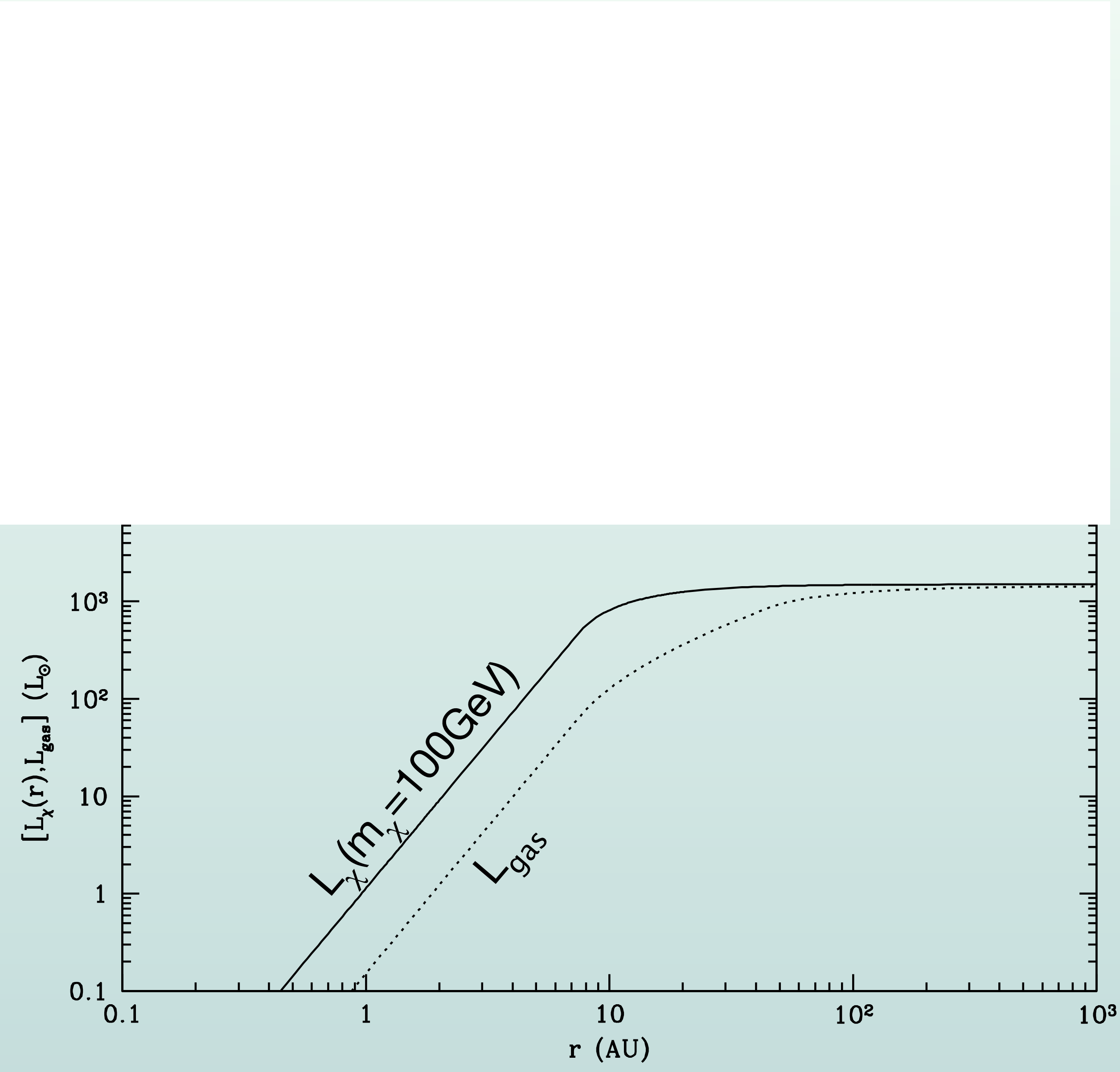

Enclosed Luminosity Profiles of "Equilibrium" Configurations

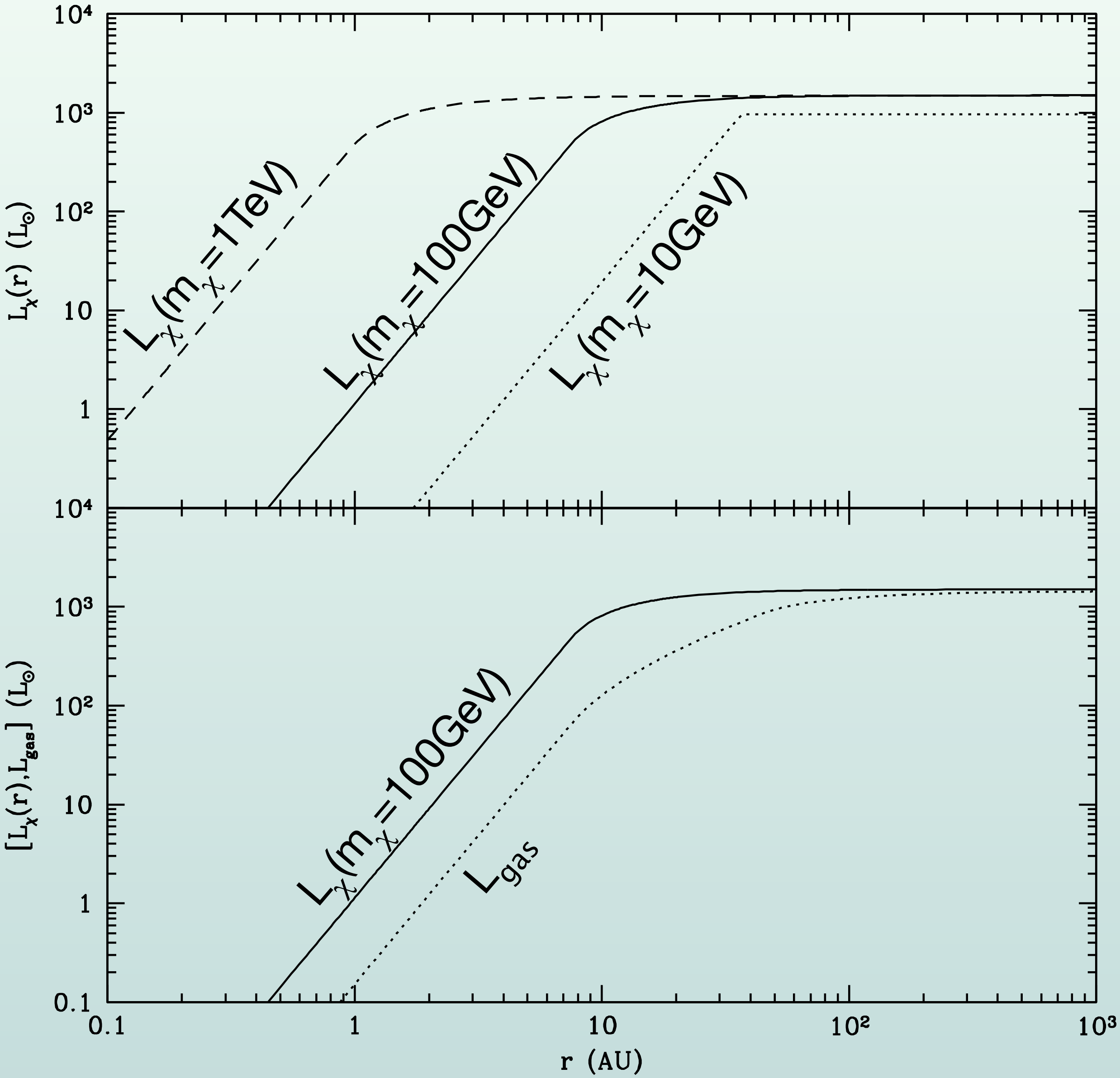

Enclosed Luminosity Profiles of "Equilibrium" Configurations

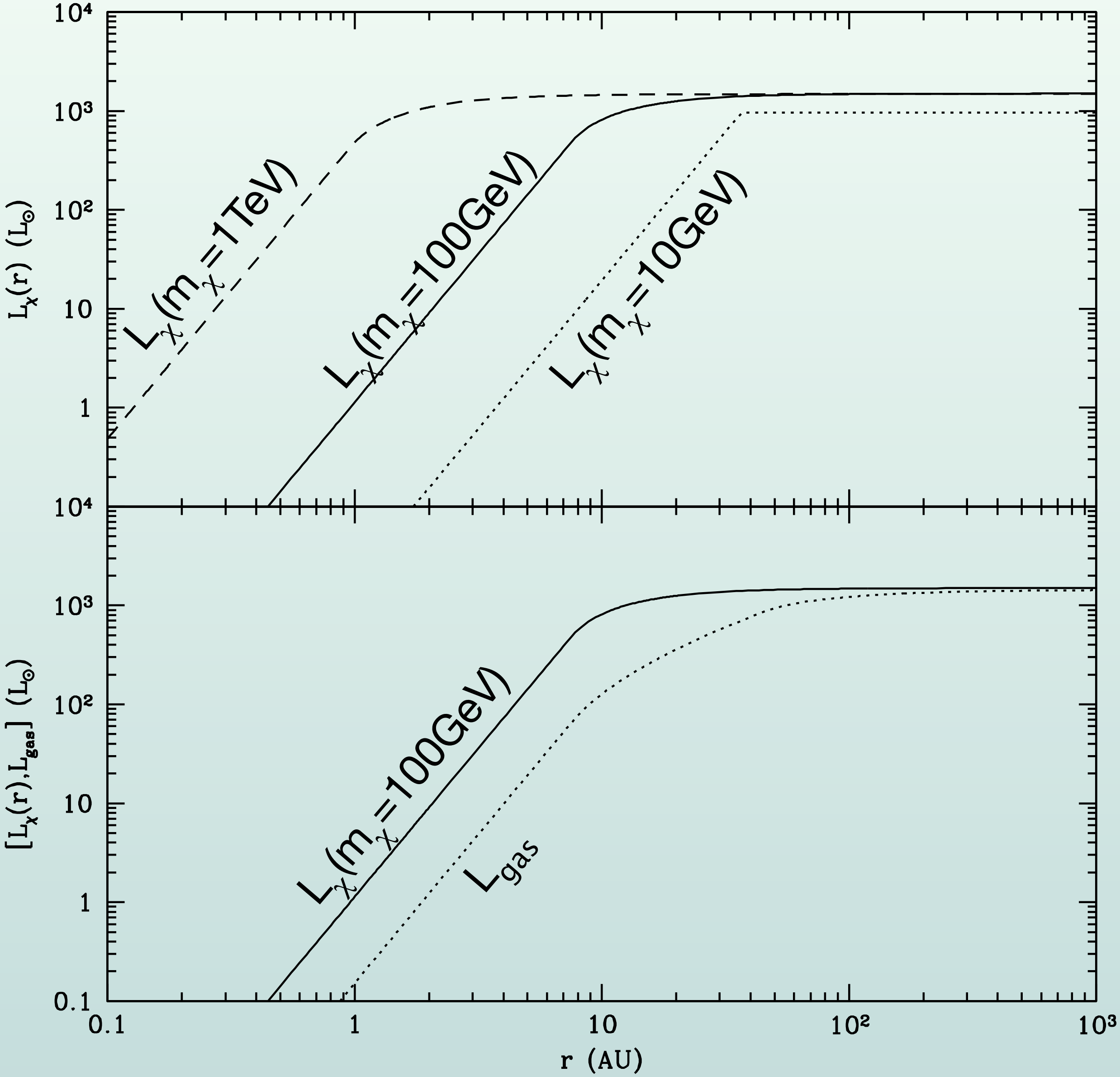

Subsequent evolution:

Baryons continue to accrete causing the star to need a larger luminosity to be supported.

Even if no additional DM accretes, the WIMP annihilation luminosity still rises dramatically as the star contracts:

$$L_\chi \simeq 1000 \left(\frac{r_*}{r_{*,0}}\right)^{-3} L_\odot$$

Enclosed Luminosity Profiles of "Equilibrium" Configurations

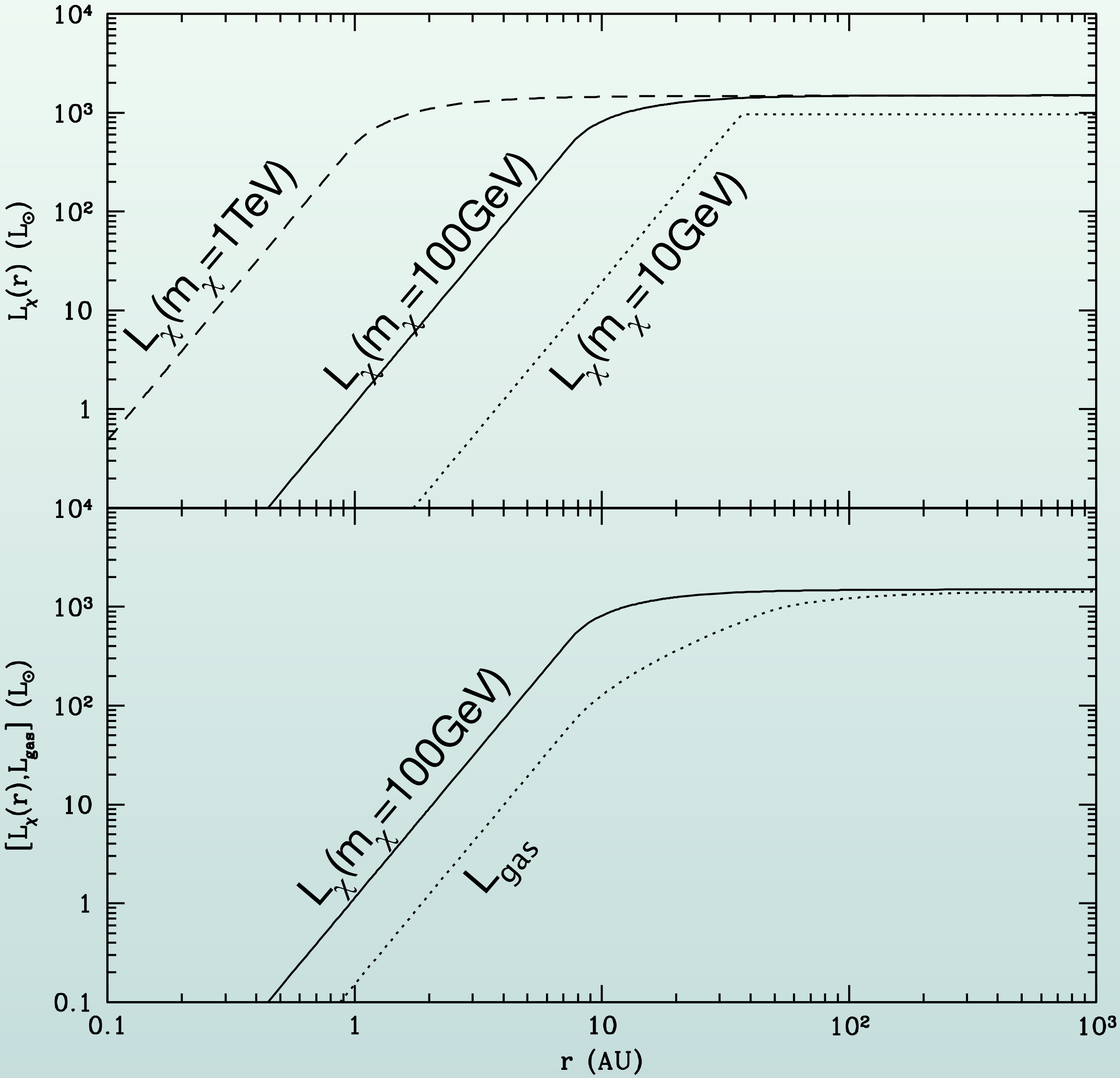

Subsequent evolution:

Baryons continue to accrete causing the star to need a larger luminosity to be supported.

Even if no additional DM accretes, the WIMP annihilation luminosity still rises dramatically as the star contracts:

$$L_\chi \simeq 1000 \left(\frac{r_*}{r_{*,0}}\right)^{-3} L_\odot$$

Contraction from 10AU to 1AU leads to L~$10^6 L_\odot$, enough to support a ~$100 M_\odot$ star. The depletion time becomes similar to the growth time ~10^5yr.

Enclosed Luminosity Profiles of "Equilibrium" Configurations

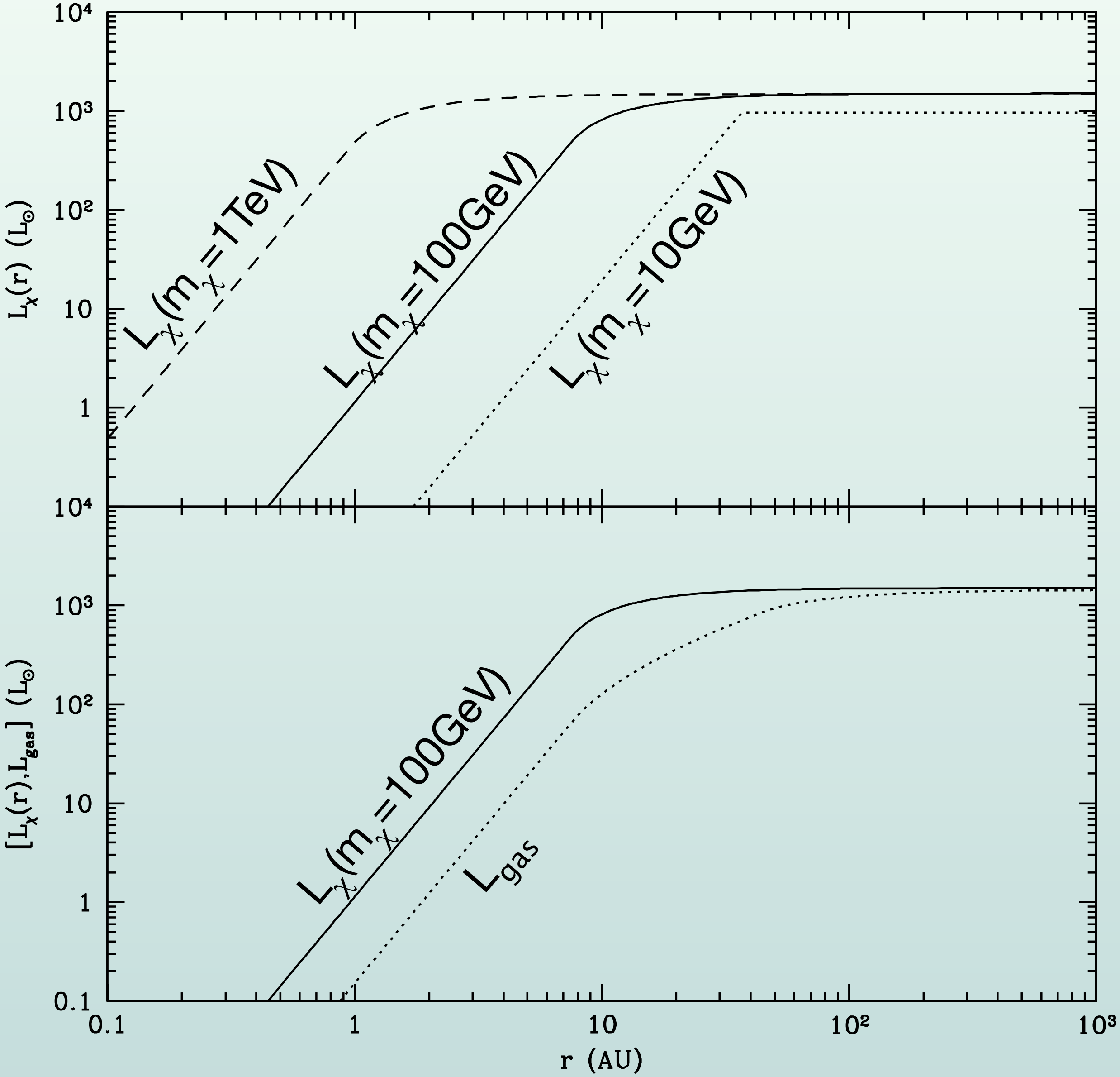

Subsequent evolution:

Baryons continue to accrete causing the star to need a larger luminosity to be supported.

Even if no additional DM accretes, the WIMP annihilation luminosity still rises dramatically as the star contracts:

$$L_\chi \simeq 1000 \left(\frac{r_*}{r_{*,0}}\right)^{-3} L_\odot$$

Contraction from 10AU to 1AU leads to $L \sim 10^6 L_\odot$, enough to support a $\sim 100 M_\odot$ star. The depletion time becomes similar to the growth time $\sim 10^5$yr.

WIMP annihilation heating may delay contraction to the main sequence and thus radiative feedback truncation of accretion, which could lead to supermassive Pop III.1 stars.

Protostellar accretion rate

Tan & McKee 2008

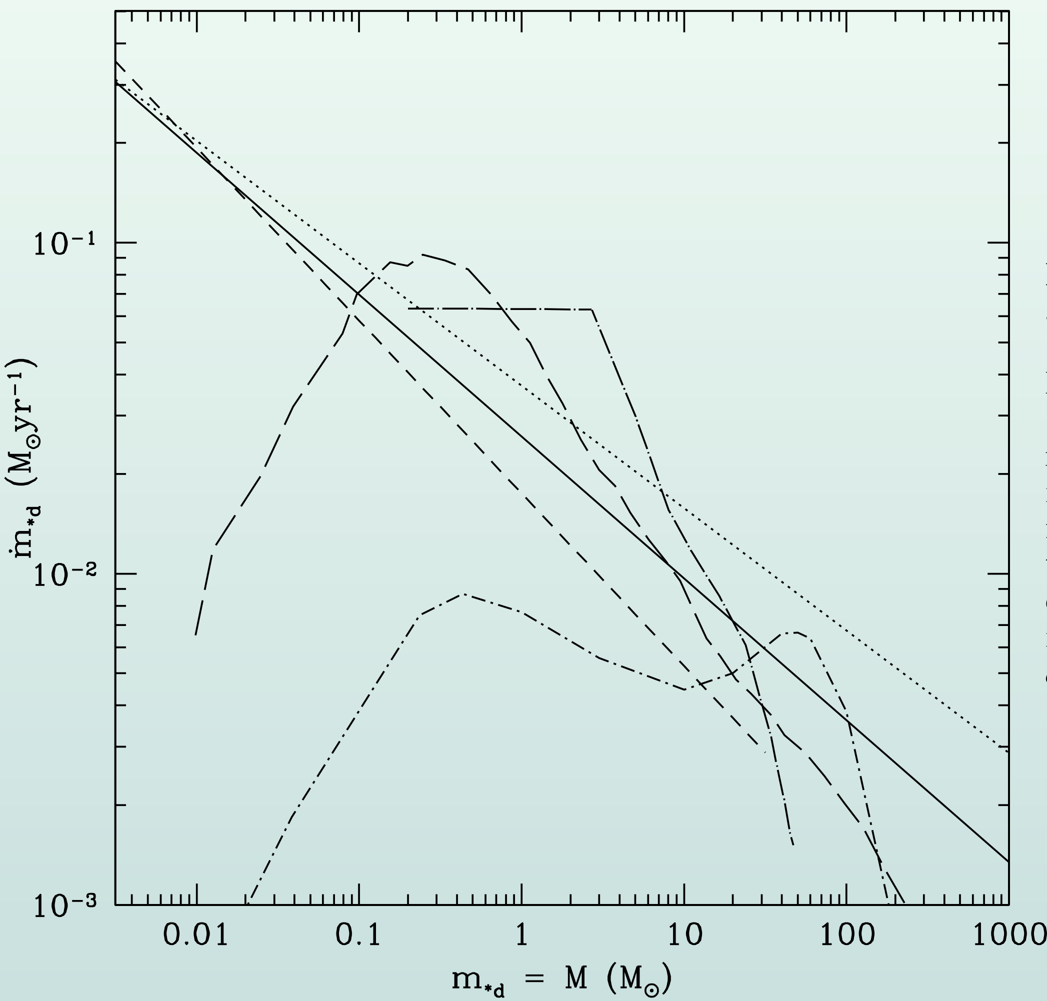

FIGURE 1. Mass accretion rate onto the protostar+disk as a function of their total mass m_{*d} for the case of negligible stellar feedback. *Solid* line is the fiducial model from Tan & McKee [26] (with $K' = 1$) from eq. (4). *Dotted* line is from the 1D model of Omukai & Nishi [27]. *Dashed* line is the analytic result from Ripamonti et al. [28]. *Dot-dashed* line is the settling inflow rate at the final stage of the simulation of Abel et al. [23], now as a function of the enclosed mass. Note that the decline of this rate at small masses is due to the lack of the full set of high density cooling processes in their simulation. *Long-dashed* line is the equivalent quantity from Yoshida et al.[31]. *Dot-long-dashed* line is the sink particle accretion rate of Bromm & Loeb [25].

Protostellar radius

Tan & McKee 2008

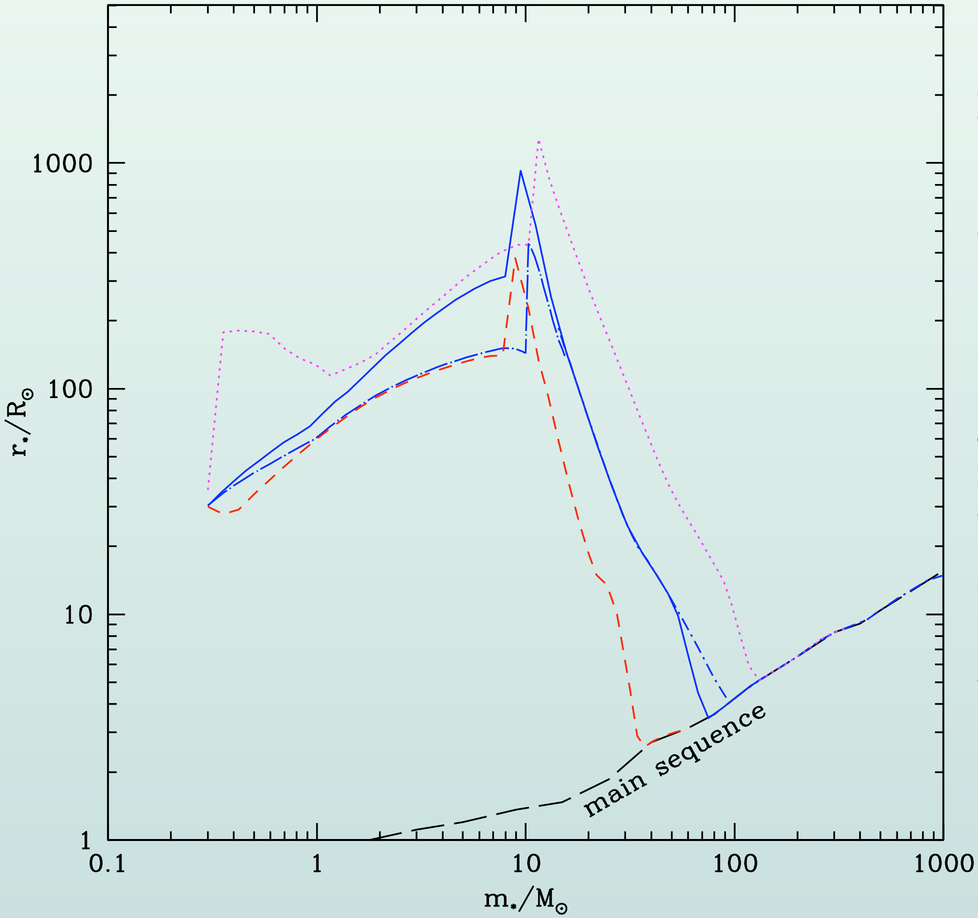

FIGURE 2. Evolution of protostellar radius with mass, based on the model of Tan & McKee [26]. All models shown have a rotation parameter $f_{\rm Kep} = 0.5$. The *solid* line shows the evolution of the fiducial model with $K' = 1$, a Shakura-Sunyaev disk viscosity parameter of $\alpha_{\rm ss} = 0.01$, and a reduction of accretion rate due to feedback effects [15], which becomes important for $m_* \gtrsim 50 M_\odot$. The star joins the main sequence [36], shown by the *long dashed* line, at about $80 M_\odot$. The *dot-dashed* line, visible only from $50-100 M_\odot$, shows the same model but with no reduction in accretion rate due to feedback effects. The *dot-long-dashed* line, visible up to about $20 M_\odot$ shows the fiducial model, but with $\alpha_{\rm ss} = 0.3$ (appropriate for viscosity driven by self-gravity [37]). The *dotted* line shows the fiducial model but with $K' = 2$, while the *dashed* line shows the $K' = 0.5$ case.

Protostellar Disk Radial Structure

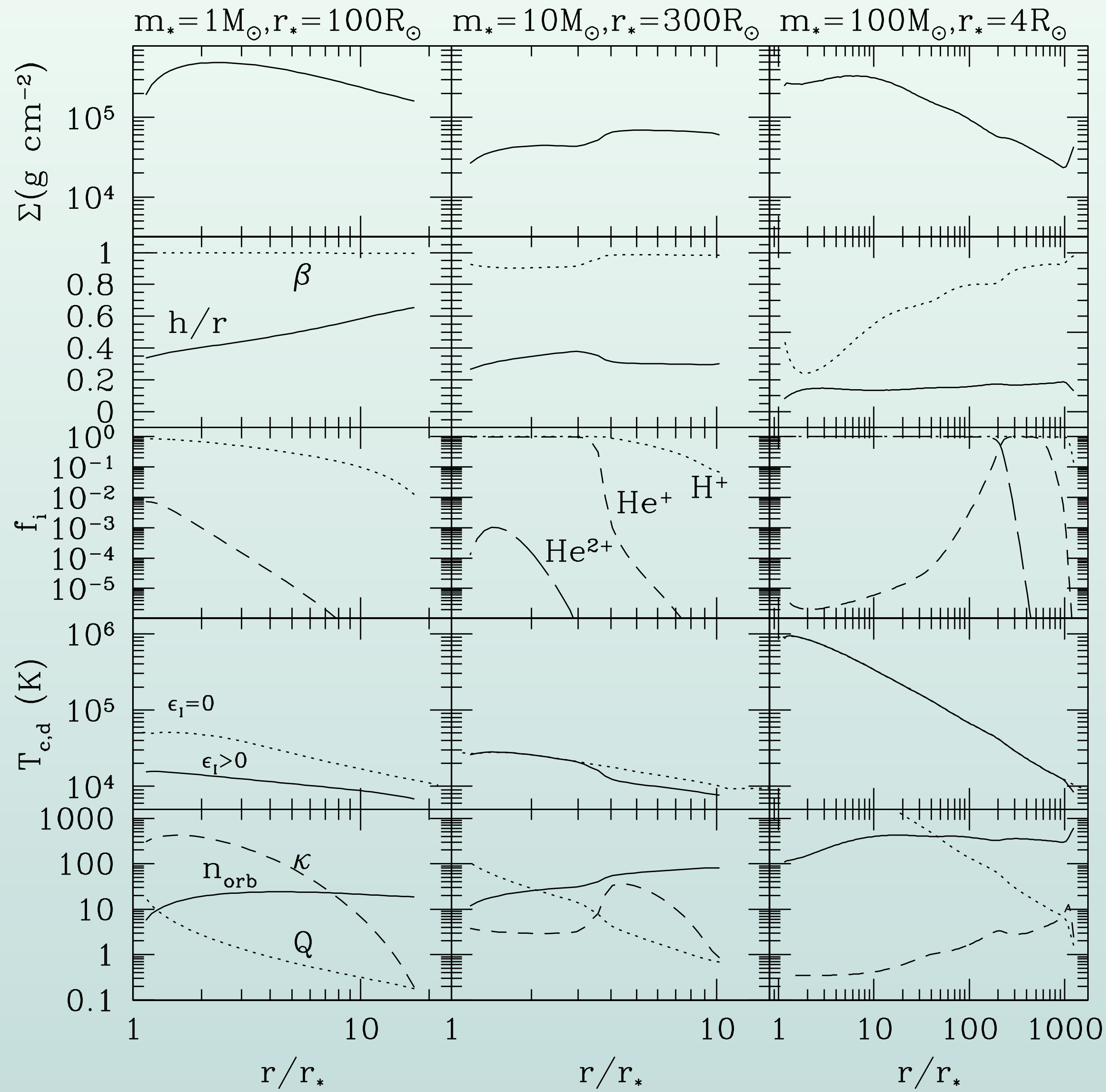

FIGURE 3. Protostellar disk structure [40] for models with $\alpha_{ss} = 0.01$ and $m_* = 1, 10, 100 M_\odot$, for which $r_* = 100, 300, 4 R_\odot$ and $\dot{m}_* = (17, 6.4, 2.4) \times 10^{-3} M_\odot\ \mathrm{yr}^{-1}$, respectively, i.e. from eq. 4 with no feedback. From top to bottom the panels show (1) surface density, Σ; (2) ratio of scaleheight to radius, h/r, and ratio of gas pressure to total pressure, β; (3) midplane ionization fractions of H^+, He^+, He^{2+}; (4) disk midplane temperature, $T_{c,d}$ (the dotted lines show results for when the ionization energy is neglected); (5) number of orbits before accretion to the star, n_{orb}, Toomre Q stability parameter, and Rosseland mean opacity κ, evaluated at the midplane. Note that all quantities are azimuthal and temporal averages of the disk, which, being turbulent, would exhibit local fluctuations.

Protostellar Disk Vertical Structure

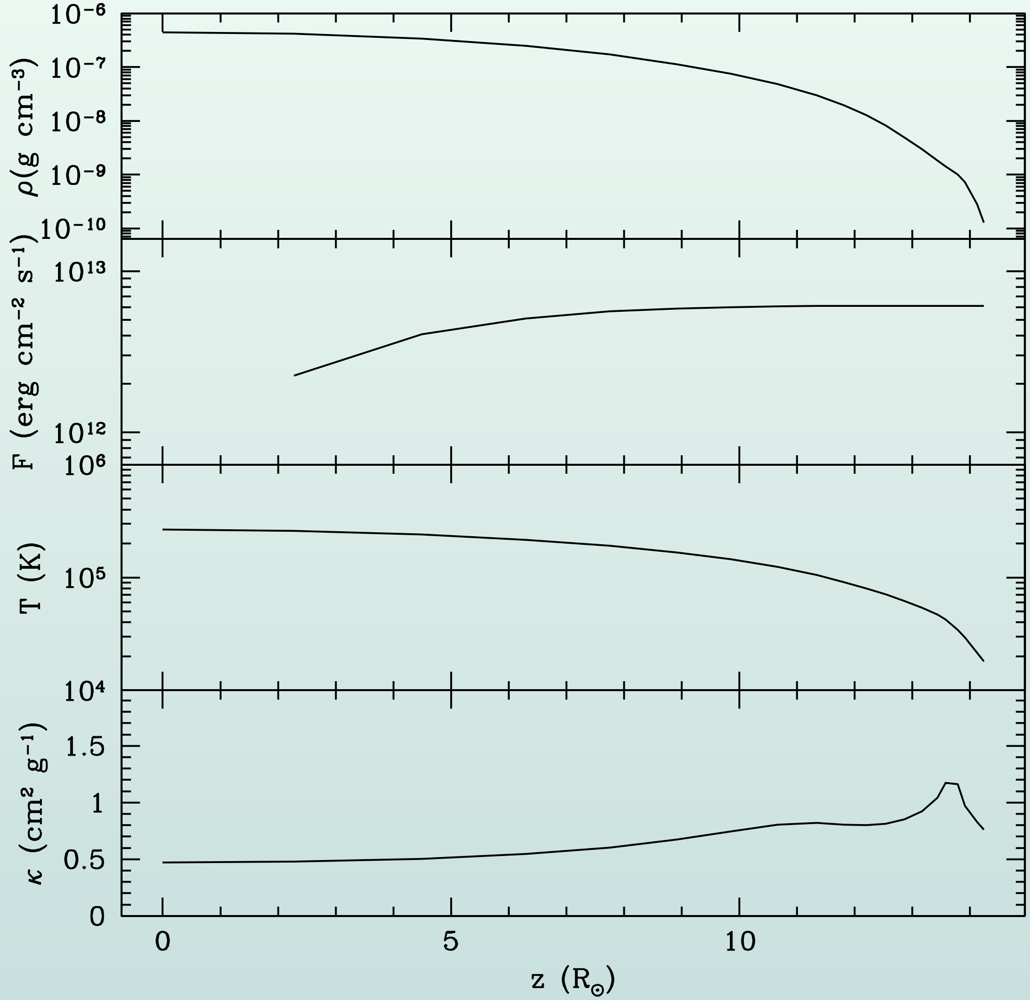

FIGURE 4. Vertical structure of the accretion disk at $r = 10r_* \simeq 43R_\odot$ for $m_* = 100\,M_\odot$, $K' = 1$, $f_{\rm Kep} = 0.5$ and no reduction in accretion efficiency due to feedback.

Protostellar Luminosity

Tan & McKee 2008

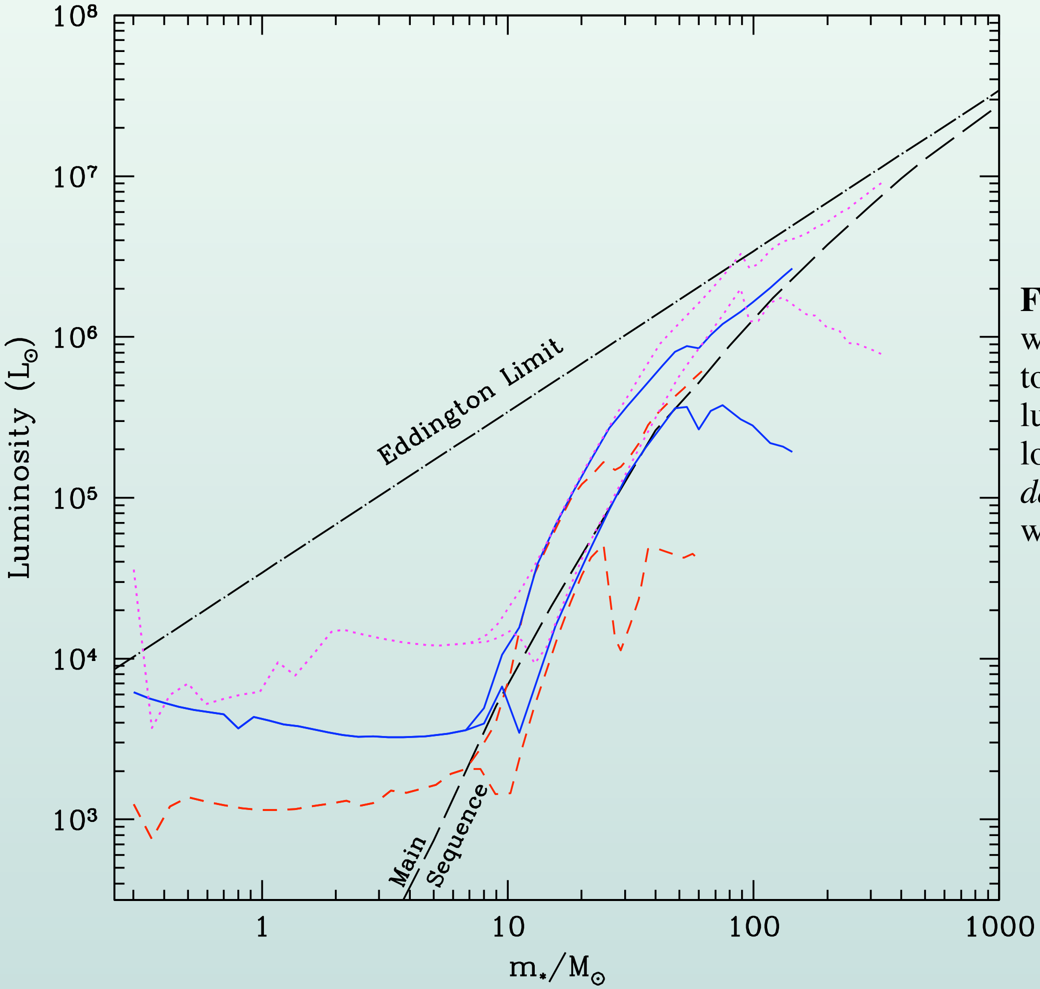

FIGURE 5. Protostellar bolometric luminosities for models with $K' = 0.5, 1, 2$ (*dashed, solid, dotted* lines). In each case the total luminosity is shown with the higher line and the accretion luminosity (boundary layer + inner disk) is shown with the lower line. The Eddington limit is indicated with the *dot-long-dashed* line and the zero age main sequence luminosity [36] with the *long-dashed* line.

Protostellar Ionizing Luminosity

Tan & McKee 2008

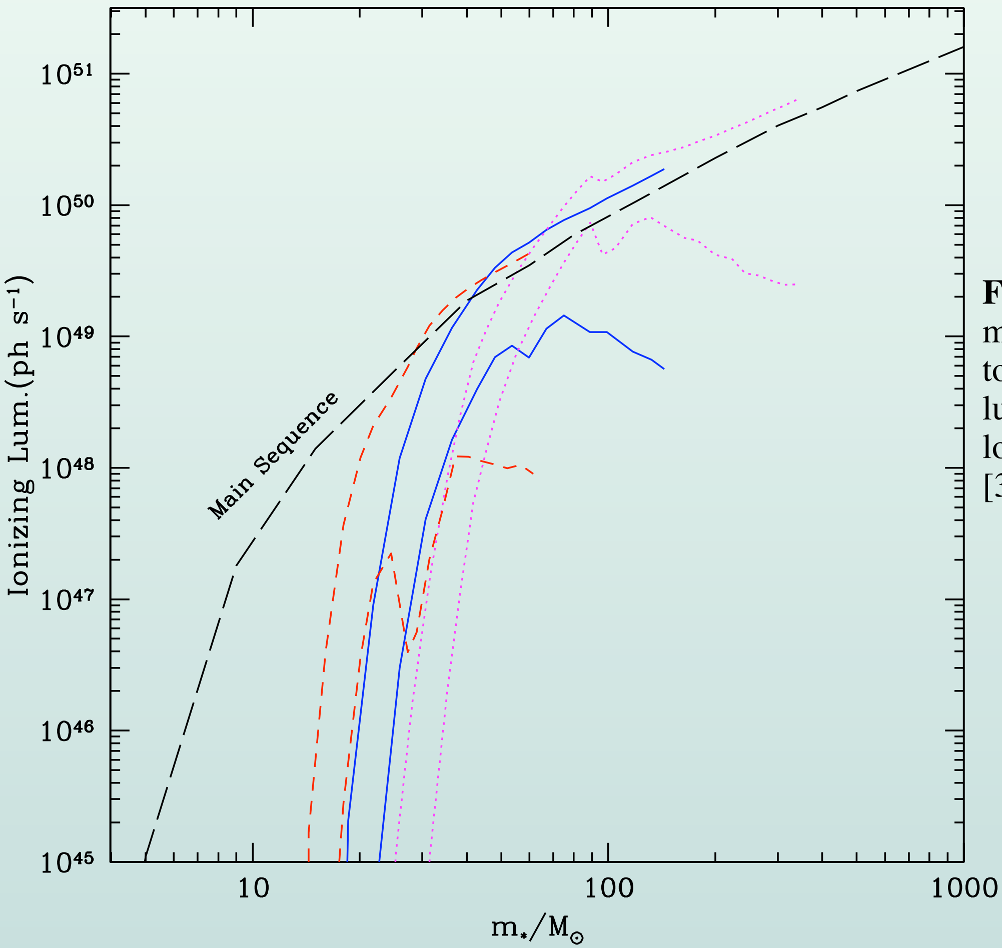

FIGURE 6. Protostellar H-ionizing photon luminosities for models with $K' = 0.5, 1, 2$ (*dashed, solid, dotted* lines). The total luminosity is shown with the higher line and the accretion luminosity (boundary layer + inner disk) is shown with the lower line. The zero age main sequence H-ionizing luminosities [36] are indicated with the *long-dashed* line.

Mass Scales of Pop III.1 Protostellar Feedback

TABLE 1. Mass Scales of Population III.1 Protostellar Feedback

K'	$f_{\rm Kep}$	$T_i/(10^4\ {\rm K})$	$m_{*,\rm pb}\ (M_\odot)^*$	$m_{*,\rm eb}\ (M_\odot)^\dagger$	$m_{*,\rm evap}\ (M_\odot)^{**}$
1	0.5	2.5	45.3	50.4	$137^\ddagger$
1	0.75	2.5	37	41	137
1	0.25	2.5	68	81	143
1	0.125	2.5	106	170	173
1	0.0626	2.5	182	$330^\S$	256
1	0.5	5.0	35	38	120
1	0.25	5.0	53.0	61	125
0.5	0.5	2.5	23.0	24.5	57
2.0	0.5	2.5	85	87	321

* Mass scale of HII region polar breakout.

† Mass scale of HII region near-equatorial breakout.

** Mass scale of disk photoevaporation limited accretion.

‡ Fiducial model.

§ This mass is greater than $m_{*,\rm evap}$ in this case because it is calculated without allowing for a reduction in $\dot{m}_*$ during the evolution due to polar HII region breakout.

Magnetic Fields: Saturation Points

Tan & Blackman (2004)

$$\overline{B}_r \sim 49\mathrm{G}(\alpha_{ss}/0.01)^{1/2}(m_*/M_\odot)^{1/4}(\dot{m}_*/0.01M_\odot\mathrm{yr})^{1/2}(r/10^{13}\mathrm{cm})^{-3/4}(h/10^{12}\mathrm{cm})^{-1/2}$$

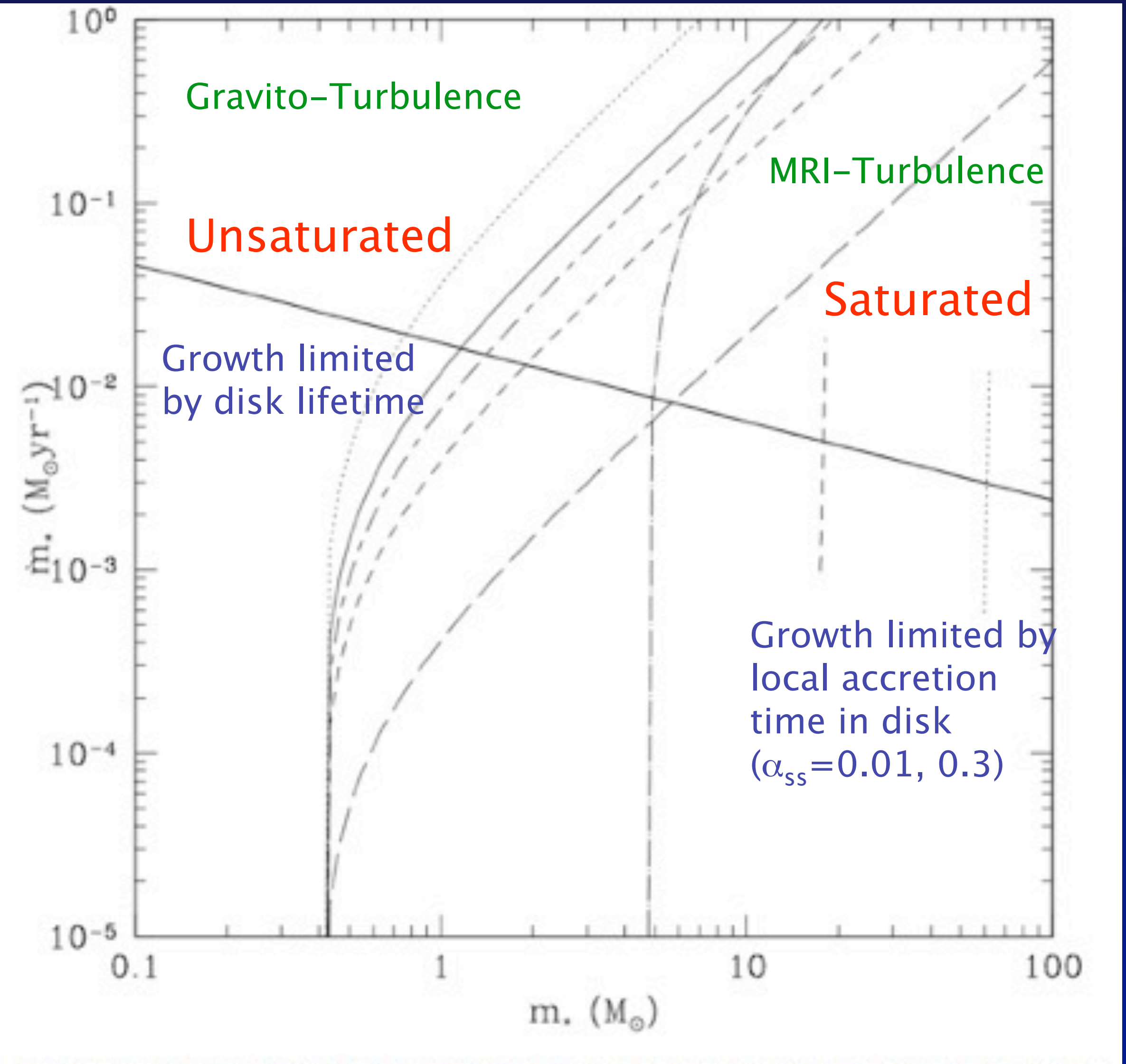

Exponential growth of seed field ($B \sim 10^{-16}$G) eventually becomes resistively limited (Blackman & Field 2002).

$t \sim m_*/\dot{m}_*$

Magnetic Fields: Saturation Points

Tan & Blackman (2004)

$$\overline{B}_r \sim 49\mathrm{G}(\alpha_{ss}/0.01)^{1/2}(m_*/M_\odot)^{1/4}(\dot{m}_*/0.01M_\odot\mathrm{yr})^{1/2}(r/10^{13}\mathrm{cm})^{-3/4}(h/10^{12}\mathrm{cm})^{-1/2}$$

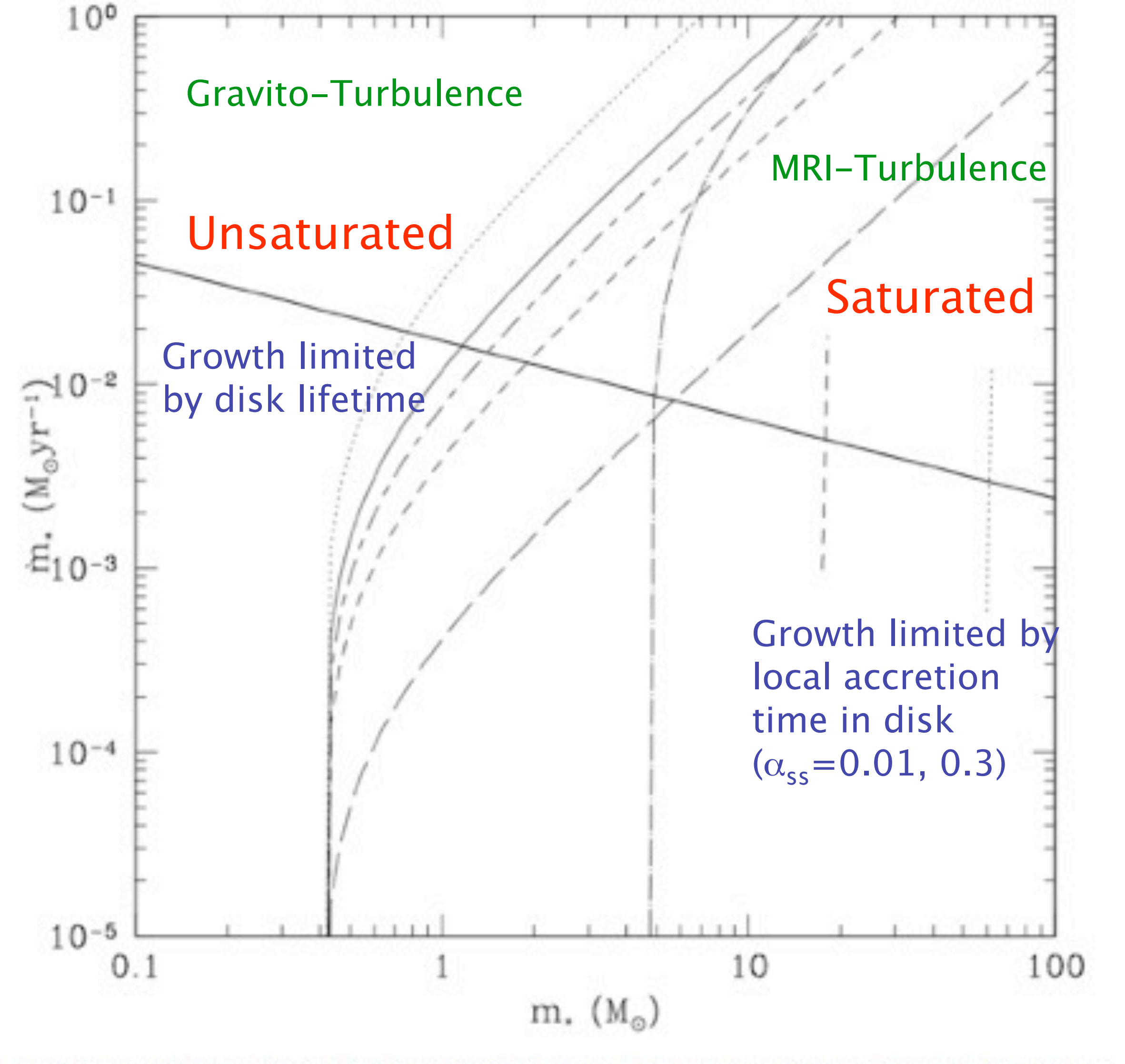

Exponential growth of seed field ($B \sim 10^{-16}$G) eventually becomes resistively limited (Blackman & Field 2002).

$t \sim m_* / \dot{m}_*$

Either Gravito– or MRI–driven turbulence can provide viscosity to remove angular momentum.

Magnetic Fields: Inverse Helical Dynamo

Blackman & Field (2002)

Turbulence in disk amplifies field strength, eventually saturating due to back reaction of B-field (Tan & Blackman 2004).

Large-scale helicity is generated in each hemisphere, leading to strong, coherent, large-scale B-fields, which rise up to form a corona and outflow.

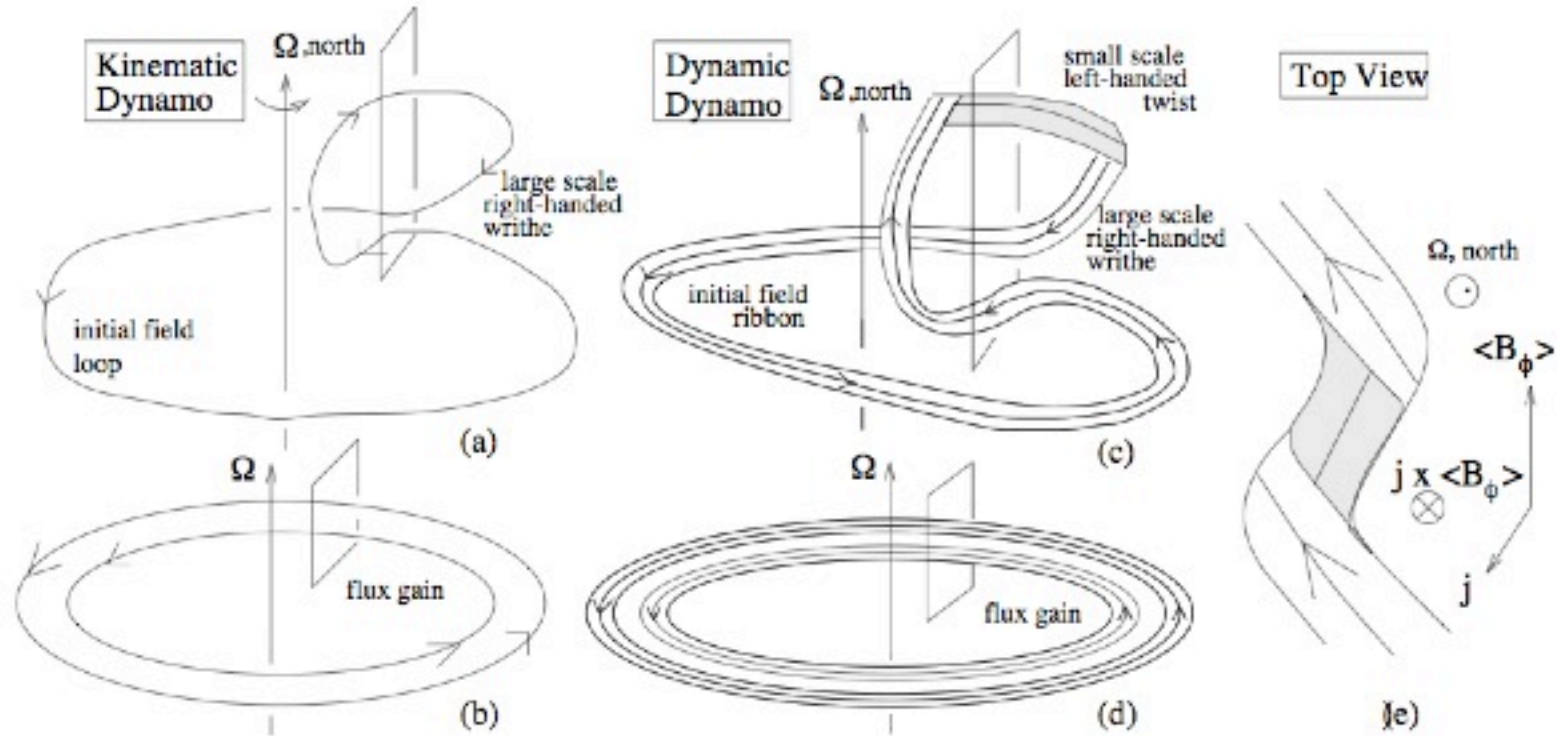

Figure 2. Kinematic helical dynamo diagram (left) ignores magnetic helicity conservation. In dynamic theory field should be replaced by ribbon, showing the conservation (Blackman & Brandenburg 2003).

Magnetic Fields: Dynamical Effect of Outflows

Tan & Blackman (2004); Machida ea. (2006)

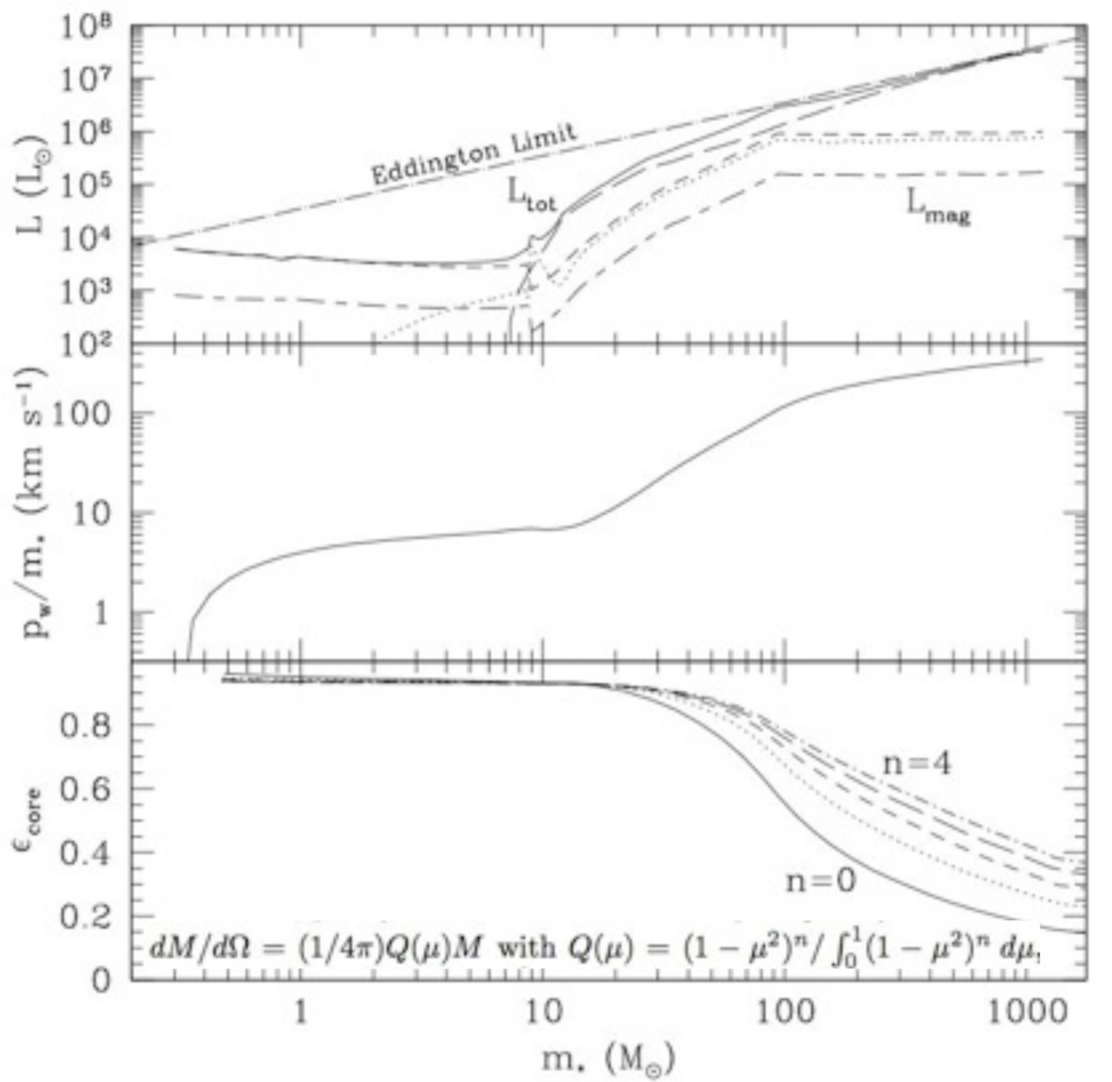

$$\frac{dp_w}{d\Omega} = \frac{p_w}{4\pi} \frac{1}{\ln(2/\theta_0)(1+\theta_0^2-\mu^2)}$$

Outflow momentum angular distribution (Matzner & McKee 1999)

Outflow power from Poynting flux

Efficiency of accretion from core due to outflow

Instantaneous Star Formation Efficiency

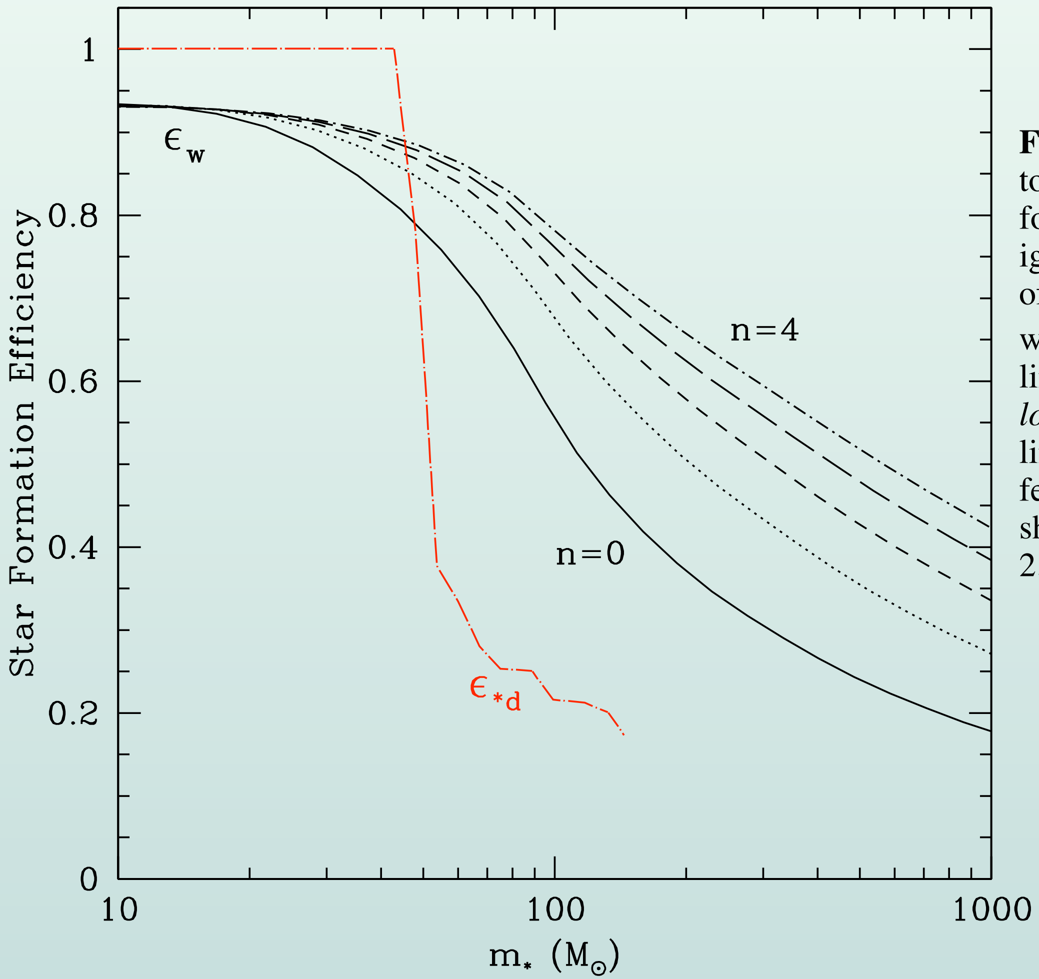

FIGURE 11. Evolution of star formation efficiency, ε_w, due to erosion of a $1000 M_\odot$ gas core by protostellar outflows winds for the fiducial $f_{\rm Kep} = 0.5$ and $K' = 1$ case, with $\alpha_{\rm ss} = 0.01$, and ignoring radiative feedback processes [40]. The density profile of the initial core is specified by $dM/d\Omega = (1/4\pi)Q(\mu)M$, with $\mu = \cos\theta$ and $Q(\mu) = (1-\mu^2)^n / \int_0^1 (1-\mu^2)^n \, d\mu$. *Solid* line is $n = 0$ (isotropic core), *dotted* is $n = 1$, *dashed* is $n = 2$, *long-dashed* is $n = 3$, *dot-dashed* is $n = 4$. The *dot-long-dashed* line shows the instantaneous efficiency, ε_{*d}, due to radiative feedback processes (i.e. H II region breakout, limited by disk-shadowing) for the fiducial model ($f_{\rm Kep} = 0.5$, $K' = 1$, $T_{i,4} = 2.5$), indicating their greater importance at $m_* \gtrsim 50 M_\odot$.

Disk Models (Tan & McKee 2004; Tan & Blackman 2004)

α=0.3

Surface density

Thickness

Ionization

Temperature
T_c , T_{eff}

Toomre $Q = \frac{c_s \Omega}{\pi G \Sigma}$

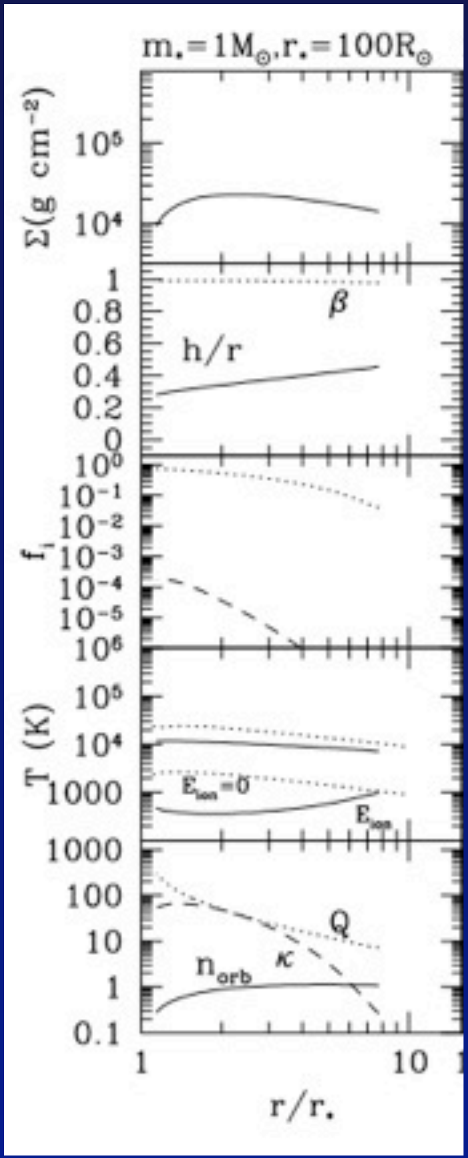

$\dot{m}_*$ $17 \times 10^{-3} M_\odot/yr$

Disk Models (Tan & McKee 2004; Tan & Blackman 2004)

α=0.3

Surface density

Thickness

Ionization

Temperature

T_c , T_{eff}

Toomre $Q = \frac{c_s \Omega}{\pi G \Sigma}$

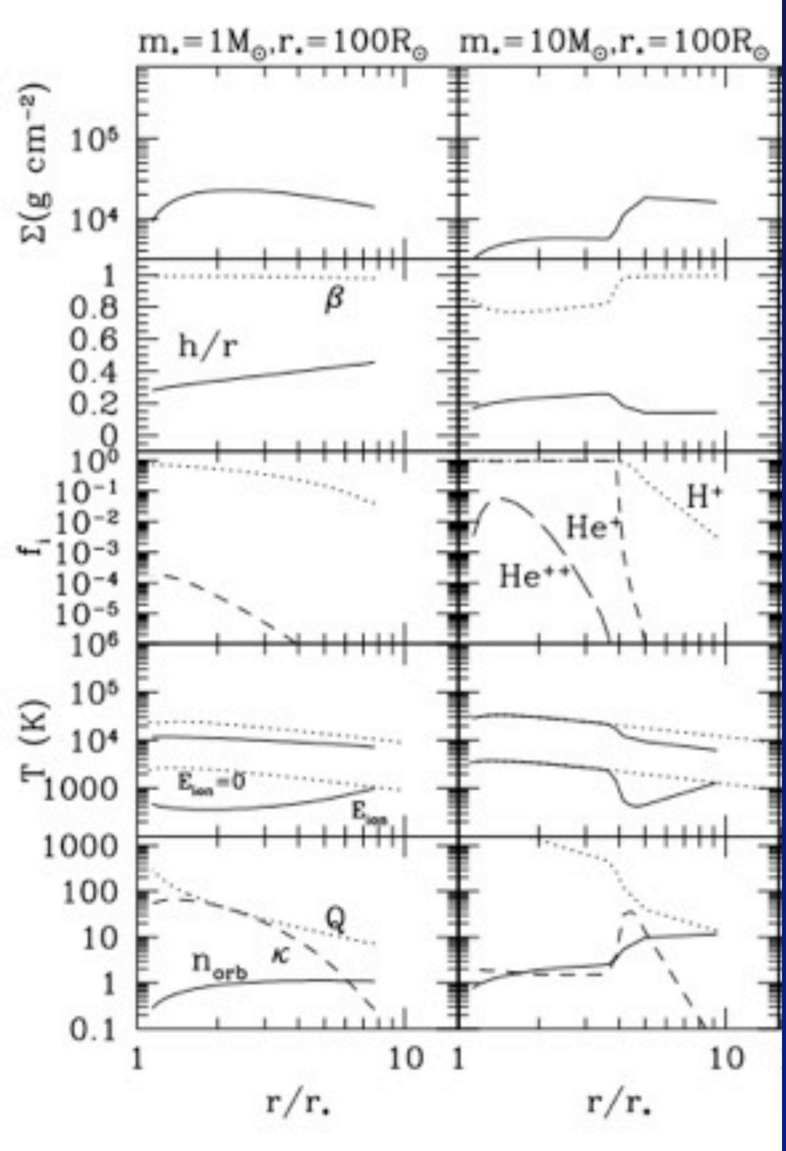

$\dot{m}_*$ 17x10^{-3}M$_\odot$/yr 6.4x10^{-3}M$_\odot$/yr

Disk Models (Tan & McKee 2004; Tan & Blackman 2004)

$\alpha = 0.3$

Surface density

Thickness

Ionization

Temperature

T_c , T_{eff}

Toomre $Q = \dfrac{c_s \Omega}{\pi G \Sigma}$

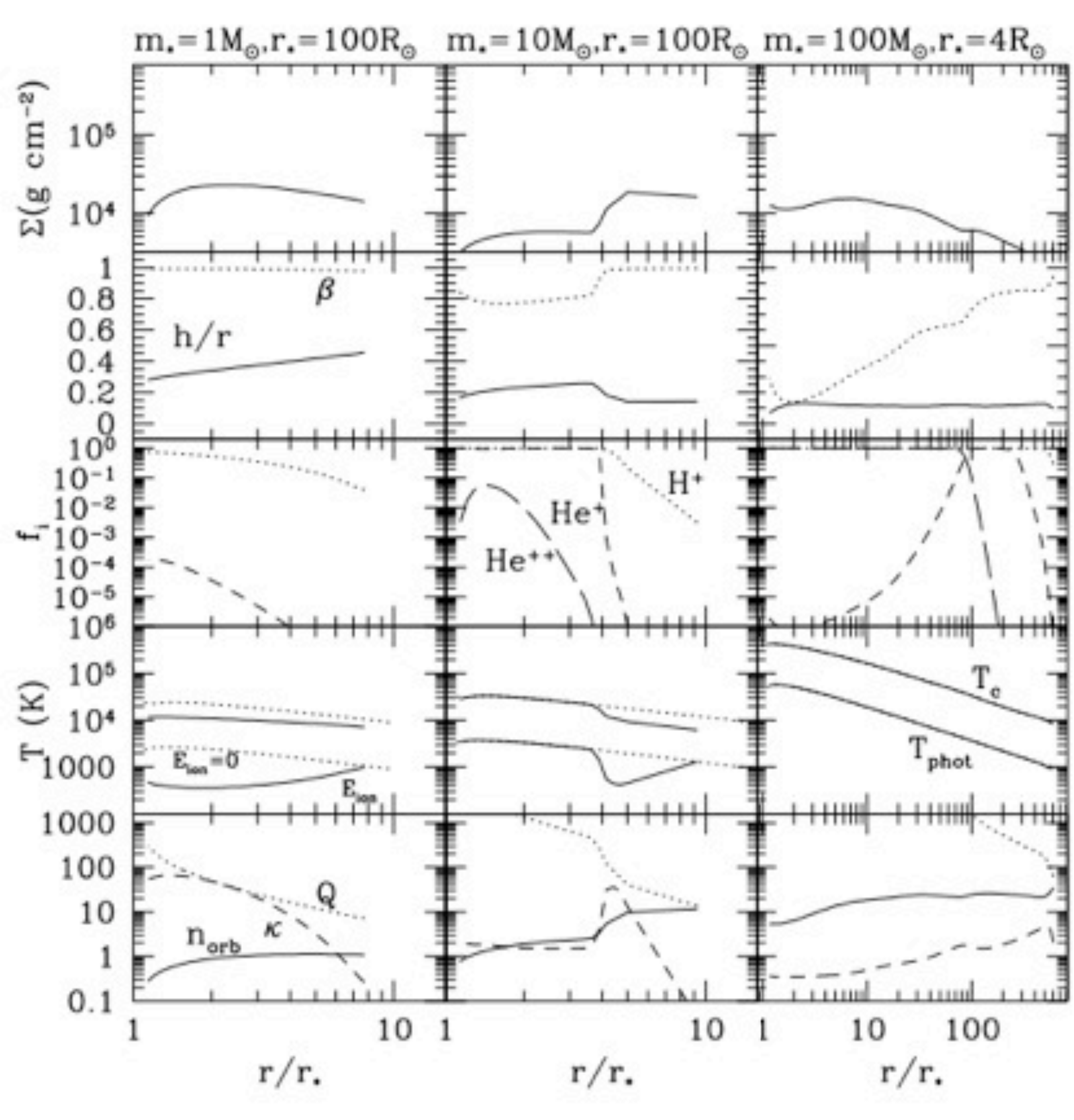

$\dot{m}_*$ 17x10^{-3}M$_\odot$/yr 6.4x10^{-3}M$_\odot$/yr 2.4x10^{-3}M$_\odot$/yr

Disk Models (Tan & McKee 2004; Tan & Blackman 2004)

α=0.3

Surface density

Thickness

Ionization

Temperature

T_c , T_{eff}

Toomre $Q = \frac{c_s \Omega}{\pi G \Sigma}$

Disks are stable

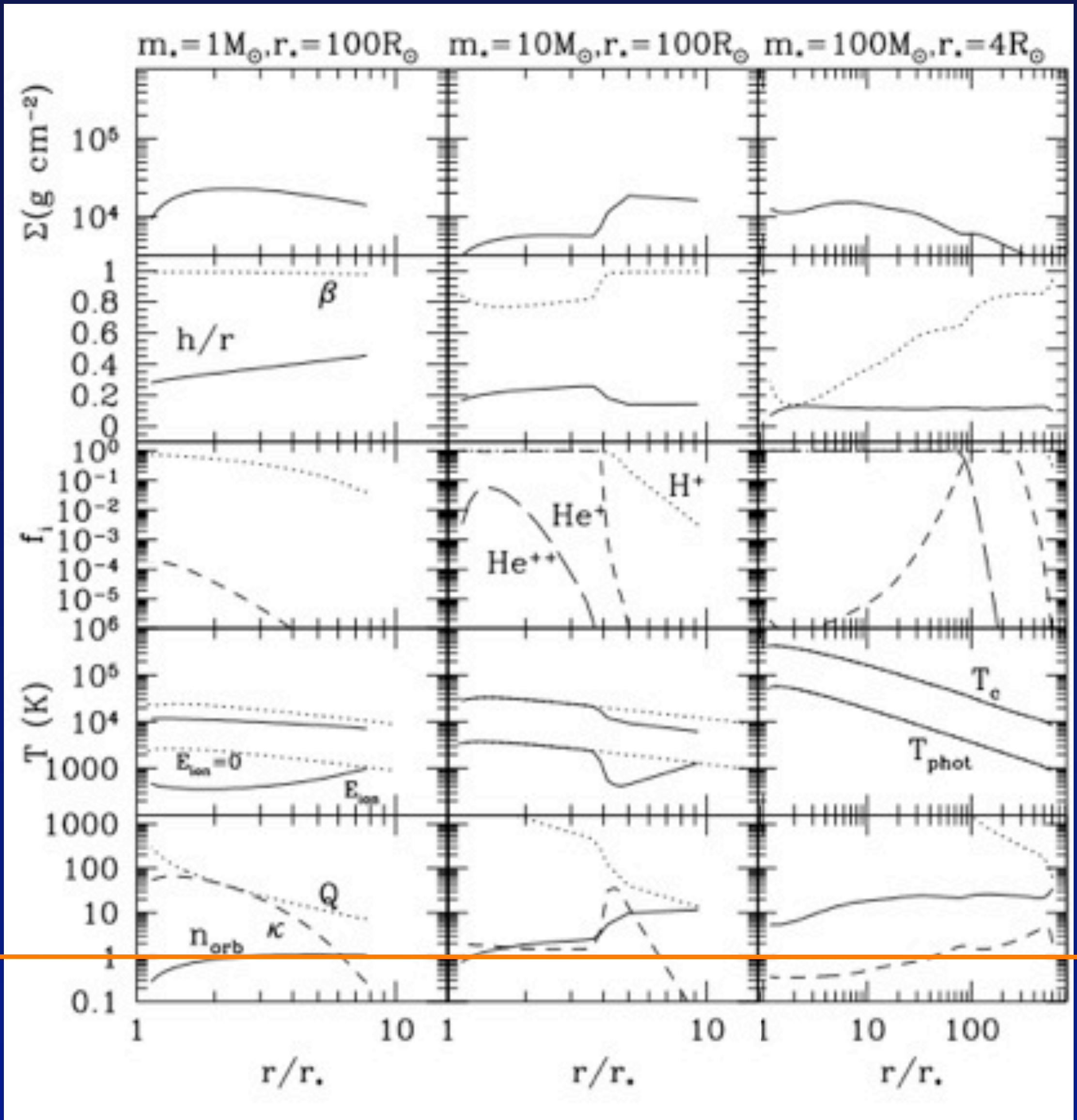

$\dot{m}_*$ 17x10^{-3}M⊙/yr 6.4x10^{-3}M⊙/yr 2.4x10^{-3}M⊙/yr

Implications of IMF for supernovae and metal enrichment

Metal production and dispersal via winds and supernovae depends on m_*

Pair Instability SNe for $m_*>140M_\odot$, Massive BH formation for $m_*>260M_\odot$

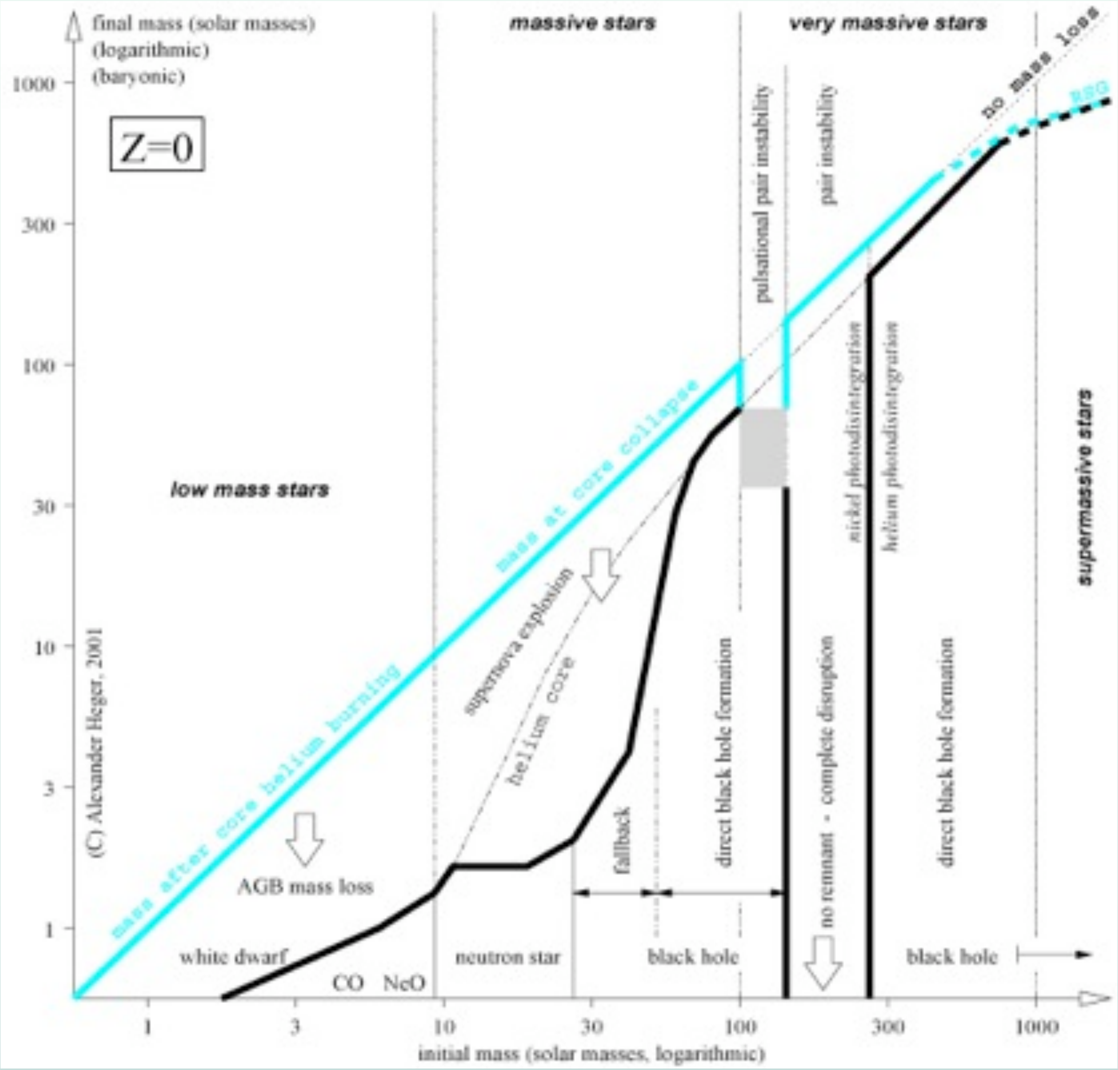

Fate of NON-ROTATING metal-free stars (Heger & Woosley 2002)

Abundance patterns from metal poor halo stars

Heger & Woosley (2008)

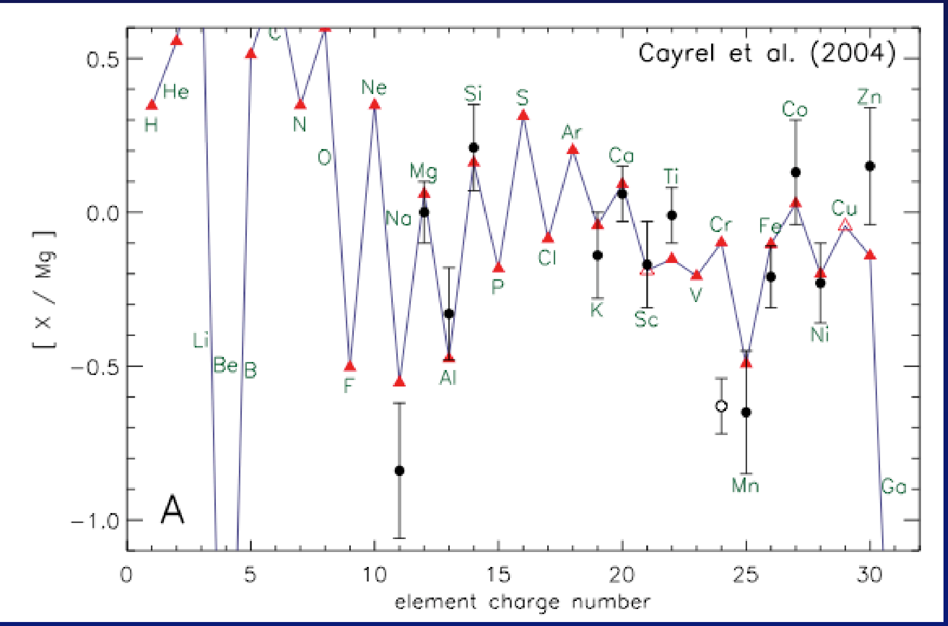

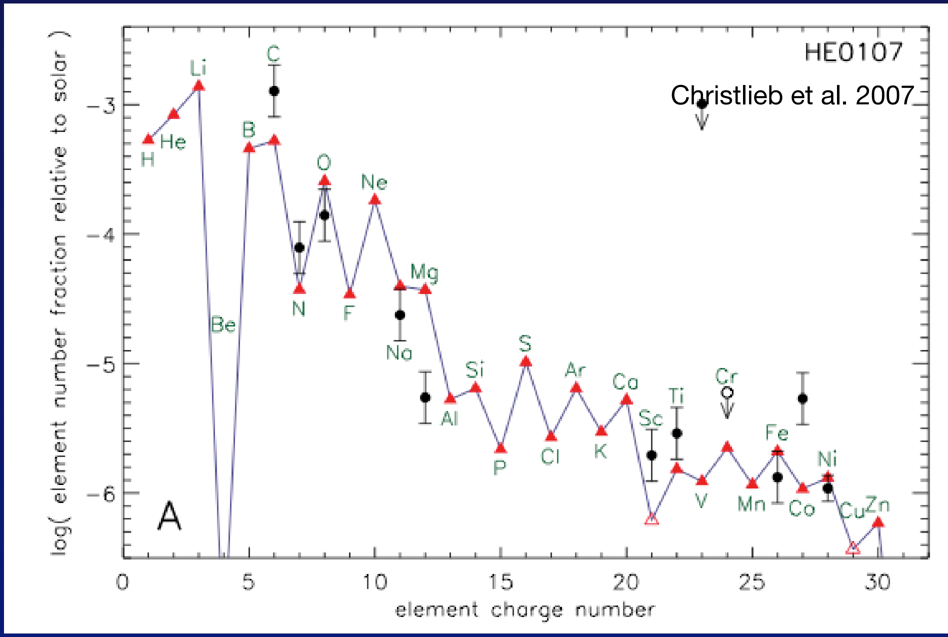

Gaussian IMF peaked at $11 M_\odot$ with width ±0.3dex

Single star: $20.5 M_\odot$

-> very massive Pop III stars are rare in environments probed by Galactic halo stars.

Implications for SMBH formation

It appears difficult to form a star that is massive enough so its final pre-SN mass is $>260M_\odot$, thus Pop III stellar remnants are likely to be relatively low-mass black holes.

Implications for SMBH formation

It appears difficult to form a star that is massive enough so its final pre-SN mass is $>260M_\odot$, thus Pop III stellar remnants are likely to be relatively low-mass black holes.

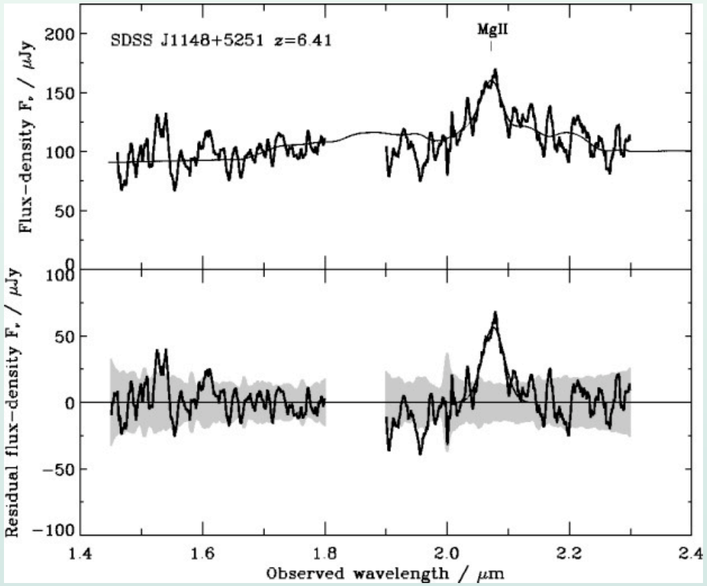

$3\times10^9 M_\odot$ BH at z=6.41

Fan et al. & Willott et al. (2003)

Age of Universe is 872Myr

Time since z=20 is 690Myr

Salpeter growth time is 45Myr

(for radiative efficiency = 0.1)

So need an initial mass of $660M_\odot$

Implications for SMBH formation

It appears difficult to form a star that is massive enough so its final pre-SN mass is >260M$_\odot$, thus Pop III stellar remnants are likely to be relatively low-mass black holes.

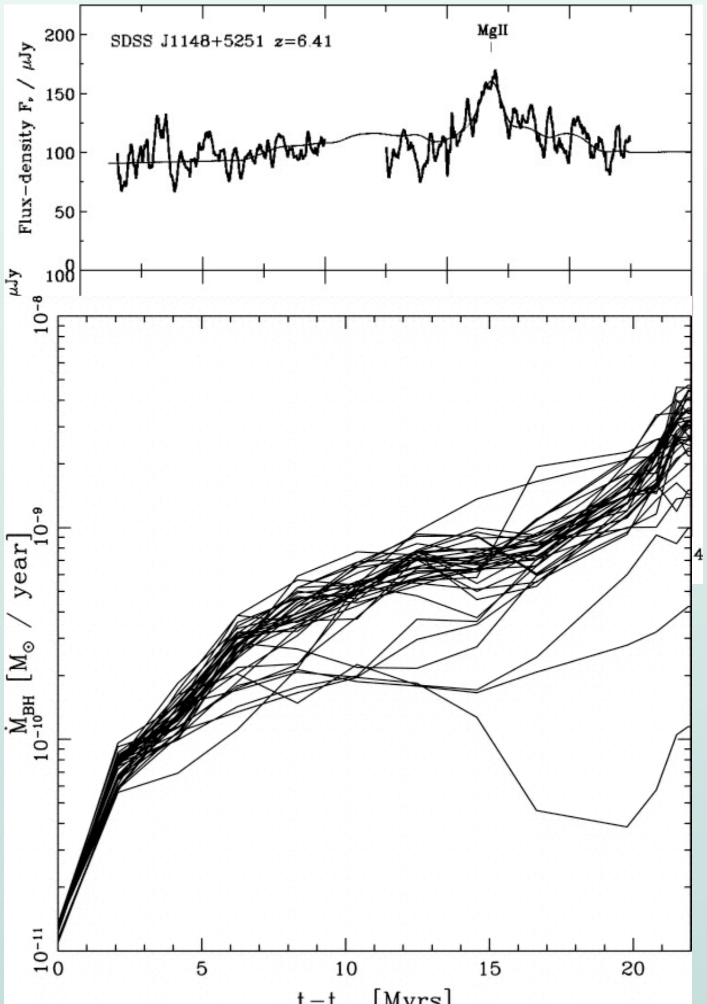

3x10^{9}M$_\odot$ BH at z=6.41

Fan et al. & Willott et al. (2003)

Age of Universe is 872Myr

Time since z=20 is 690Myr

Salpeter growth time is 45Myr (for radiative efficiency = 0.1)

So need an initial mass of 660M$_\odot$

However, actual accretion rates of PopIII remnants are likely to be much smaller (10^{-3}) than Eddington (O'Shea et al. 2004).

It appears to be difficult to form SMBHs from PopIII star remnants. Is there a different astrophysical mechanism?

Feedback and Pop III.2 Star Formation

Pop III.1 stars will likely ionize their host minihalo, suppress H_2 formation in very nearby halos, drive ionization fronts into nearby halos (perhaps inducing star formation - Whalen et al. 08)

Pop III.2 stars have their initial conditions significantly affected by astrophysical sources.

We expect the primary effect is due to ionizing radiation: gas that has been ionized and then recombines, has a high residual e^- fraction, which catalyzes H_2 and HD production.

HD cooling -> K' ~0.1. Greif & Bromm (2006) estimate $m_* \sim 10 M_\odot$

Transition to Pop II:

Critical Metallicity (Z_{crit}) for cooling to be dominated by metals

The cooling rate due to primordial coolants (H_2, HD) will depend on temperature, density and ionization history.

The cooling rate due to metals will depend on temperature, density, abundance pattern, dust content.

Estimates of Z_{crit} : $10^{-3.5}$ fine structure lines C, O and no H_2

(Bromm & Loeb 2003)

10^{-6} small dust grains

(Omukai et al. 2005)

$\sim 10^{-2}$ for gas phase metals if include H_2

(Jappsen et al. 2007)

Transition to Pop II:

Critical Metallicity (Z_{crit}) for cooling to be dominated by metals

The cooling rate due to primordial coolants (H_2, HD) will depend on temperature, density and ionization history.

The cooling rate due to metals will depend on temperature, density, abundance pattern, dust content.

Estimates of Z_{crit} : $10^{-3.5}$ fine structure lines C, O and no H_2

(Bromm & Loeb 2003)

10^{-6} small dust grains

(Omukai et al. 2005)

$\sim 10^{-2}$ for gas phase metals if include H_2

(Jappsen et al. 2007)

Stellar evolution is likely to have a more sensitive dependence on metallicity ($Z_{crit} \sim 10^{-8}$) i.e. CNO cycle (Meynet)

Transition from Pop III

- Pop III cores supported by thermal pressure
- Present-day cores and protoclusters supported by magnetic fields and turbulence
- Magnetic fields and turbulence unlikely to be effective in post-PopIII regions

  (B-fields probably too weak; turbulence damps out)

Transition from Pop III

- Pop III cores supported by thermal pressure
- Present-day cores and protoclusters supported by magnetic fields and turbulence
- Magnetic fields and turbulence unlikely to be effective in post-PopIII regions

  (B-fields probably too weak; turbulence damps out)

- Post-PopIII regions may be able to cool effectively via HD and/or metals-dust
- If c_s << virial velocity of halo, then gas should collapse to form a rotationally supported thin disk: possible fragmentation.

  (Lodato & P. Natarajan 2006; Clark, Glover & Klessen 2007)

  However, continued infall and merging of halos may maintain turbulence (Wise & Abel 2007)

Conclusions

Approximately convergent initial conditions for star formation: set by H_2 cooling. Mostly thermal pressure support + slow cooling -> no/little (disk) fragmentation -> single ~massive star in each mini-halo (no clusters of primordial stars). DM heating?

Conclusions

Approximately convergent initial conditions for star formation: set by H_2 cooling. Mostly thermal pressure support + slow cooling -> no/little (disk) fragmentation -> single ~massive star in each mini-halo (no clusters of primordial stars). DM heating?

Need analytic model to follow the growth of the protostar: accretion rate; accretion disk; protostellar evolution; feedback.

Large (~AU) protostar, contracts to main sequence for $m_* > 30 M_\odot$

This is when feedback processes start to become important.

Conclusions

Approximately convergent initial conditions for star formation: set by H_2 cooling. Mostly thermal pressure support + slow cooling -> no/little (disk) fragmentation -> single ~massive star in each mini-halo (no clusters of primordial stars). DM heating?

Need analytic model to follow the growth of the protostar: accretion rate; accretion disk; protostellar evolution; feedback.

Large (~AU) protostar, contracts to main sequence for $m_* > 30 M_\odot$

This is when feedback processes start to become important.

Feedback processes depend on core rotation and accretion rate: Gradual reduction in SF efficiency because of ionizing and radiation pressure feedback for $m_* > 30 M_\odot$. Final mass in fiducial case (K'=1, $f_{Kep}=0.5$), is ~$160 M_\odot$, set by ionizing feedback on core and disk.

Conclusions

Approximately convergent initial conditions for star formation: set by H_2 cooling. Mostly thermal pressure support + slow cooling -> no/little (disk) fragmentation -> single ~massive star in each mini-halo (no clusters of primordial stars). DM heating?

Need analytic model to follow the growth of the protostar: accretion rate; accretion disk; protostellar evolution; feedback.

Large (~AU) protostar, contracts to main sequence for $m_* > 30 M_\odot$

This is when feedback processes start to become important.

Feedback processes depend on core rotation and accretion rate: Gradual reduction in SF efficiency because of ionizing and radiation pressure feedback for $m_* > 30 M_\odot$. Final mass in fiducial case (K'=1, f_{Kep}=0.5), is ~160$M_\odot$, set by ionizing feedback on core and disk.

Changing accretion rate by factor of ~5 (K'=0.5-2) leads to final masses in the range ~60 – 300$M_\odot$ (seeds for SMBHs?)

Conclusions

Approximately convergent initial conditions for star formation: set by H_2 cooling. Mostly thermal pressure support + slow cooling -> no/little (disk) fragmentation -> single ~massive star in each mini-halo (no clusters of primordial stars). DM heating?

Need analytic model to follow the growth of the protostar: accretion rate; accretion disk; protostellar evolution; feedback.

Large (~AU) protostar, contracts to main sequence for $m_* > 30 M_\odot$

This is when feedback processes start to become important.

Feedback processes depend on core rotation and accretion rate: Gradual reduction in SF efficiency because of ionizing and radiation pressure feedback for $m_* > 30 M_\odot$. Final mass in fiducial case (K'=1, f_{Kep}=0.5), is ~160$M_\odot$, set by ionizing feedback on core and disk.

Changing accretion rate by factor of ~5 (K'=0.5-2) leads to final masses in the range ~60 - 300$M_\odot$ (seeds for SMBHs?)

Impact of PopIII stars on subsequent SF: suppressed cooling due to FUV background; enhanced cooling from metals/dust and ionization catalyzed H_2/HD -> rotational supported, fragmenting cores? Eventual build up of B-field support to resemble present-day SF clusters.

Conclusions

Approximately convergent initial conditions for star formation: set by H_2 cooling. Mostly thermal pressure support + slow cooling -> no/little (disk) fragmentation -> single ~massive star in each mini-halo (no clusters of primordial stars). DM heating?

Need analytic model to follow the growth of the protostar: accretion rate; accretion disk; protostellar evolution; feedback.

Large (~AU) protostar, contracts to main sequence for $m_* > 30 M_\odot$

This is when feedback processes start to become important.

Feedback processes depend on core rotation and accretion rate: Gradual reduction in SF efficiency because of ionizing and radiation pressure feedback for $m_* > 30 M_\odot$. Final mass in fiducial case (K'=1, f_{Kep}=0.5), is ~$160 M_\odot$, set by ionizing feedback on core and disk.

Changing accretion rate by factor of ~5 (K'=0.5-2) leads to final masses in the range ~60 – $300 M_\odot$ (seeds for SMBHs?)

Impact of PopIII stars on subsequent SF: suppressed cooling due to FUV background; enhanced cooling from metals/dust and ionization catalyzed H_2/HD -> rotational supported, fragmenting cores? Eventual build up of B-field support to resemble present-day SF clusters.

Hydrogen Ionizing Luminosities along the Primordial Zero Age Main Sequence

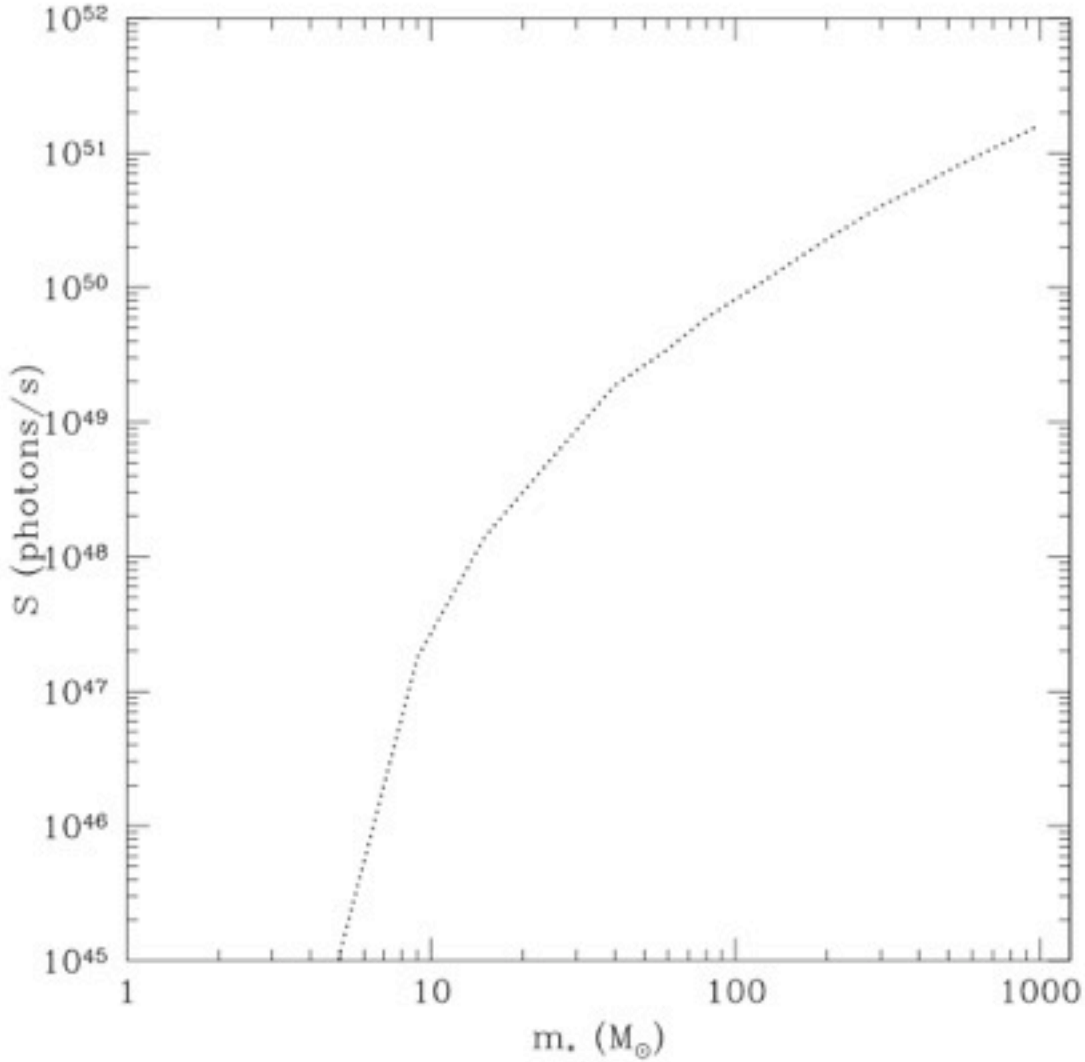

Tumlinson & Shull 2000; Bromm et al. 2001; Ciardi et al. 2001; Schaerer 2002

Implications of IMF for supernovae and metal enrichment

Metal production and dispersal via winds and supernovae depends on m_*

Pair Instability SNe for $m_*>140M_\odot$, Massive BH formation for $m_*>260M_\odot$

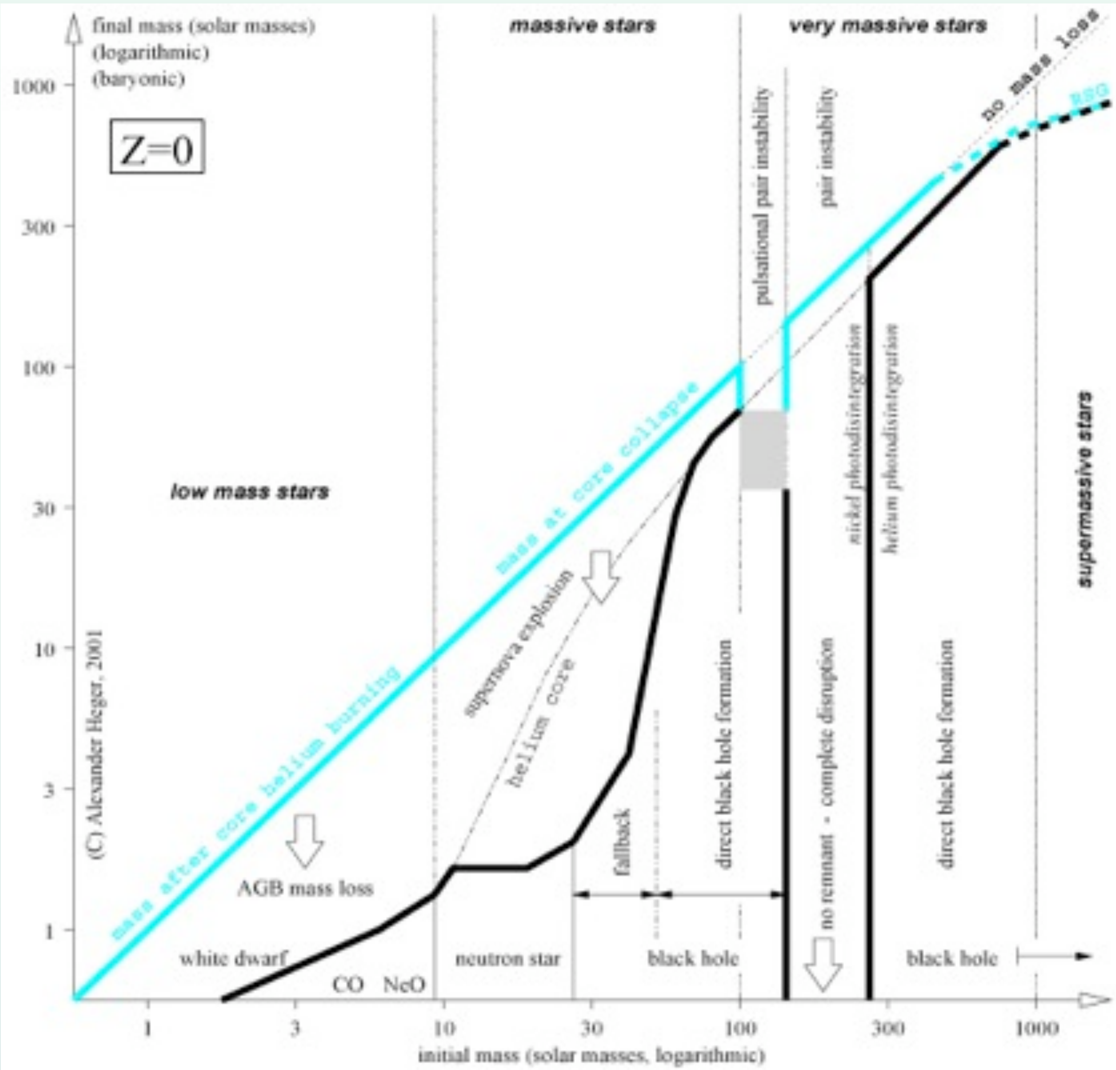

Fate of NON-ROTATING metal-free stars (Heger & Woosley 2002)

Growth of Cosmic Structure During the Dark Ages

1. Recombination z ≈1200, start of "dark ages"
2. Thermal equilibrium matter-CBR until z ≈160
   $M_{Jeans} \simeq 10^5 M_{\odot} \propto (T/\rho^{1/3})^{3/2}$: independent of z
   e.g. globular clusters
3. Thermal decoupling, $T \propto (1+z)^2$; $M_{Jeans} \propto (1+z)^{3/2}$

Growth of Cosmic Structure During the Dark Ages

1. Recombination z ≈1200, start of "dark ages"
2. Thermal equilibrium matter-CBR until z ≈160
   $M_{Jeans} \simeq 10^5 M_\odot \propto (T/\rho^{1/3})^{3/2}$: independent of z
   e.g. globular clusters
3. Thermal decoupling, $T \propto (1+z)^2 \; ; \; M_{Jeans} \propto (1+z)^{3/2}$
4. "First Light"
5. Reionization,
   e.g. galaxies

$$T \simeq 10^4 K \; ; \; M_{Jeans} \simeq 10^{9-10} \left(\frac{1+z_{ion}}{10}\right)^{3/2} M_\odot$$

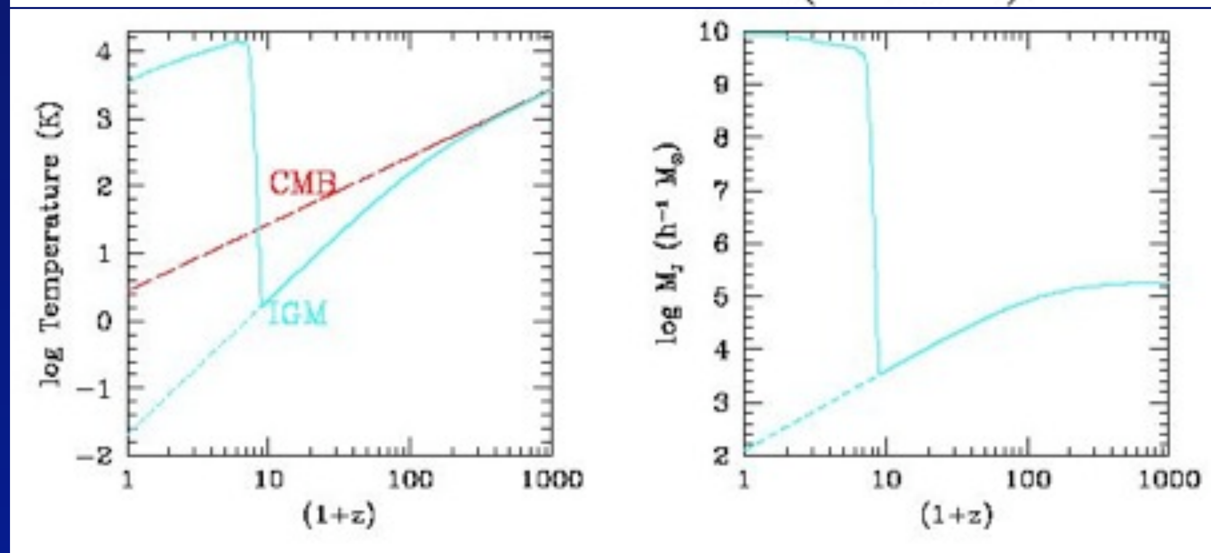

Madau (2002)

Evolution of the Protostar : Radius

Initial condition

$m_* = 0.04\ M_\odot$

$r_* = 14\ R_\odot$

(Ripamonti et al. 02)

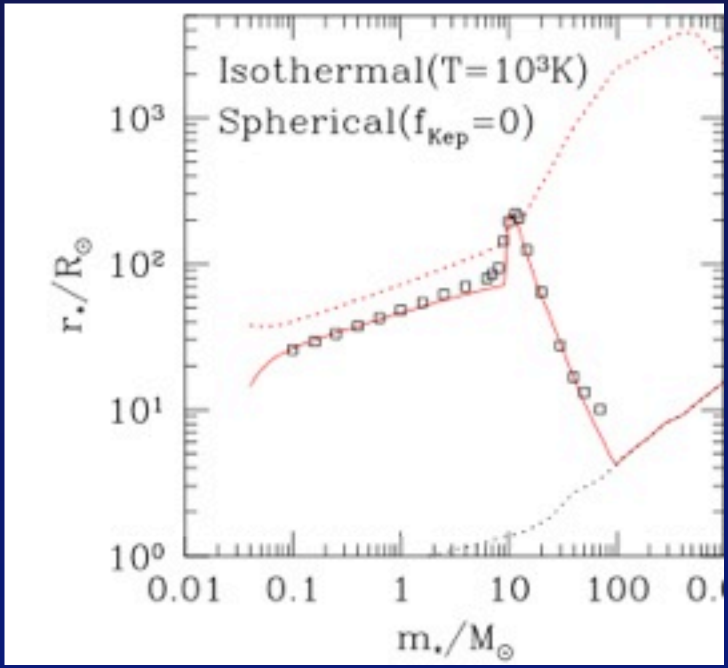

Evolution of the Protostar : Radius

Comparison with Stahler et al. (1986), Omukai & Palla (2001)

Initial condition

$m_* = 0.04\ M_\odot$

$r_* = 14\ R_\odot$

(Ripamonti et al. 02)

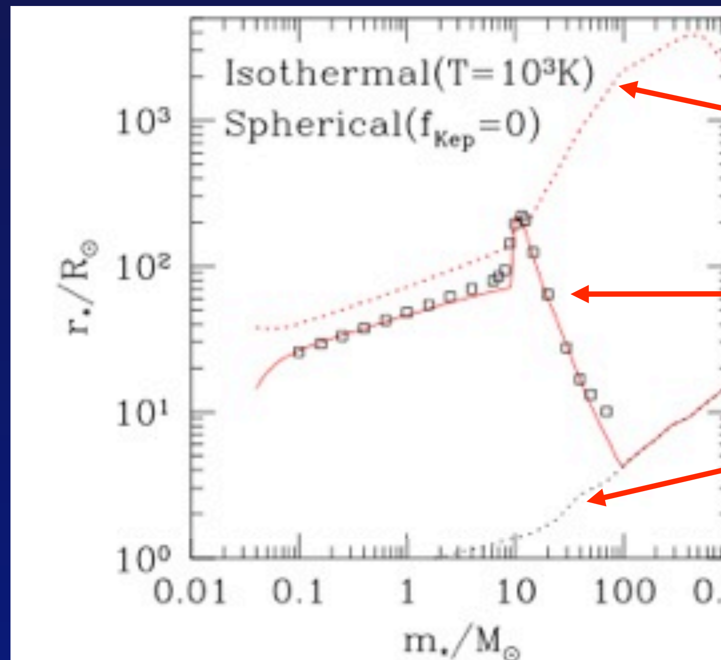

Photosphere

Accretion Shock

Main Sequence (Schaerer 2002)

Evolution of the Protostar : Radius

Comparison with Stahler et al. (1986), Omukai & Palla (2001)

Initial condition

$m_* = 0.04\ M_\odot$

$r_* = 14\ R_\odot$

(Ripamonti et al. 02)

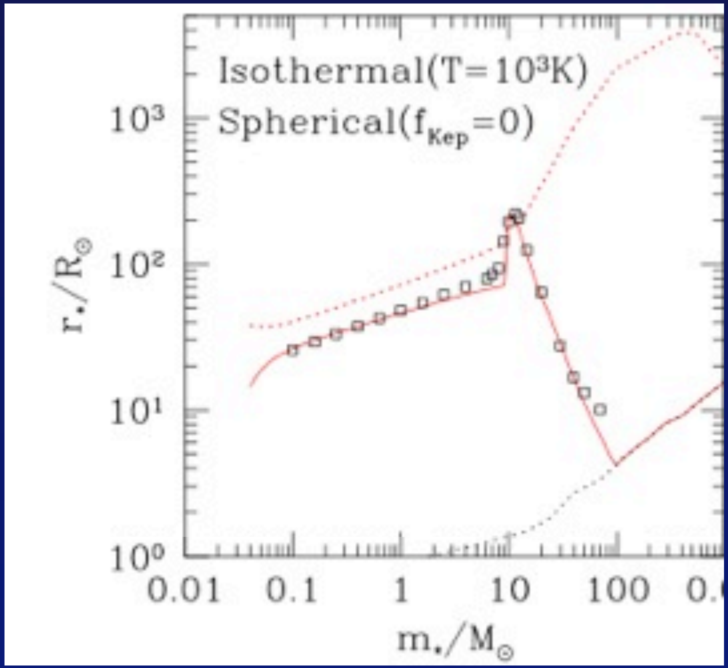

Evolution of the Protostar : Radius

Comparison with Stahler et al. (1986), Omukai & Palla (2001)

Initial condition

$m_* = 0.04\ M_\odot$

$r_* = 14\ R_\odot$

(Ripamonti et al. 02)

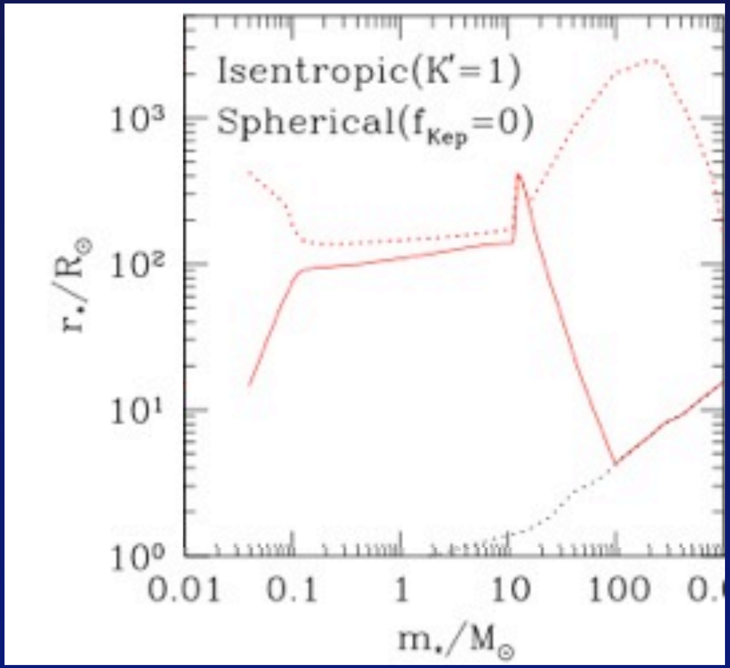

Evolution of the Protostar : Radius

Comparison with Stahler et al. (1986), Omukai & Palla (2001)

Initial condition

$m_* = 0.04\ M_\odot$

$r_* = 14\ R_\odot$

(Ripamonti et al. 02)

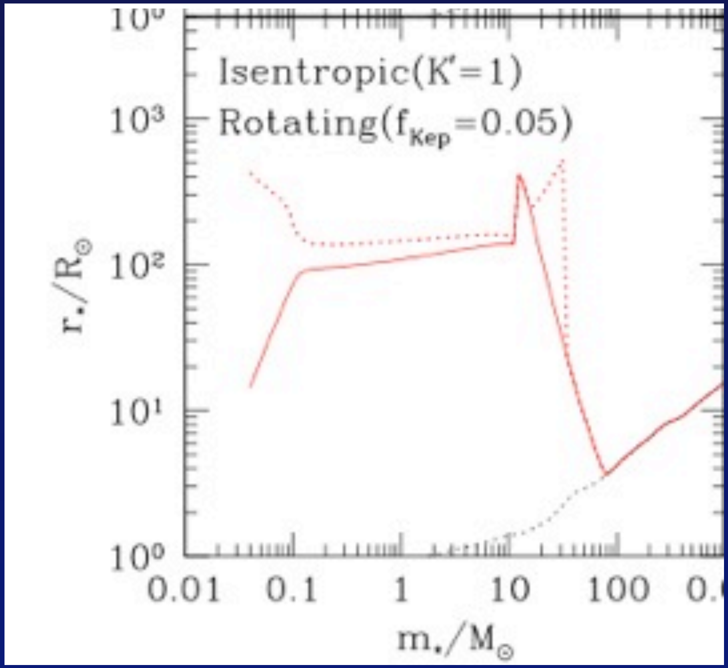

Evolution of the Protostar : Radius

Comparison with Stahler et al. (1986), Omukai & Palla (2001)

Initial condition

$m_* = 0.04\ M_\odot$

$r_* = 14\ R_\odot$

(Ripamonti et al. 02)

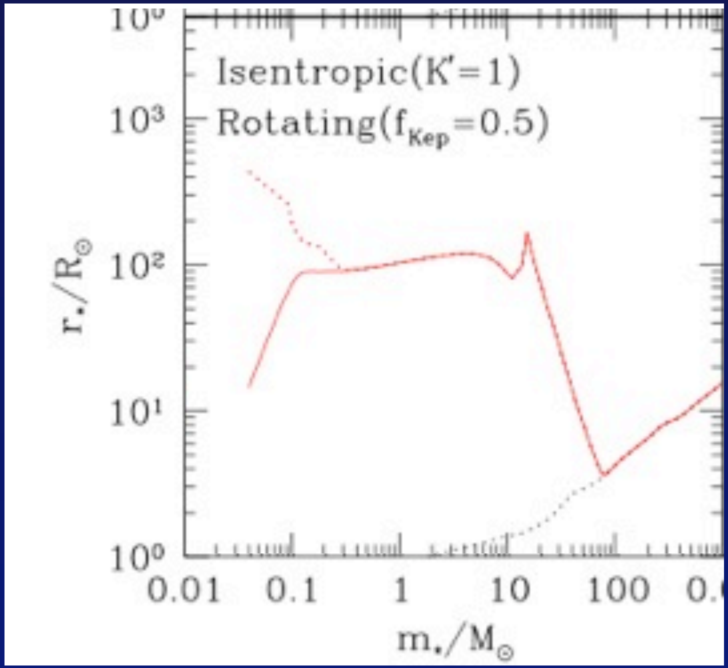

Evolution of the Protostar : Radius

Comparison with Stahler et al. (1986), Omukai & Palla (2001)

Initial condition

$m_* = 0.04\ M_\odot$

$r_* = 14\ R_\odot$

(Ripamonti et al. 02)

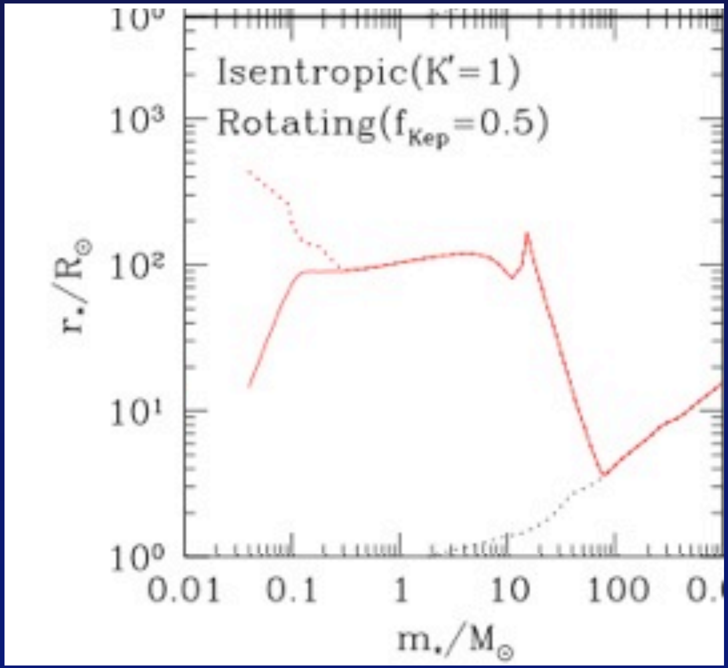

Protostar is large (~100 $R_\odot$) until it is older than t_{Kelvin}

Contraction to Main Sequence

Accretion along Main Sequence

Redshift dependence of IMF: Pop III.1

Redshift dependence of K'

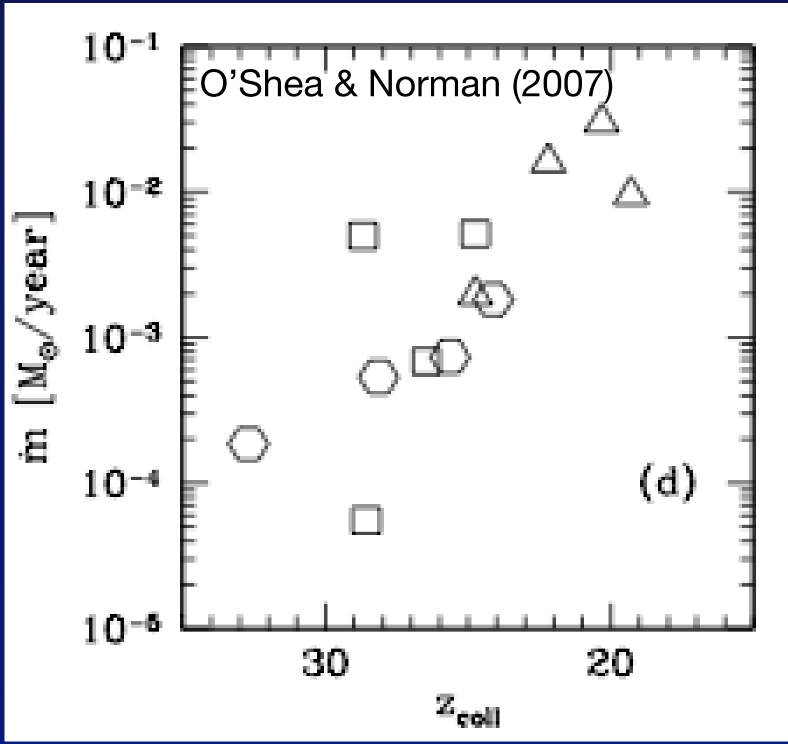

K' increases from ~0.37 at z=30 to ~4.3 at z=20.

For PopIII.1 stars ->$m_* = 40M_\odot$ to $900M_\odot$

Redshift dependence of IMF: Pop III.1

Redshift dependence of K’

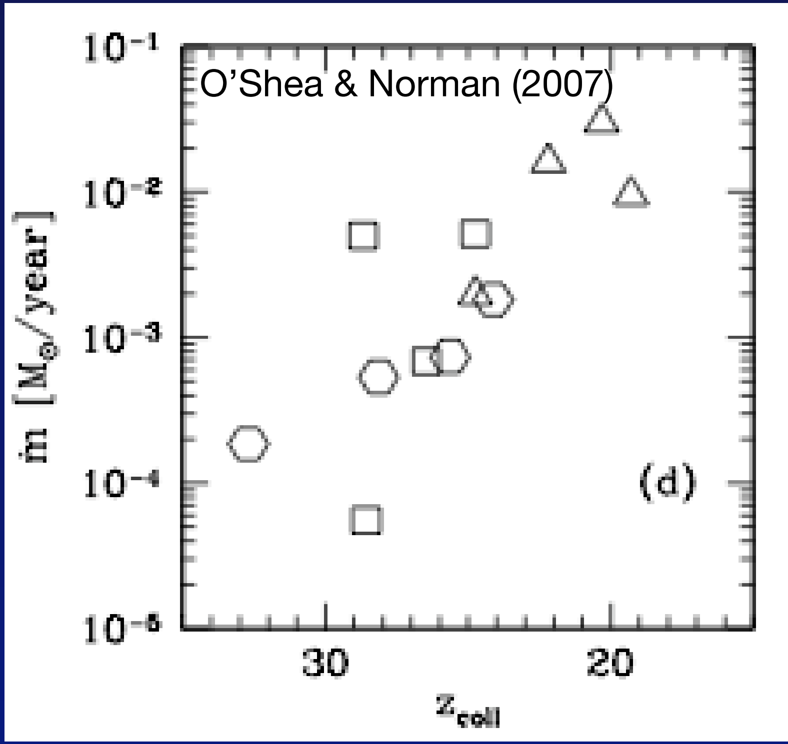

K’ increases from
~0.37 at z=30 to
~4.3 at z=20.

For PopIII.1 stars ->m_*= 40$M_\odot$ to 900$M_\odot$

However, maybe Pop III.1 stars no longer exist by z=20
because of stellar feedback from previous stars.

Overview of Physical Scales

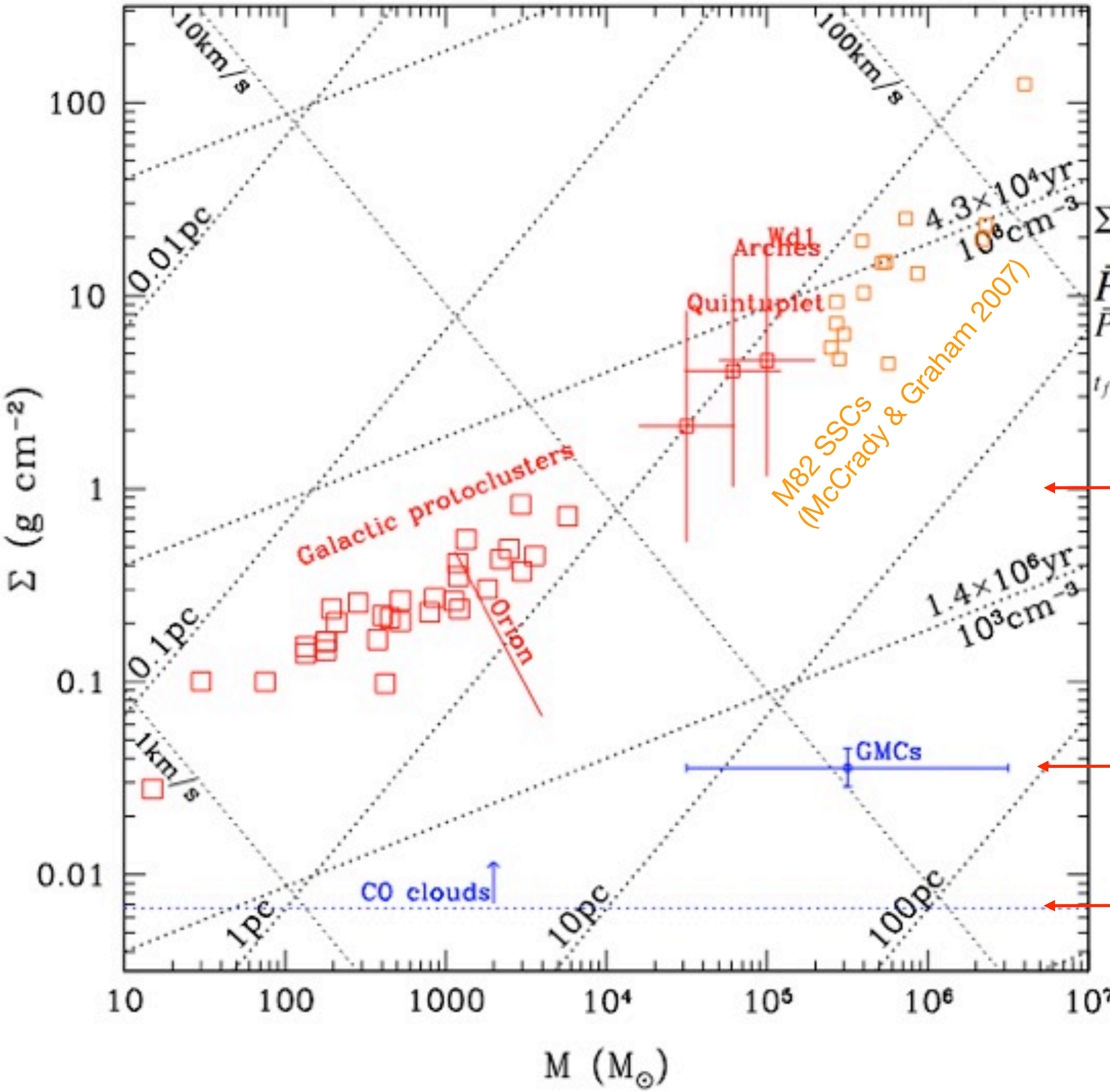

$$\Sigma \equiv \frac{M}{\pi R^2}$$

$$\bar{P} \simeq G\Sigma^2$$

$$\bar{P}/k = 4.3 \times 10^8 \Sigma^2\, K\, cm^{-3}$$

$$t_{ff} = \left(\frac{3\pi}{32G\rho}\right)^{1/2}$$

$A_V = 200$
$A_{8\mu m} = 8.1$
$N_H = 4.2 \times 10^{23} cm^{-2}$
$\Sigma = 4800\ M_\odot\ pc^{-2}$

$A_V = 7.5$
$A_{8\mu m} = 0.30$
$N_H = 1.6 \times 10^{22} cm^{-2}$
$\Sigma = 180\ M_\odot\ pc^{-2}$

$A_V = 1.4$
$N_H = 3.0 \times 10^{21} cm^{-2}$
$\Sigma = 34\ M_\odot\ pc^{-2}$

Overview of Physical Scales

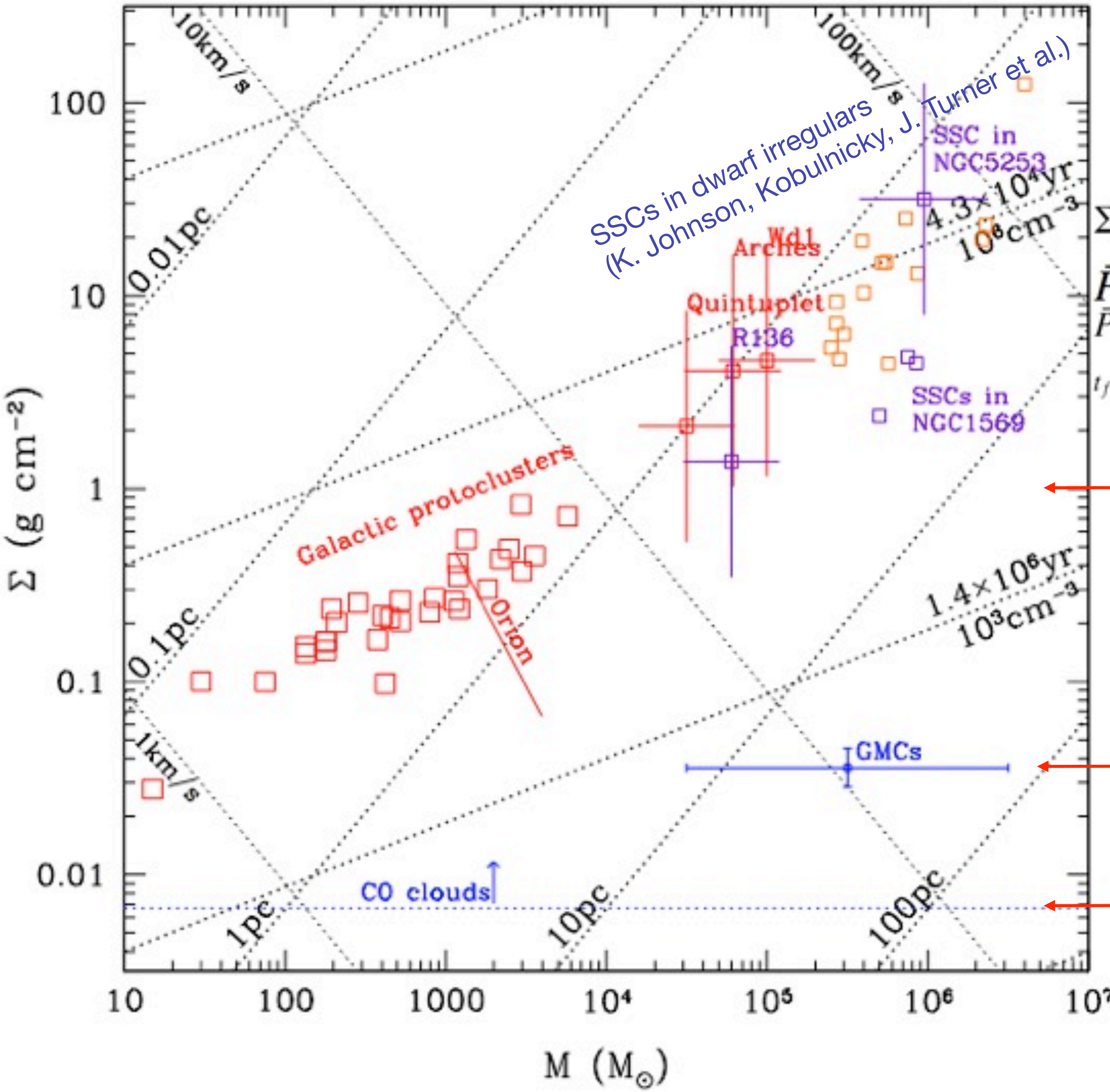

$$\Sigma \equiv \frac{M}{\pi R^2}$$

$$\bar{P} \simeq G\Sigma^2$$

$$\bar{P}/k = 4.3 \times 10^8 \Sigma^2\, K\, cm^{-3}$$

$$t_{ff} = \left(\frac{3\pi}{32 G\rho}\right)^{1/2}$$

$A_V = 200$
$A_{8\mu m} = 8.1$
$N_H = 4.2 \times 10^{23} cm^{-2}$
$\Sigma = 4800\ M_\odot\ pc^{-2}$

$A_V = 7.5$
$A_{8\mu m} = 0.30$
$N_H = 1.6 \times 10^{22} cm^{-2}$
$\Sigma = 180\ M_\odot\ pc^{-2}$

$A_V = 1.4$
$N_H = 3.0 \times 10^{21} cm^{-2}$
$\Sigma = 34\ M_\odot\ pc^{-2}$

Overview of Physical Scales

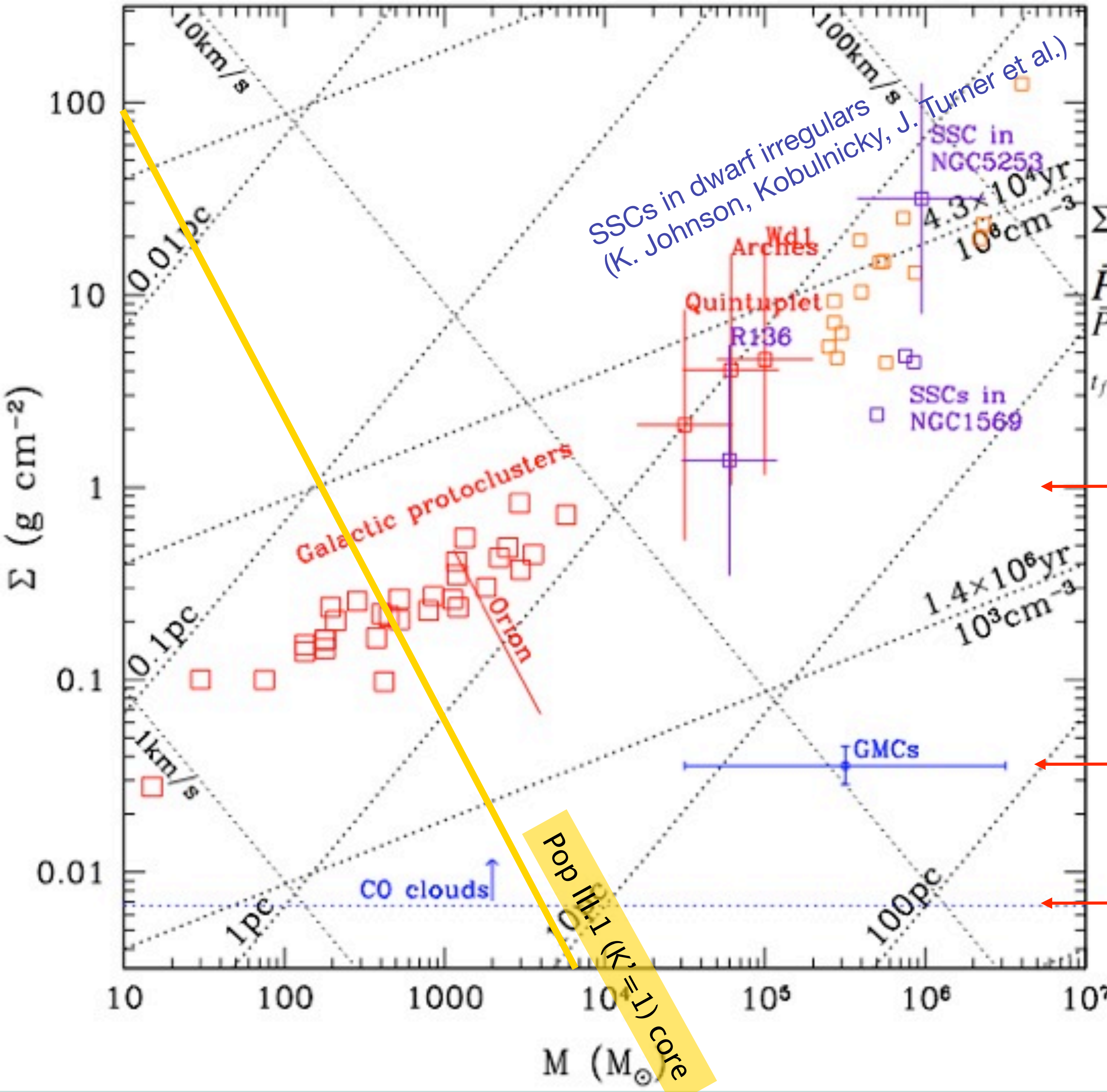

$$\Sigma \equiv \frac{M}{\pi R^2}$$

$$\bar{P} \simeq G\Sigma^2$$

$$\bar{P}/k = 4.3 \times 10^8 \Sigma^2\, K\, cm^{-3}$$

$$t_{ff} = \left(\frac{3\pi}{32 G\rho}\right)^{1/2}$$

$A_V=200$
$A_{8\mu m}=8.1$
$N_H=4.2\times10^{23}cm^{-2}$
$\Sigma=4800\ M_\odot\ pc^{-2}$

$A_V=7.5$
$A_{8\mu m}=0.30$
$N_H=1.6\times10^{22}cm^{-2}$
$\Sigma=180\ M_\odot\ pc^{-2}$

$A_V=1.4$
$N_H=3.0\times10^{21}cm^{-2}$
$\Sigma=34\ M_\odot\ pc^{-2}$

Overview of Physical Scales

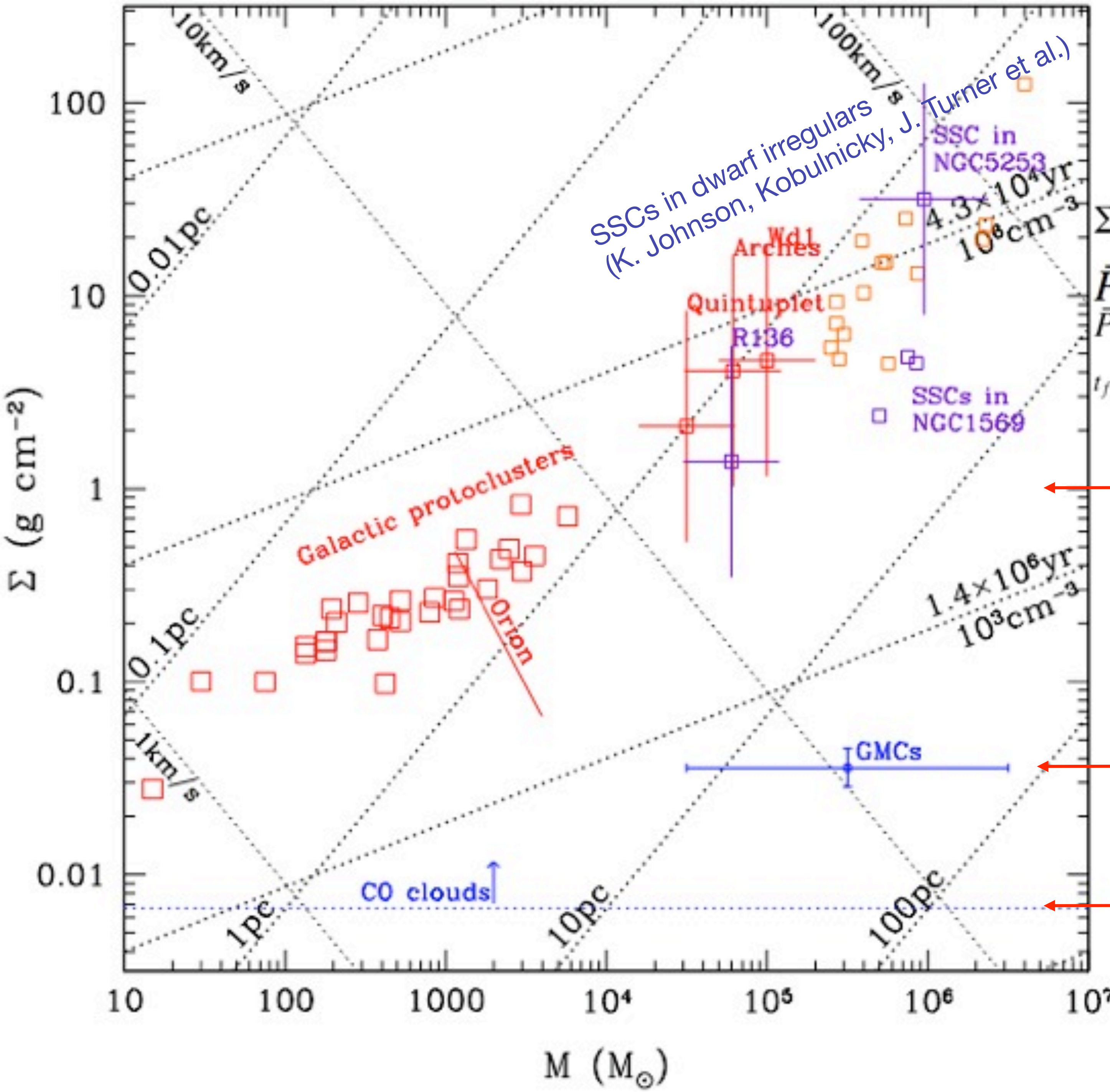

$$\Sigma \equiv \frac{M}{\pi R^2}$$

$$\bar{P} \simeq G\Sigma^2$$

$$\bar{P}/k = 4.3 \times 10^8 \Sigma^2\, K\, cm^{-3}$$

$$t_{ff} = \left(\frac{3\pi}{32 G\rho}\right)^{1/2}$$

$A_V = 200$
$A_{8\mu m} = 8.1$
$N_H = 4.2\times10^{23}$cm^{-2}
$\Sigma = 4800\ M_\odot$ pc^{-2}

$A_V = 7.5$
$A_{8\mu m} = 0.30$
$N_H = 1.6\times10^{22}$cm^{-2}
$\Sigma = 180\ M_\odot$ pc^{-2}

$A_V = 1.4$
$N_H = 3.0\times10^{21}$cm^{-2}
$\Sigma = 34\ M_\odot$ pc^{-2}

Overview of Physical Scales

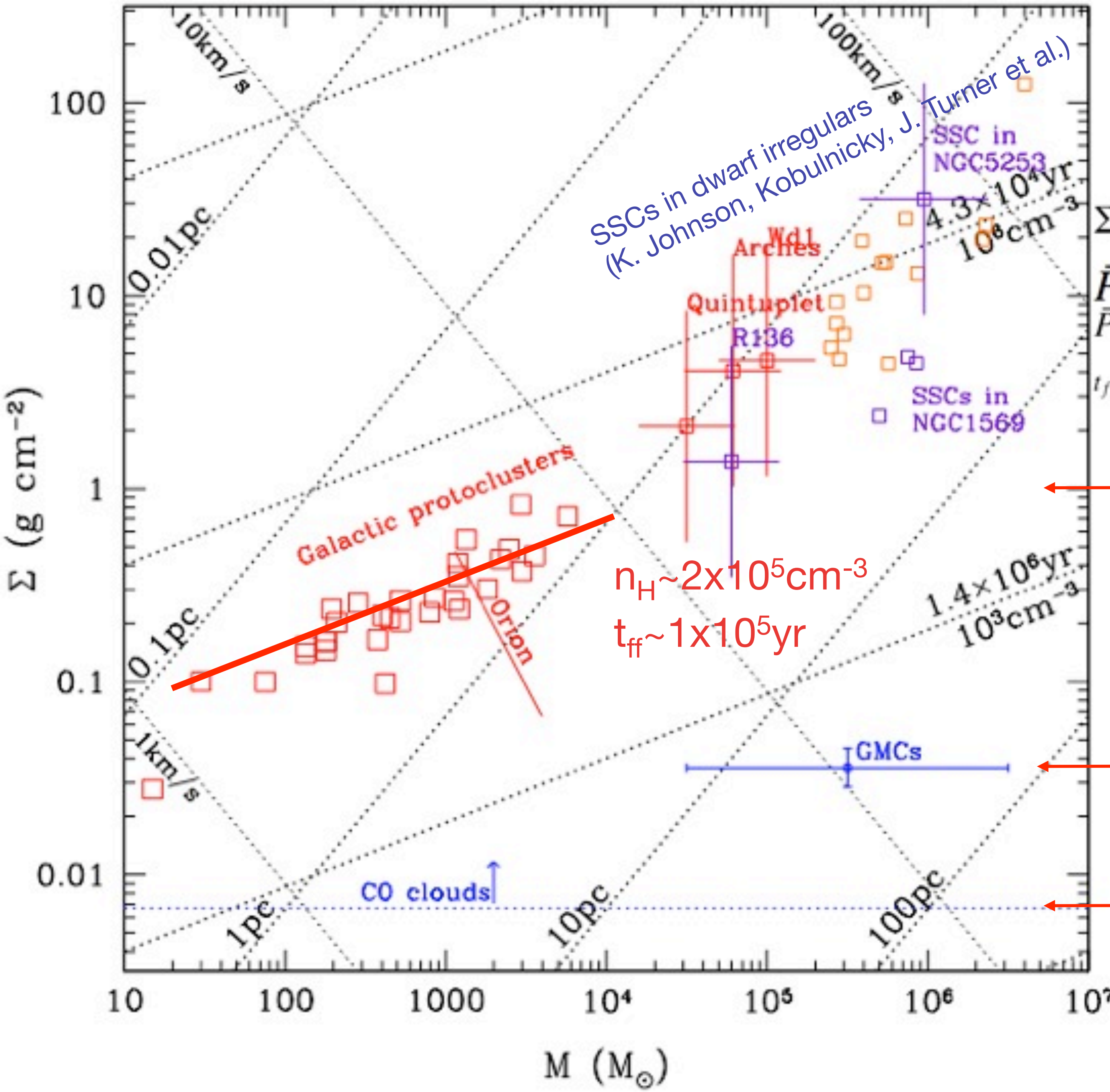

$$\Sigma \equiv \frac{M}{\pi R^2}$$

$$\bar{P} \simeq G\Sigma^2$$

$$\bar{P}/k = 4.3\times10^8\Sigma^2\, K\, cm^{-3}$$

$$t_{ff} = \left(\frac{3\pi}{32G\rho}\right)^{1/2}$$

$A_V=200$
$A_{8\mu m}=8.1$
$N_H=4.2\times10^{23}$cm^{-2}
$\Sigma=4800\ M_\odot$ pc^{-2}

$A_V=7.5$
$A_{8\mu m}=0.30$
$N_H=1.6\times10^{22}$cm^{-2}
$\Sigma=180\ M_\odot$ pc^{-2}

$A_V=1.4$
$N_H=3.0\times10^{21}$cm^{-2}
$\Sigma=34\ M_\odot$ pc^{-2}